Biocomplexity: the autonomous agroecological alternative

by

Theresa Wei Ying Ong

A dissertation submitted in partial fulfillment
of the requirements for the degree of
Doctor of Philosophy
(Ecology and Evolutionary Biology)
in the University of Michigan
2017

Doctoral Committee:
Professor John H. Vandermeer, Chair
Associate Professor Timothy James
Associate Professor Annette Ostling
Professor Ivette Perfecto

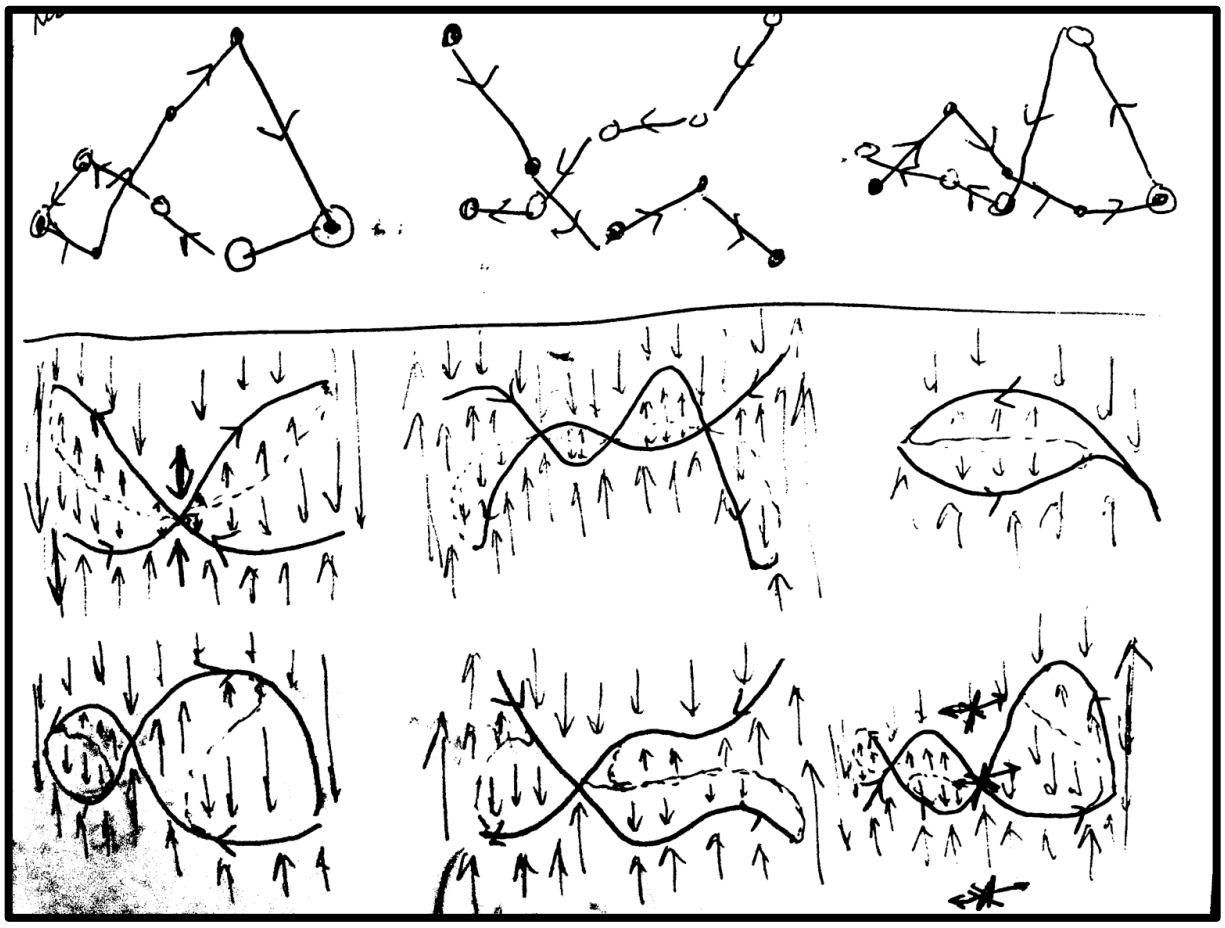

"Our truth is the intersection of independent lies."

-Richard Levins

Theresa Wei Ying Ong

weiyingo@umich.edu

ORCID: 0000-0002-7291-5205

DEDICATION

To the purple mountains and out of the box discussions.

ACKNOWLEDGEMENTS

If I were to trace the winding path that led me to where I am here with you today, I would have to begin in Malaysia where I was born, but not raised. I would not be here if my mother and father had not sacrificed everything to bring us to the United States and give me and my three brothers educational opportunities that were otherwise impossible. Though I was born in the tropics I was raised in the urban streets of Los Angeles, which left me with a perspective of the world that this thesis would be incomplete without. Those streets were a necessary contrast to the rolling mountains I would discover at Williams College, which I would have never have experienced without support from One Voice. This program asked me to look beyond what was easy and familiar, and never asked anything of me but simply to reflect on my past and hope for the future.

I have to thank David Smith for teaching me how to distinguish the identity of various roadkill, the birdsongs of Isle Royale, the behaviors of *Pseudacris triseriata* and *crucicfer,* and the muffled lyrics behind the Subterranean Homesick Blues. It is curious that that first foray into ecology would bring me from Williams to Michigan where I would later meet the man Joan Edwards had described to me as a charismatic genius—John Vandermeer. There are no words to describe what John means to me. His infective enthusiasm for all things complex, his undying belief in me, his relentless but always supportive and sometimes strange mentorship in

everything scientific, political and personal was integral to my life and work for the past eight years. I will always be grateful that you put me into the "Math" group in Field Ecology, though admittedly at the time I would have much preferred catching the charismatic mini-fauna. Field Ecology deserves thanks in itself: the course, professors (John Vandermeer, Ivette Perfecto, Catherine Badgley, Chris Dick), students and insights learned left a permanent impression on everything I have done since. Thank you to Ivette Perfecto for teaching me the politics of food and always being a model of what a strong female leader could and should be in a field lacking color. Thank you also to the other members of my committee: Tim James who never gave up on me or our project and Annette Ostling who always made me feel like an equal. Thanks to Yin Long Qiu for re-inventing practical botany with me and teaching me about Chinese history. I would not have been able to do this thesis if I had not taken Charlie Doering's introductory nonlinear dynamics course.

The Perfectomeer lab and the extended Frontiers program were like my second family. Special thanks to Aaron Iverson, Linda Marin, Mariana Valencia, Beatriz Otero, Kaleigh Fisher, Ivan Monagan, Mairin Balisi, Kristel Sanchez, Susanna Campbell, Cindy Bick, Zachary Hajian-Forooshani, Kevin Li, Gordon Fitch, Eliot Jackson, Hailey Schurr, Colin Donihue, Lauren Schmidtt, Kim Williams-Guillén, Iman Sylvain, Jessica Robinson, Kristopher Harmon, Naim Edwards, Chatura Vaidya, and Bolívar Aponte Rolón whom together made this place feel like home. Extra special thanks to Dave Allen, Doug Jackson and Senay Yitbarek—cofounders of OOTB. Without them I would never have learned the sensitive side of Robert Foster Wallace, that essential stochasticity is merely human inadequacy (if you are an engineer), and that each day should begin with a new theory. To my cohort and other EEB and SNRE students: Gyuri Barabas, Ed Baskerville, Shawn Colborn, Corbin Kuntze, Alex Smith and Alex Taylor, thanks

for all the good times. I am grateful to Ash Zemenick, Kate Mathis, Aldo de la Mora, Gustavo Bautista and Cody Thompson for their friendship on the Finca, and would also like to thank my friends Allison Ho, Daniel Kowalsky, Anastashia Maggee, Patty Liao and Brennan Madden for their free help as research assistants, and all of the adventures and mis-adventures we have had in Ann Arbor and beyond.

I would like to extend my greatest gratitude to the staff in the Department of Ecology and Evolutionary Biology for their assistance in all things small and large. Particular thanks to: Cindy Carl, Gail Kuhnlein and Jane Sullivan who made life so much easier for me. Thank you also to the Department at large and the Rackham Graduate School for consistently funding this dissertation. Science for the People and the New World Agriculture and Ecology Group were constant sources of inspiration.

Thank you to the co-authors of my chapters including John Vandermeer, Dave Allen, Kevin Li, Damie Pak, Azucena Lucatero, L'Oreal Hawkes, Tim James and MaryCarol Hunter. My students have been an endless source of pride: L'Oreal Hawkes, Azucena Lucatero, Damie Pak, Tim Kuzel, Madeline Baroli, Kerrel Spivey, Anderson Shu, Corrinne Erickson, and Jessica Ruff. Much of this thesis would not be possible without them. Thank you to my brothers Elwin, Jeffery and Richard for also not wanting to be medical doctors and leading by example. And finally, thanks to Adam, for reminding me of my roots and providing all of the necessary conditions for completing this thesis and transitioning to that next phase.

PREFACE

The term "natural" has always perplexed me. According to Merriam-Webster, "*natural"* means "existing in or caused by nature; not made or caused by humankind." At first glance this would appear to be one of those frustrating-and-not-very-useful definitions where parts of a word are used to define the word itself. Yet in this definition lies a subtle, but very deliberate delineation between what is nature and what is human. Modern day ecology is very different from its early beginnings. In the past, ecologists by in large worked in "pristine" habitats untouched by humans, or sought to recapture the essence of "nature" in areas that were already sullied by human hands. This mindset was not altogether unfounded; human presence had thinned the eggshells of bald eagles, lit the Cuyahoga River on fire, poisoned the fish and people of Japan and turned the Amazon into office paper and houses. From this emerged the notion that nature needed conservation, and unfortunately the conclusion that conservation required the removal of humans.

This was the beginning of "nature" reserves— parks that would exclude humans and protect "nature." But what was the best design? Was it better to have several small parks or a single large? On the one hand, a single large park could support a greater diversity of organisms. On the other hand, dispersal between several small parks could minimize the risk that a random act of "nature" would cause populations across all parks to go extinct at once. A critique in ecology is that we are continuously rehashing old concepts. Nowadays you can find ecologists

everywhere: in farms, in cities, in laboratories. But simply replace parks with agriculture and the classic S-S-O-S-L (several small or single large) debate becomes something very close to the contemporary land sharing-land sparing debate. The land sparing argument is one that sources from a predilection for conservation—keep one large, very intensely managed industrial farm rather than fragmenting a landscape with many, small, less intensive agro-ecological alternatives. Yet what is more concerning? Threat of environmental impact by large corporations (legally considered humans, though evidence suggests they are psychopathic ones), or a group of small-holder farmers trying to hold on to their traditional farming practices and the land they have farmed for generations?

As ecologists, we are always seeking to bring nature to human-managed systems, yet what exactly do we seek to capture? When we look across a fragmented landscape the lines we see are a mixture of "natural" formations and those created by humans. What is the distinction? Whether quantified in terms of species, interactions, landscape features, soil texture or any number of variables, we tend to measure the value of nature in terms of its complexity. Human-managed systems do tend to be simplifying: we turn diverse rainforests into monocultures of timber and soybean, we till soils and homogenize the layers that have taken millions of years to stratify, we pour concrete over the billions of microorganisms alive in the earth to create grey, monotone cities. But at what cost?

Complexity has long-been both the defining feature and main struggle for ecology as a discipline. We seek to understand the nature of interactions between elements of diverse biological systems, yet interactions between elements in the simplest of systems are plagued with complexities. The three-body problem in physics is the perfect example: take one celestial body whose precise location is known, add another and they will rotate relative to each other in a

predictable fashion. Take three and chaos emerges. As a rule of thumb, nothing in ecology has less than three elements. Though complexity may be standard for ecological systems, its effects on system stability are less so. The classic diversity-stability debate in ecology explored this very question. Elton used heuristics to contrast the stability of diverse, natural systems with the plagues of pests and disease common in simplified agricultural landscapes. May would challenge that assertion with food web models that likened diverse assemblages to a house of cards, more likely to fall over with the addition of every card. McCann, Huxel and Hastings would claim that weak interactions were the glue that held the cards in place. All of this occurred while ecologists were increasingly acknowledging the role of stochasticity and chaos in driving ecosystem dynamics, and this acknowledgement arising as those ecosystem dynamics continued to move towards collapse.

People live on this planet and "pristine" nature is an increasing rarity. I have always struggled with the concept of "nature" precisely because humans are excluded by definition. If "nature" is natural then what is human? More importantly, if humans must be excluded to conserve nature, how is nature to survive our increasing imposition? Given the simple ingredients for chaos, surely, there is no reason why a human-managed system must be less complex than a natural one. Chaos itself is a misnomer. Though unpredictable it is also deterministic, with structure and bounds that are describable. Whether and in what cases those structures and bounds are amenable to human-managed systems is the motivating question behind this thesis.

TABLE OF CONTENTS

LIST OF FIGURES

Figure

LIST OF TABLES

Table

ABSTRACT

This dissertation examines biocomplexity in agroecological systems. Throughout the dissertation, theoretical frameworks are developed, and then validated using empirical and observational studies. Three major themes are explored: 1) autonomous biological control, 2) fragmented landscapes, and 3) the complex and irreversible consequences of human-management for ecosystem states.

In autonomous biological control, interactions between diverse assemblages of natural enemies are hypothesized to maintain pest populations consistently below economic thresholds. Chapters I-III test whether autonomous biological control can be achieved through strong negative coupling of biological control agents that are ineffective in isolation. Competing agents wrestle for dominance, but are unable to persist in isolation. Pests move chaotically between control by one or the other agent, yet remain for long timescales at densities below economic thresholds. Coupling biological control agents may also reduce spatial clustering in pests, eliminating local outbreaks.

Chapters IV-V assess the population structures of pest-natural enemy systems across fragmented urban landscapes. Fragmentation can structure populations along a continuum between metapopulations and source-sinks. Dispersal from sources to sinks synchronizes population fluctuations, while isolation in metapopulations causes asynchrony. This structure leaves signatures on the spatio-temporal dynamics of populations. Asynchrony can reduce

variances in populations to levels lower than their mean sizes would predict, causing the exponent of a well known scaling law, Taylor's law to move towards 1. Thus, calculations of Taylor's law may help in addressing where populations in fragmented landscapes exist on the continuum between metapopulations and source-sinks. This approach paired with a microsatellite analysis of aphid population genetics suggest that urban gardens in Ann Arbor may represent sinks for dispersing aphids.

Chapters VI and VII examine the potential for management decisions to irreversibly impact biological control and agriculture. When parameters in simple population and nutrient dynamic models are correlated, complicated hysteretic patterns including "unattainable" stable states emerge. Certain desirable ecosystem states, once lost, may never be recovered.

In summary, biocomplexity very easily emerges from interactions between components of diverse agricultural systems. Spatial heterogeneity, a defining characteristic of agriculture, further increases this complexity. These complexities can be leveraged to promote the success of agroecological alternatives to harmful conventional practices.

INTRODUCTION

In 1958, Charles Elton observed that agriculture was prone to insect and disease outbreaks (Elton 1958). The dominant form of agriculture at the time consisted of large monocultures, a homogeneity that stood in stark contrast to the diverse vegetation of natural forests. Elton posited that within forests, a diversity of organisms acted as natural enemies of herbivores and pathogens that were prevented from becoming the pests common of agriculture. He presumed that lack of vegetative and structural diversity in agriculture limited its natural enemy diversity and would go on to suggest, "if wilderness is in retreat, we ought to introduce some of its stability and richness into the landscapes from which we grow our natural resources." This call remains appropriate today, as the dominant form of agriculture in the developed world continues to consist of monocultures that simplify landscapes and depend heavily on inputs of fertilizers and pesticides (Pimentel et al. 1992, 2005). Concern for its environmental, health, and societal impacts drives many to call for transitions from conventional agriculture to agro-ecological alternatives (Giller et al. 1997, Vandermeer 2010). These alternatives seek to capture the stability and richness of nature that Elton alluded to by emulating its complexity (Lewis et al. 1997, Vandermeer et al. 2010) . However, the consequences of complexity on system stability are not well understood (May 1972, Murdoch 1975, Hastings 1993, McCann 2000, May 2001, Allesina and Tang 2012). Though nature is inarguably complex, it may or may not be stable.

In the early 1920s, Alfred Lotka and Vito Volterra independently derived equations to describe the population dynamics of predators and prey (Volterra 1927, Lotka 1978). Even when

considering simple systems composed of two units (predator and prey), complex patterns emerge. The equations predict stable coexistence but in the form of cycles; prey populations grow exponentially, followed by population growth for predators, a decline in prey, starvation of predators, and a repeat of the cycle in perpetuity. Here is an example where stability and complexity can coincide. Though the dynamics are complicated, neither the predator nor the prey ever goes extinct. Predator-prey cycles are commonly observed in nature, the most famous example being the lynx and hare cycles derived from the Hudson Bay Company's records of fur pelts dating back to 1845 (Elton and Nicholson 1942). Yet when Gause combined predator *Paramecium* and their *Didinium* prey in well-mixed laboratory flasks, he failed to observe cycles (Gause 1934, Gause et al. 1936). This would become a common theme for ecology. Nature and theories suggested that complex systems could be stable, but empirical tests were less convincing.

Alexander Nicholson would later argue that neither Gause's experiments nor the Lotka-Volterra equations were realistic approximations of nature (Nicholson 1933, 1954). Both the experiments and the theory lacked the complexity of natural systems, and therefore could not adequately represent real predator-prey dynamics. As a consequence, Nicholson and Bailey developed an alternative model, based on a parasitoid wasp-host system (Nicholson and Bailey 1935) with generational effects included using a discrete time framework. At first the model failed to produce stable predator-prey cycles, but by adding aspects more realistic for parasitoid-host biology, the model was eventually coerced to do— rather than assume that hosts were randomly distributed, the model imposed a more realistic clumped distribution.

In 1958 Huffaker re-attempted to demonstrate predator-prey cycles in an experiment (Huffaker 1958). Considering Nicholson's arguments, Huffaker introduced space to a predator-prey system composed of mites distributed on carefully arranged arrays of oranges. Yet space

alone was insufficient to cause coexistence between predators and their prey. Only by adding greater spatial heterogeneity, where prey were aided in dispersal and predators were hindered, was Huffaker finally able to demonstrate cycles. In combination, Nicholson and Huffaker's results revealed the importance of complexity in effecting coexistence between predators and prey.

Yet real ecological systems are not two-dimensional. They are composed of a diversity of organisms interacting with one another and their environment at various spatial and temporal scales. Robert May disrupted Elton's presumption that diversity begets stability when he showed in 1972 that increasing the number of species in a food web model reduced the stability of the overall system (May 1972). Rather than considering stability as persistence of species for long timescales as Gause, Nicholson and Huffaker had done before him, May analyzed individual equilibrium points for their Lyapunov stability characteristics, finding that food webs were essentially like a house of cards, every additional card or species made the whole system more likely to collapse (move towards an equilibrium point that had one of the species in the community at zero). Again ecologists were confronted with a paradox: May's model predicted that diverse systems were inherently unstable, yet most real systems included a diversity of organisms that appeared to coexist in a stable manner (McCann 2000). After many decades, McCann, Hastings and Huxel provided one potential explanation. May's model was composed of very strong links between species in the food web, but McCann et al. showed that if the links between species were much weaker, diversity could actually increase stability (McCann et al. 1998). Most recently, researchers found that increasing the intensity of higher-order interactions among species could also reverse May's diversity-stability conclusion (Bairey et al. 2016).

Although adding more species decreases the stability of two-way interactions, three-way interactions are not affected, and four-way interactions actually increase in stability.

There is great difficulty in assessing the effect of diversity on system stability because once a third component, another predator or competitor for resources, is added, dynamics go from complicated to impossible to predict. Edward Lorenz first demonstrated this in 1963, when he developed a simple three-component model to describe atmospheric convection (Lorenz 1963). At that time, computers were fairly new tools in research. Lorenz used a computer to project changes in the three variables of his model, but when he repeated his analysis for the same initial conditions, he found that the results diverged exponentially. Lorenz discovered that the divergence resulted from a miniscule rounding error he had made when inputting the initial conditions for his second run. This led him to discover that when a dynamic system is composed of three or more variables, projections can be sensitive to initial conditions. Any small difference in initial conditions causes an exponential, yet deterministic divergence in the results, a concept that became known as deterministic chaos. Before this discovery, variability in ecological datasets was assumed random, but Lorenz's results implied that this variation could be deterministic—a point that would start another long-standing debate in ecology on whether variation in real-data is primarily stochastic or deterministic (Andrewartha 1954, Hairston et al. 1960, Ehrlich and Birch 1967, Slobodkin et al. 1967, Andrewartha and Birch 1986, Grenfell et al. 1998). After discovering that both stochasticity and deterministic chaos are relatively common, ecologists settled on the idea that it did not matter whether the ultimate source of variation was deterministic, but how that variation influenced system stability (Hastings et al. 1993).

The ubiquity of multi-dimensionality and context-dependency in nature mean there are few, if any, generalizable concepts in ecology. To arrive at general laws, ecologists traditionally

take a reductionist approach; we strip complex systems down to components and assess pair-wise interactions in isolation. This has led to many advances in ecology, not the least of which includes predator-prey theory. Yet complexity is arguably the most general law in ecology. Reductionist approaches purposefully remove or reduce complexity to improve understanding, however, doing so also reduces our ability to approximate real ecological systems. Thus, to arrive at a greater understanding of complexity in ecology, this dissertation combines reductionist and holistic methods; first separating components of complex systems and then combining them to observe their synergistic effects. Yet it is important to note that simple systems can be quite complicated in their own right. Lorenz's remarkable demonstration of deterministic chaos in three-dimensional systems was overshadowed by May's demonstration in 1976 that deterministic chaos can occur in a one-dimensional system (May 1976). May showed that in a simple model of logistic population growth, time lags could cause a population to over or under-shoot carrying capacities. Populations constantly had to readjust, increasing or decreasing their populations to account for under or overshooting beyond carrying capacity, creating chaotic dynamics in a simple one-dimensional system.

Though the methods and conclusions for past work contributing to the diversity-stability debate are various, all of them begin with the presumption that components within complex systems are stable in isolation. For the first time, this dissertation reverses that assumption and asks what happens when we couple two unstable consumer-resource interactions. Considering Elton's original framework, it is perhaps not surprising that much of the early work in population ecology focused on biological control systems where natural enemies are applied to control pest problems in agriculture (Nicholson and Bailey 1935, Levins 1969, Murdoch 1975, Luck 1990). I follow that tradition here. In the first chapter I develop a theoretical framework for coupling

unstable systems, followed by experimental validations in the second chapter and extensions into space in the third.

Huffaker first established the importance of space for stabilizing predator-prey mechanisms, sparking MacArthur and Wilson's forays into island-biogeography theory where the number of species that an island could sustain was made into a function of the distance to a mainland and the size of the island (Huffaker 1958, MacArthur and Wilson 1967). Richard Levins would extend these ideas in metapopulation theory, replacing the islands with habitat patches in fragmented landscapes (Levins 1969). Levins noted that high-dispersal between small sink patches could maintain persistence of species even if there were no large source patches in the landscape (Levins 1969, Pulliam 1988). As a result, habitat fragmentation patterns and dispersal between patches would become standard ways of conceptualizing the role of space for species coexistence (Gotelli 1991, Hanski and Gilpin 1991, Hanski and Ovaskainen 2000). One debate that arose from this work was whether when designing parks with the goal of conserving species, it was better to include several small parks or devote funds to a single large park. The single-large or several-small (SLOSS) debate was a practical realization of whether populations were better preserved in metapopulations or source-sinks (MacArthur and Wilson 1967, Diamond 1975). Today most of what ecologists would classify as pristine, natural habitat exists in a fragmented state. Agriculture and urban sprawl are primarily responsible for fragmenting that habitat, and if we are to effectively conserve small remnant populations, it is important to understand how the populations respond to landscape fragmentation patterns (Harrison and Bruna 1999).

It is tempting to classify a fragmented landscape as a source-sink or metapopulation simply on the size and frequency of habitat patches. Ecologists have recognized that there is

nuance in this description and landscapes are more likely to lie on a continuum with metapopulations and source-sinks acting as the extremes of a spectrum (Jackson et al. 2014). Whether or not populations exist as source-sinks or metapopulations, ecologists agree that dispersal between patches is necessary for long-term persistence. To insure proper dispersal, Perfecto et al. argue that the quality of the matrix connecting patches of remnant habitat must be improved (Perfecto et al. 2009). Often that improvement requires an increase in the complexity of the matrix, or in Elton's sense, incorporating some wilderness into agriculture and urban systems. As of yet however, there is no means to evaluate how permeable landscapes are as a whole for dispersing wildlife. In chapters four and five I challenge static representations of landscape structure by suggesting that the permeability of the matrix between habitat patches can very easily influence where populations lie on the continuum between metapopulation and source-sink. To test this hypothesis I developed a method for measuring permeability based on a universal scaling law between population means and variances known as Taylor's law. This law implies a power function relationship between population means and variances, which I use to interpret how organisms in a fragmented urban landscape perceive its structure. I first create this theoretical framework, and then apply it to survey data of aphids and their natural enemies in the city of Ann Arbor. In chapter five I confirm my expectations on how aphids perceive landscape structure via a population genetics study.

The first five chapters of this dissertation explore the biological and structural complexities of agriculture, but the last two chapters are reserved for agriculture's most complex feature: human management. In 1990, Luck manipulated the Lotka-Volterra equations to represent a biological control agent-pest system (Luck 1990). From this he developed what Arditi and Berryman would later refer to as the biological control paradox (Arditi and Berryman

1991). Much like the then popular paradox of enrichment, Luck showed that increasing the efficiency of control agents would have the counter-intuitive effect of decreasing its control over the pest. He showed that overexploitation by a control agent could cause boom-bust dynamics in the pest. Outbreaks emerge if specialized control agents decline after overexploiting pests. Thus, seemingly constructive changes in agricultural management to improve the efficiency of biological control agents (ie. improving habitat quality) could have unintentional effects on the stability of pest populations. Poor or misguided management choices like these, if reversible should have no large consequences for agriculture and the people whose livelihoods depend on it. Yet ecologists are increasingly recognizing that human-managed systems are prone to large and irreversible shifts in ecosystem states known as critical transitions (Scheffer 2009). The most famous example is the case of cod fisheries (Petrie et al. 2009). From the 1850s to the late 1980s cod fisheries had fairly consistent harvests of cod. Fisheries increased harvest rates at a steady rate over the years, until in 1992 cod populations suddenly collapsed. Despite efforts to reduce harvest rates to pre-collapse conditions, the cod did not rebound. The system experienced a critical transition from a high population to a low population equilibrium, two alternative stable states that exist at the same harvest rate. Which state the system was in, appeared not to depend on current harvest rates, but past ones. Here again is another concept of stability, the resilience of systems to change (McCann 2000). Ecologists have recently begun to acknowledge that alternative stable states are common: eutrophication of lakes, savannas to forest transitions, and healthy to bleached coral reefs are a few examples (Scheffer and Carpenter 2003, Scheffer 2009, Petrie et al. 2009, Hirota et al. 2011, Staver et al. 2011). These transitions are driven by changes in some "driver" variable: nutrient loads, precipitation or acidity for the examples above. In reality there are many potential interacting driver variables. Yet no studies have addressed how

interactions between driver variables may influence critical transitions. Instead ecologists tend to focus on detecting or preventing large transitions (Scheffer et al. 2012). The inherent irreversibility, or hysteresis, of these systems has received much less attention. In chapter six I explore how interactions between carrying capacity and growth rates of biocontrol agents can drive complex hysteretic patterns in equilibrium densities of pests. I discuss how management choices in agriculture can have large, complicated and irreversible consequences for pest control. In the final chapter, I extend the complex hysteretic framework I developed for biocontrol to soil-nutrient dynamics. Using a simple nutrient-soil feedback model, I ask how correlations between max nutrient recycling rates and loss rates may influence patterns of hysteresis when farmers transition from organic to conventional management and vice versa (Carpenter et al. 1999). Finally, I experimentally test whether agroecological transitions can cause hysteresis in crop yields and nutrient dynamics, and whether empirically derived patterns of hysteresis conform to theoretical predictions.

The aforementioned goal of this dissertation is to understand the feasibility of transitioning between conventional and agroecological alternatives that incorporate greater complexities. Taken together this dissertation carefully examines various features of biocomplexity and how its risks and benefits may be balanced to more effectively create agroecological alternatives.

Literature Cited

Allesina, S., and S. Tang. 2012. Stability criteria for complex ecosystems. Nature 483:205–208.

Andrewartha, H. G. 1954. The Distribution and Abundance of Aninmals: By HG Andrewartha and LC Birch. University of Chicago Press.

Andrewartha, H. G., and L. C. Birch. 1986. The ecological web: more on the distribution and abundance of animals. University of Chicago Press.

Arditi, R., and A. A. Berryman. 1991. The biological control paradox. Trends in ecology & evolution 6:32.

Bairey, E., E. D. Kelsic, and R. Kishony. 2016. High-order species interactions shape ecosystem diversity. Nature Communications 7:12285.

Carpenter, S. R., D. Ludwig, and W. A. Brock. 1999. Management of eutrophication for lakes subject to potentially irreversible change. Ecological Applications 9:751–771.

Diamond, J. M. 1975. The island dilemma: Lessons of modern biogeographic studies for the design of natural reserves. Biological Conservation 7:129–146.

Ehrlich, P. R., and L. C. Birch. 1967. The“ balance of nature” and“ population control.” The American Naturalist 101:97–107.

Elton, C., and M. Nicholson. 1942. The ten-year cycle in numbers of the lynx in Canada. The Journal of Animal Ecology:215–244.

Elton, C. S. 1958. The ecology of invasions by plants and animals. Methuen, London 18.

Gause, G. F. 1934. The Struggle for Existence. Courier Dover Publications.

Gause, G., N. Smaragdova, and A. Witt. 1936. Further studies of interaction between predators and prey. The Journal of Animal Ecology:1–18.

Giller, K. E., M. H. Beare, P. Lavelle, A.-M. N. Izac, and M. J. Swift. 1997. Agricultural intensification, soil biodiversity and agroecosystem function. Applied Soil Ecology 6:3–16.

Gotelli, N. J. 1991. Metapopulation Models: The Rescue Effect, the Propagule Rain, and the Core-Satellite Hypothesis. American Naturalist 138:768–776.

Grenfell, B. T., K. Wilson, B. F. Finkenstädt, T. N. Coulson, S. Murray, S. D. Albon, J. M. Pemberton, T. H. Clutton-Brock, and M. J. Crawley. 1998. Noise and determinism in synchronized sheep dynamics. Nature 394:674–677.

Hairston, N. G., F. E. Smith, and L. B. Slobodkin. 1960. Community structure, population control, and competition. The american naturalist 94:421–425.

Hanski, I., and M. Gilpin. 1991. Metapopulation dynamics: brief history and conceptual domain. Biological Journal of the Linnean Society 42:3–16.

Hanski, I., and O. Ovaskainen. 2000. The metapopulation capacity of a fragmented landscape. Nature 404:755–758.

Harrison, S., and E. Bruna. 1999. Habitat Fragmentation and Large-Scale Conservation: What Do We Know for Sure? Ecography 22:225–232.

Hastings, A. 1993. Complex interactions between dispersal and dynamics: lessons from coupled logistic equations. Ecology:1362–1372.

Hastings, A., C. L. Hom, S. Ellner, P. Turchin, and H. C. J. Godfray. 1993. Chaos in Ecology: Is Mother Nature a Strange Attractor? Annual Review of Ecology and Systematics 24:1–33.

Hirota, M., M. Holmgren, E. H. Van Nes, and M. Scheffer. 2011. Global resilience of tropical forest and savanna to critical transitions. Science 334:232–235.

Huffaker, C. B. 1958. Experimental studies on predation: Dispersion factors and predator-prey oscillations. Hilgardia 27:343–383.

Jackson, D., D. Allen, I. Perfecto, and J. Vandermeer. 2014. Self-organization of background habitat determines the nature of population spatial structure. Oikos 123:751–761.

Levins, R. 1969. Some Demographic and Genetic Consequences of Environmental Heterogeneity for Biological Control. Bulletin of the Entomological Society of America 15:237–240.

Lewis, W. J., J. C. van Lenteren, S. C. Phatak, and J. H. Tumlinson. 1997. A total system approach to sustainable pest management. Proceedings of the National Academy of Sciences 94:12243–12248.

Lorenz, E. N. 1963. Deterministic Nonperiodic Flow. Journal of the Atmospheric Sciences 20:130–141.

Lotka, A. J. 1978. The growth of mixed populations: Two species competing for a common food supply. Pages 274–286 The Golden Age of Theoretical Ecology: 1923–1940. Springer Berlin Heidelberg.

Luck, R. F. 1990. Evaluation of natural enemies for biological control: A behavioral approach. Trends in Ecology & Evolution 5:196–199.

MacArthur, R. H., and E. O. Wilson. 1967. The Theory of Island Biogeography. Princeton University Press.

May, R. M. 1972. Will a Large Complex System be Stable? Nature 238:413–414.

May, R. M. 1976. Simple mathematical models with very complicated dynamics. Nature 261:459–467.

May, R. M. 2001. Stability and Complexity in Model Ecosystems. Princeton University Press.

McCann, K., A. Hastings, and G. R. Huxel. 1998. Weak trophic interactions and the balance of. Nature 395:794–798.

McCann, K. S. 2000. The diversity–stability debate. Nature 405:228–233.

Murdoch, W. W. 1975. Diversity, complexity, stability and pest control. J. appl. Ecol 12:795–807.

Nicholson, A. J. 1933. Supplement: the balance of animal populations. The Journal of Animal Ecology:131–178.

Nicholson, A. J. 1954. An outline of the dynamics of animal populations. Australian journal of Zoology 2:9–65.

Nicholson, A. J., and V. A. Bailey. 1935. The Balance of Animal Populations.—Part I. Proceedings of the Zoological Society of London 105:551–598.

Perfecto, I., J. H. Vandermeer, and A. L. Wright. 2009. Nature's Matrix: Linking Agriculture, Conservation and Food Sovereignty. Earthscan.

Petrie, B., K. T. Frank, N. L. Shackell, and W. C. Legget. 2009. Structure and stability in exploited marine fish communities: quantifying critical transitions. Fisheries Oceanography 18:83–101.

Pimentel, D., U. Stachow, D. A. Takacs, H. W. Brubaker, A. R. Dumas, J. J. Meaney, D. E. Onsi, and D. B. Corzilius. 1992. Conserving Biological Diversity in Agricultural/Forestry Systems. BioScience 42:354–362.

Pimentel, D., R. Zuniga, and D. Morrison. 2005. Update on the environmental and economic costs associated with alien-invasive species in the United States. Ecological Economics 52:273–288.

Pulliam, H. R. 1988. Sources, Sinks, and Population Regulation. The American Naturalist 132:652–661.

Scheffer, M. 2009. Critical transitions in nature and society. Princeton University Press.

Scheffer, M., and S. R. Carpenter. 2003. Catastrophic regime shifts in ecosystems: linking theory to observation. Trends in Ecology & Evolution 18:648–656.

Scheffer, M., S. R. Carpenter, T. M. Lenton, J. Bascompte, W. Brock, V. Dakos, J. van de Koppel, I. A. van de Leemput, S. A. Levin, E. H. van Nes, M. Pascual, and J. Vandermeer. 2012. Anticipating Critical Transitions. Science 338:344–348.

Slobodkin, L. B., F. E. Smith, and N. G. Hairston. 1967. Regulation in terrestrial ecosystems, and the implied balance of nature. The American Naturalist 101:109–124.

Staver, A. C., S. Archibald, and S. A. Levin. 2011. The global extent and determinants of savanna and forest as alternative biome states. Science 334:230–232.

Vandermeer, J. H. 2010. The Ecology of Agroecosystems. Jones & Bartlett Publishers.

Vandermeer, J., I. Perfecto, and S. Philpott. 2010. Ecological Complexity and Pest Control in Organic Coffee Production: Uncovering an Autonomous Ecosystem Service. BioScience 60:527–537.

Volterra, V. 1927. Variazioni e fluttuazioni del numero d'individui in specie animali conviventi. C. Ferrari.

CHAPTER I

Coupling unstable agents in biological control

Theresa Wei Ying Ong & John H. Vandermeer

published in *Nature Communications*, 2015.

doi:10.1038/ncomms6991

1.1 Abstract

It has long been a goal of farm policy to manage production in such a way that expensive off-farm inputs and negative environmental consequences can be simultaneously minimized. One generalized philosophy that has gained currency in recent years is autonomous pest control, in which complex ecological interactions are encouraged to maintain the ecosystem in a state of permanence with the pest below economic thresholds. Early experience with biological control was hampered significantly by the inherent instability of many of the control agents, suggesting that pursuit of the autonomous strategy could be difficult. Here we show that combining two unstable two-dimensional systems (pest–predator and pest–pathogen) produces a stable three-dimensional system (pest–predator–pathogen) that is robust to perturbations in initial conditions. Contrary to expectations, the inclusion of negative interactions, which are arguably a necessary

consequence of increased complexity, can stabilize unstable conditions and rescue biological control of simpler, ineffective pest management systems.

1.2 Introduction

Charles Elton[1] first juxtaposed the striking stability of natural systems and the plagues of diseases and pests so common in agricultural systems in 1958. Since then, there have been many attempts to mimic such natural systems in agriculture by releasing natural enemies of pests as biological control agents to capture the control mechanisms that presumptively led to the stability of natural systems[2]. However, both in practice and theory, biological control was difficult to stabilize[3,4,5,6]. Generalist control agents often had non-target negative effects on other beneficial insects, whereas specialist control agents disappeared as their target pest resource was eliminated[7,8]. This often led to secondary resurgence of the pest once the agent was gone, followed by an inundation of the system with more agents as they disappeared—a very costly solution[9]. These practical issues mirrored debates in the theoretical literature. In the paradox of biological control, simple predator–prey theory was used to show that the most efficient control agents caused the most extreme pest outbreaks, since efficient agents overexploited resources and died quickly, allowing pests to resurge in great numbers while agent populations slowly recovered[5]. In another example, the Nicholson–Bailey model sparked controversy since its original form, which used difference equations to describe parasitoid–host interactions, was incapable of stable interactions, and only through extensive revisions incorporating complexities of host–parasite biology was it forced to do so[4].

One overarching theme that resulted from this work was that strong interactions tend to destabilize pest control. We define unstable to mean any pest population that becomes too

extreme or variable to be practical for a farmer. This is an assigned threshold beyond which damage caused by pests to crops become economically unsustainable[5,10]. Control agents are often designed to strongly inhibit pest growth, yet these kinds of strong consumer–resource interactions are often themselves, unstable[5,11]. Most recently, theoretical work utilizing food web modules have found that weak predator–prey interactions can help stabilize unstable systems[12]. These models show that unpredictable, chaotic dynamics can be dampened into stable equilibria by the imposition of a stable consumer–resource interaction[12]. However, since agricultural pests are defined by their propensity for unstable growth, and pests remain a major agricultural problem, it stands to reason that unstable interactions between pests and natural enemies are more common[13]. However, the question of whether two unstable interactions can be combined to produce stability has yet to be asked. If possible, then a diverse assemblage of separately unstable control agents could be combined to create a functional pest management programme, reminiscent of the stability that Elton first noticed in natural systems[1].

In addition, there has always been a disjunction between the theory of competitive exclusion and the coexistence of multiple competing natural enemies in nature that has been explained, in recent literature, through mechanisms of species complementarity, where enemies split a shared resource into separate niches, thus preventing direct competition[14]. Although there exists strong evidence that complementarity between diverse assemblages of organisms (mostly grasses and so on) may lead to stability of ecosystems in the biodiversity–ecosystem function literature, empirical evidence for complementarity in biological control is not abundant[15,16,17]. Many positive effects of natural enemy diversity on biological control are reported, but evidence tends to favour sampling effects from one strong control agent, or insurance effects where many redundant enemies buffer systems from rapid changes in the environment[16,17,18,19,20,21]. In contrast,

competition over shared resources and predation among natural enemies (intraguild predation (IGP)) are very common but almost automatically suspected of impairing biological control in empirical work and coexistence in theoretical models[16,17,22,23,24,25,26]. However, proponents of autonomous biological control argue that these same negative interactions are a natural consequence of a complex network of multiple natural enemies, and may actually help suppress pest problems by acting as a system of checks and balances limiting overexploitation by any one enemy—essentially reconciling the disjunction[27,28].

To the extent studied thus far, all herbivores are attacked by both predators/parasitoids and pathogens[26,29,30,31,32], suggesting that any system of autonomous control will automatically contain this duality of control factors. Thus, we investigate the controlling effects of first a pathogen, then a predator and finally their combination. Recently, scientists have encouraged the utilization of predators and pathogens in biological control, arguing that facilitation is more likely than competition because of differences in size, life cycles and modes of attack[29]. However, in cases where pathogens and predators are not separated by space or time, we argue that the potential for strong negative interactions is high, especially considering the evidence of non-target effects by generalist pathogens on other competing natural enemies, primarily predators[26,31]. Although studies more frequently report cases of IGP between predators, the prevalence of coexisting disease and predator control agents suggests that predators must engage in IGP with pathogens whenever they happen to consume infected prey[17,30,31,32]. We argue that in cases where infection of hosts is widespread or latent for long periods of time[33], prey choice becomes limited for predators, making IGP more likely[30]. One well-documented example is the predation of pests that harbour developing parasitoids[32]. The same argument can be made for developing fungal spores within pests, although few have attempted to test this question[30,31]. Currently, IGP is

generally considered a hindrance to biocontrol efforts, and is often used as a default explanation for non-significant or negative relationships between diversity of control agents and biocontrol[16,18,19,20,22,23], while in the theoretical literature IGP is presented as a hindrance to competitive coexistence by seeming on the surface to lead to exclusion of the intraguild prey[17,24,25,26].

In consideration of the strong negative interactions that may occur among control agents used in tandem for biological control, we combine standard Rosenzweig/MacArthur[34] and epidemic models[35] following examples in the mathematical biology literature[36,37,38,39,40,41,42] and modify them to determine whether combining two ineffective control agents (ineffective in the sense that pests remain permanently in an outbreak mode) through strong competition over a shared resource and IGP can rescue control. We find that stability can indeed be rescued, forcing us to reassess current generalizations on the effects of strong negative interspecific interactions on ecosystem stability.

1.3 Results

Model justification

In agricultural systems where crops are carefully managed, resources are rarely limiting for pests since most pest-control strategies are enacted before crop yields drop to the point where pests experience density dependence[10]. We therefore retain density independence on the prey, since we are concerned with the alternate control by disease or predator, not with some form of bottom up or otherwise control (which would be implied by including the customary 'carrying capacity' of the prey). However, in acknowledgement of the fact that competitive exclusion between the control agents is inevitable without some form of nonlinearity[43,44,45], we instill

density dependence on the predator following the example of a previous predator–prey model[46]. We choose to impose density dependence on the predator rather than the pathogen by reasoning that non-food resources such as space or nesting habitat are more likely limited in predators than pathogens due to size alone (Methods).

Thus we begin with a model where both the disease (Methods, equations (1a) and (1b)) and predator (Methods, equations (2a) and (2b)) acting alone are able to control the pest, but where the pest can, under certain circumstances, escape control from either agent (Fig. 1b,d). We take control and stability to mean any pest population that ultimately coalesces to some constant or oscillating size consistently below pest tolerance thresholds (Fig. 1a,c)[10]. For our purposes, we set tolerance thresholds to a value of 500 susceptible pest individuals after 10,000 generations. Although the specific threshold is arbitrary, the long timescale allows us to see whether populations ultimately tend towards ∞, $-\infty$ (unstable) or consistently remain within biologically realistic values (stable).

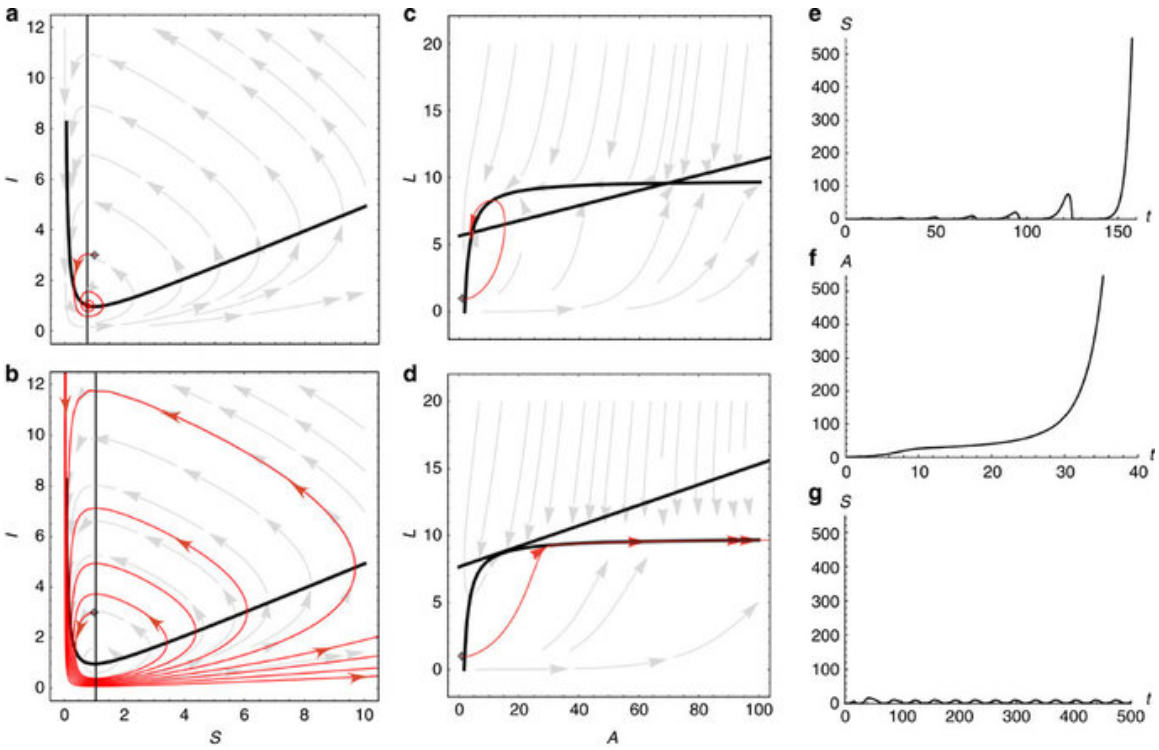

Figure 1.1 Taking unstable conditions to stable ones. Pest individuals (*S* or *A*) plotted against enemy individuals (*I*-pathogen or *L*-predator) yield phase portraits of example (a) stable and (b) unstable dynamics for subsystem 1: pathogen–pest and (c) stable and (d) unstable dynamics for subsystem 2: predator–pest. Dark black lines are zero growth isoclines, grey arrows indicate the vector field and red arrows are exemplary trajectories from initial conditions indicated by a grey dot. Corresponding time series plots for unstable subsystems 1 (e) and 2 (f), and the result of combining e and f to produce (g) system 3 (pathogen–predator–pest). The parameter values are: r=0.46, $\alpha 1$=0.9, $\alpha 2$=0.06, $\beta 1$=1, $\beta 2$=0.01, $m1$=0.47, $m2$=0.1, K=10 and ε=0.8, and the initial conditions are $S0$=1, $I0$=3 and $L0$=1 r is the per capita growth rate of the pest, $\alpha 1$ and $\alpha 2$ are the attack rates of the pathogen and the predator, respectively, $\beta 1$ and $\beta 2$ are the handling times of the pathogen and predator, respectively, $m1$ and $m2$ are the mortality rates of the pathogen and predator, respectively, K is the carrying capacity of the predator and ε is the conversion rate of infected prey consumed to predators produced.

Destabilizing the control agents

In the case of the pathogen, loss of control, instability, is characterized by boom-bust dynamics in the pest, where the booms and busts grow in magnitude with each passing cycle until reaching some large limit much beyond tolerance thresholds (Fig. 1.1b,e). In the case of the predator, instability is characterized by exponential growth of the pest once the predator reaches

its carrying capacity K, a non-renewable resource that limits predator growth due to intraspecific competition, that is, space or nesting habitat (Fig. 1.1d,f)[46]. Both kinds of dynamics are classic representations of instability in theoretical ecology[5,44,47]. Fortunately, the dynamic simplicity of our model creates clear boundaries for stable and unstable dynamics (instability criteria indicated in Methods), and allows us to dictate when control is lost (unstable) by manipulation of a few key parameters. We find that to destabilize the pathogen, we can reduce the rate at which pathogens infect susceptible pests—the attack rate ($\alpha 1$), increase the natural mortality rate of the pathogen ($m1$) or increase the time required for an infection to kill the host pest—the handling time ($\beta 1$) (Methods, equation (6)). To destabilize the predator, we can increase the rate at which the pests grow (r), decrease the amount of nesting habitat or space for the predator—the carrying capacity (K), decrease the rate at which predators attack pests ($\alpha 2$) or increase the time required for an individual predator to find, kill and consume one pest—the handling time ($\beta 2$) (Methods, equation (9)). Note that in both cases, instability (and thus pest outbreak) occurs when the control agent is weakened.

We then take these two weak, unstable control agents, and further weaken them by coupling the two systems through exploitative competition over a shared susceptible pest resource and IGP (predator consumes healthy pests, infected pests and the pathogens inside the infected pests) (Methods, equations (3a)–(3c)). We find that there indeed exist conditions where coupling two unstable control agents through negative interactions leads to stable coexistence of the two control agents and rescue of biological control (Fig. 1.1e–g). Healthy pest populations are markedly reduced when the control agents are combined and can remain at these low, stable equilibria for long timescales (Fig. 1.1e–g). Recall that to create instability the control agents were first weakened. Thus, it is reasonable to expect that the combination of two weak control

agents could rescue control, corresponding to well-known notions of species complementarity[14,15,16]. However, what is especially interesting is that control is rescued in spite of strong negative interactions imposed by IGP and the inherent competition that occurs when multiple agents share a resource (Methods, equations (3a)–(3c)). It is important to note that previous theoretical work has already shown that weak, stable consumer–resource interactions can help dampen chaotic oscillations that result from strong consumer–resource interactions[11,12]. When formulated so that one or both control-agent–pest pairs are stable to begin with, our models reproduce this same result (see Supplementary Figs 1 and 2). However, here we take the issue one step further by showing that stability can be rescued even when each component system is unstable to begin with, and even when strong negative interactions are used to couple the unstable components (Fig. 1.1e–g).

Stability hotspots

We constrained parameter values to biologically realistic values for rates, such that control-agent attack rates, handling times and mortality rates were $0<\alpha 1, \alpha 2, \beta 1, \beta 2, m1, m2<1$, then overlaid regions of parameter space where each of the independent subsystems were unstable based on the instability criteria calculated in Methods (equations (6) and (9); Fig. 1.2a–c). We strategically sampled values within each zone, paired them and determined the stability of the resulting complex system (Fig. 1.2d, see Methods). We found that parameter values on the edges of the instability regions for each independent control agent were most likely to be tipped into stable control when the two agents were combined; 9 out of 10 successful parameter combinations included at least one edge set (P=0.021, n=10, exact binomial test) (Fig. 1.2d). Increased sampling specifically for edge values revealed 13 additional successful combinations

(Fig. 1.2d, see Methods). Rescue of stability was heavily dependent on parameter sets that included predators with low handling times; 13 out of 13 successful parameter combinations involved an edge where $\beta 2 \rightarrow 0$, ($P<0.001$, $n=13$, exact binomial test) (Fig. 1.2d). Low handling times allow the predator to quickly consume both healthy and infected pests, reducing pathogen densities through competition and IGP, respectively. In this way, the predator is able to prevent the pathogen from ever becoming an epidemic and overexploiting the pests, effectively damping the unstable oscillations of the pathogen subsystem (Fig. 1.1).

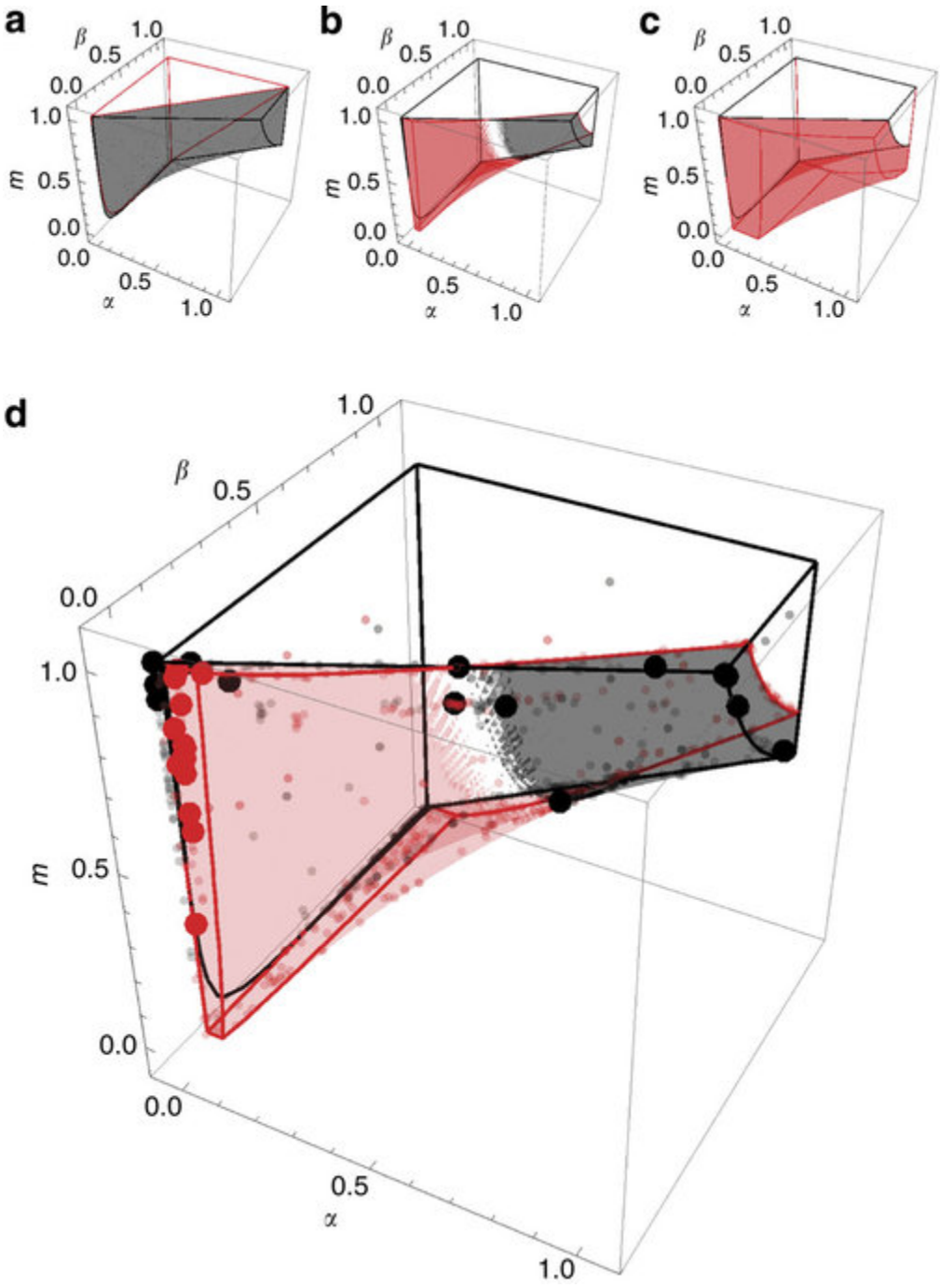

Figure 1.2 Sampling of instability regions. Regions of three-dimensional parameter space that satisfy instability criteria for subsystem 1: pathogen–pest (black outline) (6), and subsystem 2: predator–pest (red outline) (9) overlaid. Control-agent attack rates (α), handling times (β) and mortality rates (m) are varied on each axis under conditions of (a) low r or high K (r=0.0001, K=10) or (r=0.46, K=6,000), (b) medium r and K (r=0.46, K=10) and (c) high r or low K (r=0.99, K=4.5) or (r=0.46, K=2). r is the per capita growth rate of the pest, and K is the carrying capacity of the predator. Black-shaded region corresponds to parameter space where the pathogen is competitively dominant over the predator and the red-shaded region corresponds to parameter

space where the predator is dominant over the pathogen based on parameter values of α, β and m. (d) Strategically sampled unstable parameter sets for the pathogen (black dots) and predator subsystems (red dots) in the medium r and K scenario. Larger dots represent unstable pathogen (black) and predator (red) parameter sets that successfully rescued stability in the combined, complex model (ε=0.8, conversion rate of infected pests into predator abundance).

Relative strengths of agents

By further adjusting the remaining parameters, pest growth rate (r) and predator carrying capacity (K), we note that there are only three general scenarios: the instability region of the predator is always underneath the instability region of the pathogen (Fig. 1.2a), the instability regions of each control agent overlap the other in some portion of phase space (Fig. 1.2b) and the instability region of the predator always overlaps the instability region of the pathogen (Fig. 1.2c). Considering that values on the edges of instability regions are more likely to rescue control, and larger instability regions extend towards higher attack rates, lower handling times and lower mortality rates (generally implying stronger control agents), the biological interpretation of these three scenarios are: the pathogen always beats the predator (Fig. 1.2a), equal competition (Fig. 1.2b) and the pathogen always loses to the predator (Fig. 1.2c). We know that rescue of stability is highly dependent on values near the edge of the predator instability region where $\beta 2 \rightarrow 0$ (Fig. 1.2d), and notice that this stability-inducing edge first appears when there is equal competition, and grows larger as the strength of the predator over the pathogen increases (Fig. 1.2a–c). The predator must effectively keep the pathogen from becoming an epidemic to rescue control, thus only the scenarios where there is equal competition between predator and pathogen or the predator always wins results in the rescue of biological control (Fig. 1.2b,c). We note that this can be achieved by increasing the growth rate of the pest (r) or decreasing the carrying capacity of the predator (K), which causes the instability region of the predator to increase in size, overlap the instability region of the pathogen and reveal the $\beta 2 \rightarrow 0$ edge that is so necessary in limiting

the pathogen and rescuing control of the pest (Fig. 1.2). Because the size of the $\beta 2 \rightarrow 0$ edge increases as the dominance of the predator over the pathogen increases, so too should the probability of successfully rescuing stability.

Intraspecific versus interspecific competition

One of the few general laws in ecology derived from the original Lotka–Volterra competition models suggests that intraspecific competition may need to be greater than interspecific competition if multiple enemies are to coexist in a biological control programme8. In our model, we implemented a carrying capacity in our predator to represent intraspecific competition over a non-renewable resource such as nesting habitat. The predator subsystem becomes unstable and loses control of the pest when nesting habitat is more limiting than pest resources, or when intraspecific competition is high. When the pathogen is introduced, strong competition over pests prevents the predator from reaching carrying capacity while also preventing the pathogen from overexploiting pests. This implies that interspecific competition becomes greater than intraspecific competition, yet coexistence is maintained. Although our model is based largely on the original Lotka–Volterra equations[44], beginning with unstable components leads us to conclude that coexistence is maintained when interspecific competition is greater than intraspecific, the exact opposite of the classical outcome.

Strength of IGP

We note that our analysis here is not an exhaustive search of parameter space, but is intended to show the potential for stability to result spontaneously from the coupling of unstable components. By analysing each component system separately and keeping all parameters

constant when combined, we can confidently assert that each system begins as a purely unstable unit, and that stability arises solely from the negative interactions that couple the independent units together. We refrain from adjusting parameters post combination, because doing so would alter the initial stability of the component systems. Our analysis is therefore constrained to parameters that are unique to the combined system, the only one being the conversion rate of infected pests into predator offspring (ε) (Methods, equations (3a)–(3c)).

The cost of IGP (consumption of infected pests) to the predator is controlled by the parameter ε. Since the conversion rate of healthy pests into predator abundance is set to 1, an ε value <1 implies that the predator produces fewer offspring when consuming infected rather than healthy prey (Methods, equations (3a)–(3c)). We justify this by the fact that infected prey are less healthy by definition and arguably less nutritious, especially if predators are themselves susceptible to infection7,26. Time series data for varying ε show the existence of two major attractors, one where the peak abundances of predator and pathogen are synchronous (Fig. 1.3a,b,d) and one where they are asynchronous (Fig. 1.3c,e). The model is set up such that the predator consumes both uninfected/susceptible (S) and infected pests (I) with a constant attack rate ($\alpha 2$). At very low ε values, consumption of infected pests contributes little to predator recruitment, essentially acting like empty calories. Although the predator does not distinguish between healthy and infected pests directly, its population growth depends mainly on the number of healthy pests available, thus as the healthy pest population grows, so does the predator population. This results in synchrony between the predator and pathogen populations, since both depend primarily on healthy pests for recruitment. We call this the pathogen-dominant attractor, since the pathogen exerts a strong negative effect on the predator by reducing predator recruitment, and the dynamics mimic the cyclic instability of the pathogen-only subsystem (Figs

1.1b and 1.4a). As ε values approach 1, consumption of infected pests and healthy pests become equally important for predator recruitment. This causes the predator to synchronize with both healthy and infected pest populations, and a resulting asynchrony between predator and pathogen populations (Fig. 1.4a). We call this the predator-dominant attractor since there is almost no cost of IGP to the predator. By adjusting initial conditions and overlaying the resulting bifurcation plots, we can visualize the two interwoven attractors and see clear signs of hysteresis[48,49], where position on one or the other attractor depends on the initial conditions of the system (Fig. 1.5). A shift from one attractor to the other could result in a sudden increase in pest numbers resembling a regime shift, but this would only be considered a pest outbreak if pest tolerance thresholds were set particularly low (~11 for Fig. 1.5)[49]. It is important to note that for all of these simulations, the susceptible pest population remains bound to a very low range of possible values that are much below our original threshold of 500. This implies that the rescue of control from the combination of unstable agents is robust to perturbations in initial conditions and epsilon (Fig. 1.5). In other words, stability is robust.

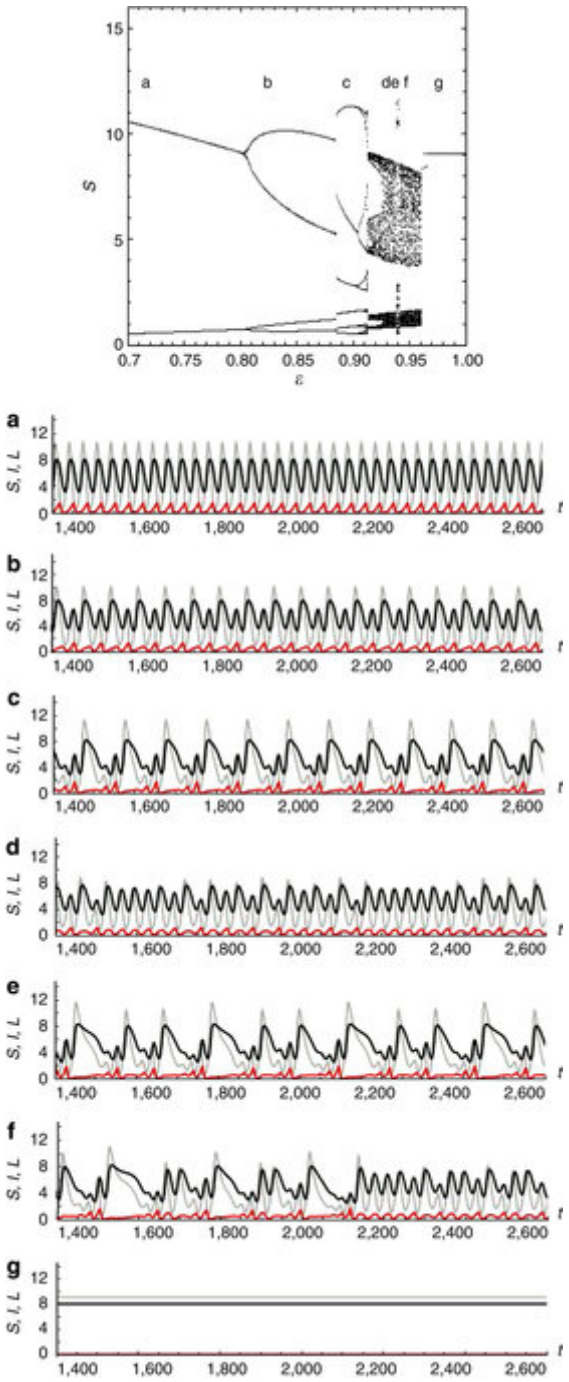

Figure 1.3 Symmetric and asymmetric dynamical behaviour. Bifurcation diagram for conversion rate parameter ε in system 3 varied from 0.70 to 1.00 evaluated for equilibrium values of the susceptible pest population S, and corresponding time series graphs plotted for (a) ε=0.70, (b) 0.85, (c) 0.90, (d) 0.93, (e) 0.94, (f) 0.96 and (g) 1.00. Grey lines are number of susceptible pests S, black lines are predators L and red lines represent infected pests or pathogens I. In a, b and d behavior is symmetric (pathogen dominant), in c and e asymmetric (predator dominant) and f mixed. All other parameter values are: r=0.46, α1=0.9, α2=0.06, β1=1, β2=0.01, m1=0.47, m2=0.1 and K=10, and the initial conditions are S0=1, I0=3 and L0=1. r is the per

capita growth rate of the pest, $\alpha 1$ and $\alpha 2$ are the attack rates of the pathogen and the predator, respectively, $\beta 1$ and $\beta 2$ are the handling times of the pathogen and predator, respectively, $m1$ and $m2$ are the mortality rates of the pathogen and predator, respectively and K is the carrying capacity of the predator.

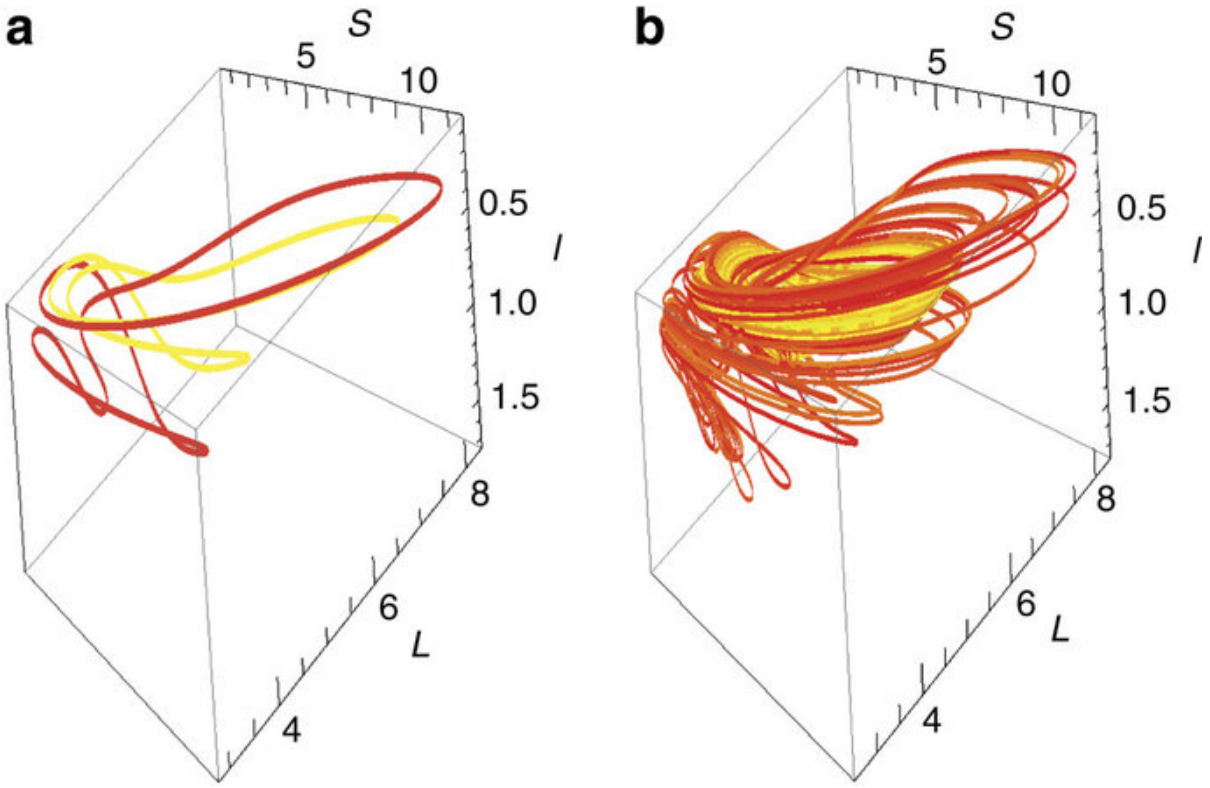

Figure 1.4 Component and combined chaotic attractors. Pest abundance (S) plotted against pathogen (I) and predator abundance (L) yields three-dimensional phase portraits for system 3 of a, two main attractors overlaid; symmetric, pathogen-dominant (yellow, ε=0.85), asymmetric, predator-dominant (red, ε=0.90), and b, chaotic attractor (ε=0.959) where colour is a function of position in phase space. All plots made using data from t=5,000 to 10,000. Other parameter values are: r=0.46, $\alpha 1$=0.9, $\alpha 2$=0.06, $\beta 1$=1, $\beta 2$=0.01, $m1$=0.47, $m2$=0.1 and K=10, and the initial conditions are $S0$=1, $I0$=3 and $L0$=1. r is the per capita growth rate of the pest, $\alpha 1$ and $\alpha 2$ are the attack rates of the pathogen and the predator, respectively, $\beta 1$ and $\beta 2$ are the handling times of the pathogen and predator, respectively, $m1$ and $m2$ are the mortality rates of the pathogen and predator, respectively, K is the carrying capacity of the predator and ε is the conversion rate of infected prey consumed to predators produced.

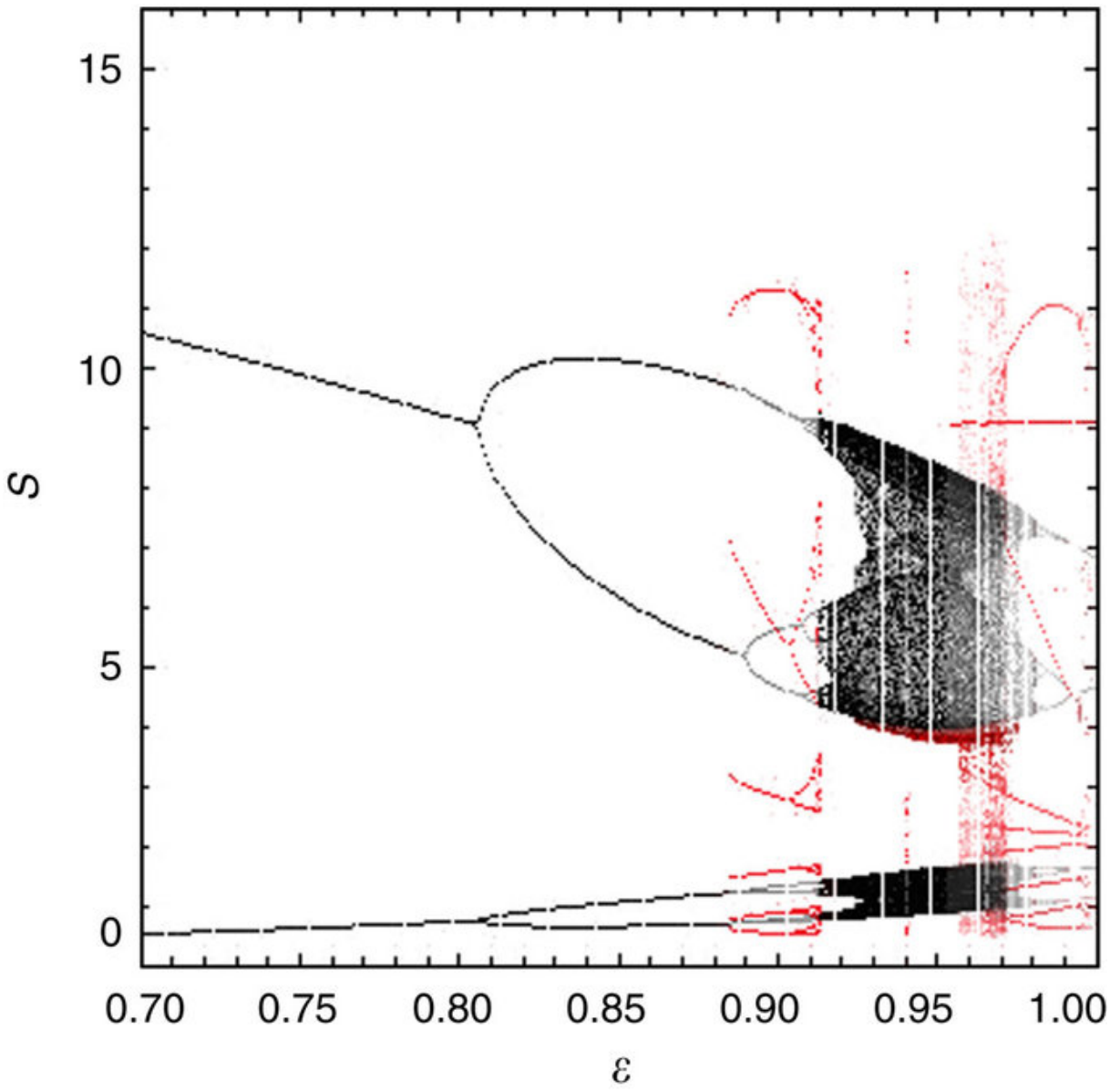

Figure 1.5 Robust stability shown through bifurcation overlays. Conversion rate parameter ε in system 3 is varied from 0.70 to 1.00 and evaluated for equilibrium values of the susceptible pest population S. Overlay of 21 bifurcation diagrams plotted at 10% opacity, each initiated under different initial conditions and all other parameters kept constant. Putative predator-dominant attractor in red, pathogen-dominant attractor in black. Initial conditions ranged from $S0$: 3 to 18, $I0$: 4 to 10 and $L0$: 11 to 13, chosen to reveal as much of each attractor as possible. The parameter values are: r=0.46, $\alpha 1$=0.9, $\alpha 2$=0.06, $\beta 1$=1, $\beta 2$=0.01, $m1$=0.47, $m2$=0.1 and and K=10. r is the per capita growth rate of the pest, $\alpha 1$ and $\alpha 2$ are the attack rates of the pathogen and the predator, respectively, $\beta 1$ and $\beta 2$ are the handling times of the pathogen and predator, respectively, $m1$ and $m2$ are the mortality rates of the pathogen and predator, respectively, K is the carrying capacity of the predator and ε is the conversion rate of infected prey consumed to predators produced.

At some values of ε in the predator–pathogen–pest system, trajectories may take the form of a complicated strange attractor, a bounded region from which all trajectories trace unique paths (Fig. 1.4b). Within the chaotic window, marked in the bifurcation plot as a dark band of infinitely many possible positions in phase space (Fig. 1.5), we observe a strange attractor that switches between two modes reflecting the basic behaviour of the two attractors previously described (Fig. 1.3f). Thus, the strange attractor has three distinct phases: predator-dominant, pathogen-dominant and a phase that appears to be switching between the two (Fig. 1.4). As each enemy appears to struggle to gain superiority over the shared resource, victory is always short-lived since both systems are unstable on their own. The winner always loses its advantage to the competitor, and the cycle repeats.

Our formulation of system 3 assumes that the predator satiates at a rate dependent on the number of all prey available (type II functional response, typical for describing predators[50]), with no discretion between infected or healthy prey (Methods, equations (3a)–(3c)). We note that altering the functional response of the predator so that it can distinguish infected and healthy prey simplifies the system such that the chaotic region shrinks, but the qualitative behaviour of rescuing stability remains the same (Supplementary Fig. 3). We formulated the pathogen with a type III functional response[50] to be indicative of a pathogen within a spatially distributed population, where disease transmission is low when the host population is low and/or highly dispersed (since contact among individuals will be low) and transmission rapidly reaches some upper limit at high population densities once a critical density of hosts accumulates (Methods, equations (1a) and (1b)). Converting the functional response of the pathogen from type III to type II has similar consequences (Supplementary Figs 4 and 5). It is also important to note that we can eliminate IGP and still rescue stability (Supplementary Fig. 6), but the negative effects of

competition over the shared resource can never be removed and thus are an inherent part of stabilizing system 3, making these results robust.

When considering the efficiencies of two competing enemies simultaneously, we note that when the efficiency of one enemy is high the other must be low. In both the predator-dominant and pathogen-dominant attractors, the susceptible pest population peaks become more extreme as the negative effect of one enemy on the other increases. The paradox of biological control[5] (where attempts to increase efficiency of control may lead to the loss of biological control) occurs at both extremes, whether the predator (high ε) or the pathogen (low ε) is most efficient. The smallest oscillations occur at intermediate ε values in the chaotic region, when the efficiencies of the two competitors are more or less equal, and neither enemy has a competitive advantage over the other (Fig. 1.5). If as is usually the case, the goal of management is to eliminate outbreaks, these results imply that strong, but fairly matched competition between enemies can help by minimizing pest population maximums.

1.4 Discussion

Thus, coupling two unstable systems with negative interactions has the counter-intuitive result of rescuing stability, creating a stable, more diverse system. Although usually suspected of hindering biological control and competitive coexistence, our results show potential for IGP and competition over shared resources to prevent outbreak dynamics and take unstable conditions to stable ones. In general, we found that strong interspecific competition can act as a stabilizing force if we begin with unstable components. These results can be tested empirically using laboratory populations of pests and control agents previously determined to be ineffective

singularly. The overabundance of competitors and IGP in systems with effective autonomous biological control has always been difficult to explain, given the standard theory[1,2,3,4,5,6,7,27,28]. Here, we suggest that the prevalence of these negative interactions between diverse assemblages in nature may in fact contribute to the consistent and stable level of natural control found in many undisturbed ecosystems[3,27,28,30,51]. We add that evidence in favour of sampling effects from one strong natural enemy[16,17,18,19,20] are curiously also consistent with dominance hierarchies among competing enemies. An understanding of the stability of component parts apart from the system as a whole may be a necessary prerequisite to determining the consequence of strong negative interactions within complex networks.

1.5 Methods

Model specifications

Subsystem 1: pathogen–pest two-dimensional system based on the modified epidemic model35, where S is the number (not proportion) of susceptible pest individuals, I is the number of pest individuals infected by the pathogen and $\phi = \frac{S}{1+\beta_1 S^2}$, a Holling type III functional response50.

$$\frac{dS}{dt} = rS - \alpha_1 SI\phi \qquad (1a)$$

$$\frac{dI}{dt} = \alpha_1 SI\phi - m_1 I \qquad (1b)$$

Subsystem 2: predator–pest two-dimensional system of equations based on the modified Rosenzweig/MacArthur model34 altered to include density dependence on the predator46, where

the predator is L (lady beetles), prey/pest is A (aphids), $\theta = \frac{1}{1+\beta_2 A}$, a Holling type II functional response50 and K is the carrying capacity of the predator, a non-renewable resource such as space or nesting habitat46.

$$\frac{dA}{dt} = rA - \alpha_2 AL\theta \qquad (2a)$$

$$\frac{dL}{dt} = \alpha_2 AL\theta\left(\frac{K-L}{K}\right) - m_2 L \qquad (2b)$$

For these models, r is the per capita growth rate of the pest, $\alpha 1$ and $\alpha 2$ are the attack rates of the pathogen and the predator, respectively, $\beta 1$ and $\beta 2$ are the times necessary for the pathogen and predator, respectively, to search, kill, eat and otherwise handle one pest and $m1$ and $m2$ are the mortality rates of the pathogen and predator, respectively.

System 3: combined pathogen–predator–pest three-dimensional system of equations, derived from $A=S+I$:

$$\frac{dS}{dt} = rS - \alpha_1 SI\phi - \alpha_2 SL\theta \qquad (3a)$$

$$\frac{dI}{dt} = \alpha_1 SI\phi - \varepsilon\alpha_2 IL\theta - m_1 I \qquad (3b)$$

$$\frac{dL}{dt} = \alpha_2 (S+\varepsilon I)L\theta\left(\frac{K-L}{K}\right) - m_2 L \qquad (3c)$$

The parameter ε is the conversion rate of infected pests into predator abundance. Since the conversion rate of healthy pests into predator abundance is effectively 1, when $\varepsilon<1$, there is a reproductive cost to engaging in IGP for the predator.

Stability analysis

Subsystem 1: the pathogen (4a) and pest (4b) isoclines, where each respective population is at equilibrium or $dI/dt=0$ and $dS/dt=0$ are as follows:

$$S = \sqrt{\frac{m_1}{\alpha_1 - \beta_1 m_1}} \qquad (4a)$$

$$I = \frac{r(1+\beta_1 S^2)}{\alpha_1 S} \qquad (4b)$$

There exists one non-zero equilibrium point where the two isoclines overlap. The arrangement of the isoclines dictates whether this equilibrium point is stable or unstable, and in practical terms whether there is control or no control of the pest (equivalent to the classic ideas of epidemic or not). As the pathogen (*I*) isocline becomes greater than the inflection point of the pest isocline (5, Fig. 1b), the equilibrium point goes from exhibiting stable damped cycles to limit cycles of ever-increasing magnitudes.

$$\sqrt{\frac{m_1}{\alpha_1 - \beta_1 m_1}} > \sqrt{\frac{1}{\beta_1}} \qquad (5)$$

Rearranging (5) gives the following instability criteria for subsystem 1 (6), which can be achieved by reducing either the attack rate of the pathogen or increasing its mortality rate or handling time.

$$\frac{\alpha_1}{\beta_1 m_1} < 2 \qquad (6)$$

Subsystem 2: the predator (7a) and pest (7b) isoclines, where dL/dt, $dA/dt=0$ are:

$$L = \frac{K(\alpha_2 A - \beta_2 m_2 A - m_2)}{\alpha_2 A} \qquad (7a)$$

$$L = \frac{r\beta_2}{\alpha_2} A + \frac{r}{\alpha_2} \qquad (7b)$$

There are two non-trivial equilibrium points where these isoclines overlap in positive space: one a stable point attractor exhibiting oscillatory behaviour and the other an unstable point repellor placed on a separatrix delimiting two basins of attraction (8) (Fig. 1c).

$$(A^*, L^*)_{1,2} = \left(\frac{\alpha_2 K - \beta_2 m_2 K - r \pm \sqrt{-4\beta_2 m_2 r K + (r + \beta_2 m_2 K - \alpha_2 K)^2}}{2\beta_2 r}, \frac{\alpha_2 K - \beta_2 m_2 K + r \pm \sqrt{-4\beta_2 m_2 r K + (r + \beta_2 m_2 K - \alpha_2 K)^2}}{2\alpha_2} \right) \quad (8)$$

A blue-sky bifurcation occurs when the slope or *y*-intercept of the pest isocline (7b) is increased such that the two equilibrium points collide (Fig. 1d), creating a half-stable point that eventually disappears 'into the clear blue sky'47. By setting the two equilibrium points equal to each other we can determine this exact point as the instability criteria for subsystem 2:

$$\frac{\alpha_2 K - \beta_2 m_2 K - r}{\sqrt{\beta_2 m_2 K r}} < 2 \quad (9)$$

Thus, increasing the growth rate of the pest r, lowering the carrying capacity of the predator K, increasing the handling time of the predator $\beta 2$ or decreasing the attack rate of the predator $\alpha 2$, can destabilize subsystem 2. All trajectories beyond this point are unstable as the predator reaches carrying capacity, and the pest continues to grow exponentially (Fig. 1d).

Model testing

Parameter sets for single control-agent components (subsystems 1 and 2) were strategically sampled within the instability regions calculated (equations (6) and (9)). Unstable parameter sets were then paired in the full model, system 3 (equations (3a)–(3c), ,), and resulting stability examined using time series data and bifurcation plots. All simulations where susceptible pest populations (S) were below a tolerance threshold of 500 individuals and neither predator, pathogen nor pest was eliminated after 10,000 time steps were considered stable.

Strategic sampling

To efficiently sample the unstable phase space of each control agent, 10 random parameter sets were pulled from (1) the entire instability region, (2) the edges bordering stability of the instability region (approaching the limits of the instability criteria—equations (6) and (9)) and (3) the region of the instability region that overlapped the instability region of the other control agent, which we will refer to as the dominant region. Predator parameter sets were fully crossed with pathogen sets, producing a total of 900 parameter combinations. Each of these parameter combinations was simulated for 10,000 time steps, and stability assessed for each. From the 10 successful combinations found, probability of rescuing stability based on region specificity was calculated using binomial exact tests.

To refine which edges were important for rescuing stability, we separated the instability regions of each control agent into the six edges that border stability. These edges correspond to parameters approaching extreme values: $\alpha 1,2 \rightarrow 1$, $\beta 1,2 \rightarrow 1$, $\beta 1,2 \rightarrow 0$, $m1,2 \rightarrow 1$, $m1,2 \rightarrow 0$, and the surface edge between unstable and stable regions where no particular parameter is at an extreme. Fifty additional parameter sets were randomly selected from each of the five extreme edges, and 100 from the surface edge for each control agent. The predator and pathogen parameter sets were then randomly matched, resulting in 350 total combinations. Each of these parameter sets was simulated, stability assessed and the probability of rescuing stability based on edge specificity calculated using binomial exact tests.

Parameterization

The parameter values for all plots are: r=0.46, $\alpha 1$=0.9, $\alpha 2$=0.06, $\beta 1$=1, $\beta 2$=0.01,

$m1$=0.47, $m2$=0.1, K=10 and ε=0.8, and the initial conditions are $S0$=1, $I0$=3 and $L0$=1, unless otherwise noted. r is the per capita growth rate of the pest, $\alpha 1$ and $\alpha 2$ are the attack rates of the pathogen and the predator, respectively, $\beta 1$ and $\beta 2$ are the handling times of the pathogen and predator, respectively, $m1$ and $m2$ are the mortality rates of the pathogen and predator, respectively, K is the carrying capacity of the predator and ε is the conversion rate of infected prey consumed to predators produced.

Bifurcation plots

To examine the effects of variables of interest (ε, f) on system dynamics, models were run for 10,000 time steps, and population peaks estimated where the first derivative of the dynamical variable of interest (in most cases, S, the susceptible pest population) was naught. To remove transience, the last 20% of values were plotted for all bifurcations.

Additional information

How to cite this article: Ong, T. W. and Vandermeer, J. H. Coupling unstable agents in biological control. *Nat. Commun.* 6:5991 doi: 10.1038/ncomms6991 (2015).

1.6 References

1.Elton, C. S. The ecology of invasions by plants and animals. *Methuen London* (1958).

2.Huffaker, C. B., Messenger, P. S. & DeBach, P. in*Biological Control* ed. Huffaker C. B. 16–67Springer (1971) at http://dx.doi.org/10.1007/978-1-4615-6528-4_2.

3.Murdoch, W. W. Diversity, complexity, stability and pest control. *J. Appl. Ecol.* 12, 795–807 (1975).

4.Nicholson, A. J. & Bailey, V. A. The balance of animal populations—part I. *Proc. Zool. Soc. London* 105, 551–598 (1935).

5.Luck, R. F. Evaluation of natural enemies for biological control: A behavioral approach. *Trends Ecol. Evol.* 5, 196–199 (1990).

6.Howarth, F. Classical biocontrol: panacea or pandora's box. *Proc. Hawaii. Entomol. Soc.* 24, 239–244 (1983).

7.Louda, S. M., Pemberton, R. W., Johnson, M. T. & Follett, P. A. Nontarget effects- the Achilles' heel of biological control? Retrospective analyses to reduce risk associated with biocontrol introductions. *Annu. Rev. Entomol.* 48, 365–396 (2003).
8.Symondson, W. O. C., Sunderland, K. D. & Greenstone, M. H. Can generalist predators be effective biocontrol agents? *Annu. Rev. Entomol.* 47, 561–594 (2002).
9.Van Lenteren, J. C. *et al*. Environmental risk assessment of exotic natural enemies used in inundative biological control. *BioControl* 48, 3–38 (2003).
10.Stern, V. M. Economic thresholds. *Annu. Rev. Entomol.* 18, 259–280 (1973).
11.May, R. M. Will a large complex system be stable? *Nature* 238, 413–414 (1972).
12.McCann, K., Hastings, A. & Huxel, G. R. Weak trophic interactions and the balance of nature. *Nature* 395, 794–798 (1998).
13.Pimentel, D., Zuniga, R. & Morrison, D. Update on the environmental and economic costs associated with alien-invasive species in the United States. *Ecol. Econ.* 52, 273–288 (2005).
14.Straub, C. S., Finke, D. L. & Snyder, W. E. Are the conservation of natural enemy biodiversity and biological control compatible goals? *Biol. Control* 45, 225–237 (2008).
15.Tilman, D. *et al*. The influence of functional diversity and composition on ecosystem processes. *Science* 277, 1300–1302 (1997).
16.Letourneau, D. K., Jedlicka, J. A., Bothwell, S. G. & Moreno, C. R. Effects of natural enemy biodiversity on the suppression of arthropod herbivores in terrestrial ecosystems. *Annu. Rev. Ecol. Evol. Syst.* 40, 573–592 (2009).
17.Schmitz, O. J. Predator diversity and trophic interactions. *Ecology* 88, 2415–2426 (2007).
18.Myers, J. H., Higgins, C. & Kovacs, E. How many insect species are necessary for the biological control of insects? *Environ. Entomol.* 18, 541–547 (1989).
19.Denoth, M., Frid, L. & Myers, J. H. Multiple agents in biological control: improving the odds? *Biol. Control* 24, 20–30 (2002).
20.Straub, C. S. & Snyder, W. E. Species identity dominates the relationship between predator biodiversity and herbivore suppression. *Ecology* 87, 277–282 (2006).
21.Perfecto, I. *et al*. Greater predation in shaded coffee farms: the role of resident neotropical birds. *Ecology* 85, 2677–2681 (2004).
22.Cardinale, B. J. *et al*. Biodiversity loss and its impact on humanity. *Nature* 486, 59–67 (2012).
23.Finke, D. L. & Denno, R. F. Predator diversity and the functioning of ecosystems: the role of intraguild predation in dampening trophic cascades. *Ecol. Lett.* 8, 1299–1306 (2005).
24.Vandermeer, J. Omnivory and the stability of food webs. *J. Theor. Biol.* 238, 497–504 (2006).
25.Amarasekare, P. Coexistence of intraguild predators and prey in resource-rich environments. *Ecology* 89, 2786–2797 (2008).
26.Rosenheim, J. A., Kaya, H. K., Ehler, L. E., Marois, J. J. & Jaffee, B. A. Intraguild predation among biological-control agents: theory and evidence. *Biol. Control* 5, 303–335 (1995).
27.Lewis, W. J., Lenteren, J. C., van, Phatak, S. C. & Tumlinson, J. H. A total system approach to sustainable pest management. *Proc. Natl Acad. Sci. USA* 94, 12243–12248 (1997).

28.Vandermeer, J., Perfecto, I. & Philpott, S. Ecological complexity and pest control in organic coffee production: uncovering an autonomous ecosystem service. *BioScience* 60, 527–537 (2010).
29.Crowder, D. W., Northfield, T. D., Strand, M. R. & Snyder, W. E. Organic agriculture promotes evenness and natural pest control. *Nature* 466, 109–112 (2010).
30.Ong, T. W. & Vandermeer, J. H. Antagonism between two natural enemies improves biological control of a coffee pest: the importance of dominance hierarchies. *Biol. Control* 76, 107–113 (2014).
31.Flexner, J. L., Lighthart, B. & Croft, B. A. The effects of microbial pesticides on non-target, beneficial arthropods. *Agric. Ecosyst. Environ.* 16, 203–254 (1986).
32.Brodeur, J. & Rosenheim, J. A. Intraguild interactions in aphid parasitoids. *Entomol. Exp. Appl.* 97, 93–108 (2000).
33.Lacey, L. A. & Brooks, W. in *Manual of Techniques in Insect pathology* (ed. Lacey L. A.) 1–15 (Academic, 1997).
34.Rosenzweig, M. L. & MacArthur, R. H. Graphical representation and stability conditions of predator-prey interactions. *Am. Nat.* 97, 209–223 (1963).
35.Kermack, W. O. & McKendrick, A. G. A contribution to the mathematical theory of epidemics. *Proc. R. Soc. Lond. Ser. Contain. Pap. Math. Phys. Character* 115, 700–721 (1927).
36.Holmes, J. C. & Bethel, W. M. *Behavioural Aspect of Parasite Transmission*. eds Cunning E. U., Wright C. A. *Zool. J. Linnean Soc* Suppl. No. 151, 123–149 (1972).
37.Anderson, R. M. *et al*. The invasion, persistence and spread of infectious diseases within animal and plant communities. *Phil. Trans. R. Soc. Lond. B* 314, 533–570 (1986).
38.Dobson, A. P. The population biology of parasite-induced changes in host behaviour. *Q. Rev. Biol.* 63, 139–165 (1988).
39.Hadeler, K. P. & Freedman, H. I. Predator-prey populations with parasitic infection. *J. Math. Biol.* 27, 609–631 (1989).
40.Freedman, H. I. A model of predator-prey dynamics as modified by the action of a parasite. *Math. Biosci.* 99, 143–155 (1990).
41.Xiao, Y. & Chen, L. Modeling and analysis of a predator–prey model with disease in the prey. *Math. Biosci.* 171, 59–82 (2001).
42.Mukherjee, D. Persistence aspect of a predator–prey model with disease in the prey. *Differ. Equ. Dyn. Syst.* 1–16 (2014).
43.Gause, G. F. *The Struggle for Existence* Courier Dover Publications (1934).
44.Volterra, V. *Variazioni e Fluttuazioni del Numero D'individui in Specie Theanimali Conviventi* C. Ferrari (1927).
45.Armstrong, R. A. & McGehee, R. Coexistence of species competing for shared resources. *Theor. Popul. Biol.* 9, 317–328 (1976).
46.Vandermeer, J. & King, A. Consequential classes of resources: subtle global bifurcation with dramatic ecological consequences in a simple population model. *J. Theor. Biol.* 263, 237–241 (2010).
47.Strogatz, S. *Nonlinear Dynamics and Chaos: with Applications to Physics, Biology, Chemistry and Engineering* Perseus Books Group (2001).
48.Abraham, R. H. & Shaw, C. D. *Self-Organized Systems* Springer (1988).
49.Scheffer, M. & Carpenter, S. R. Catastrophic regime shifts in ecosystems: linking theory to observation. *Trends Ecol. Evol.* 18, 648–656 (2003).

50.Holling, C. S. Some characteristics of simple types of predation and parasitism. *Can. Entomol.* 91, 385–398 (1959).
51.Duffy, J. E. Why biodiversity is important to the functioning of real-world ecosystems. *Front. Ecol. Environ.* 7, 437–444 (2009).

Acknowledgements

We thank Annette Ostling, Meghan Duffy, Ivette Perfecto and Doug Jackson for comments on the manuscript. The University of Michigan Rackham Graduate School provided financial support.

APPENDIX 1

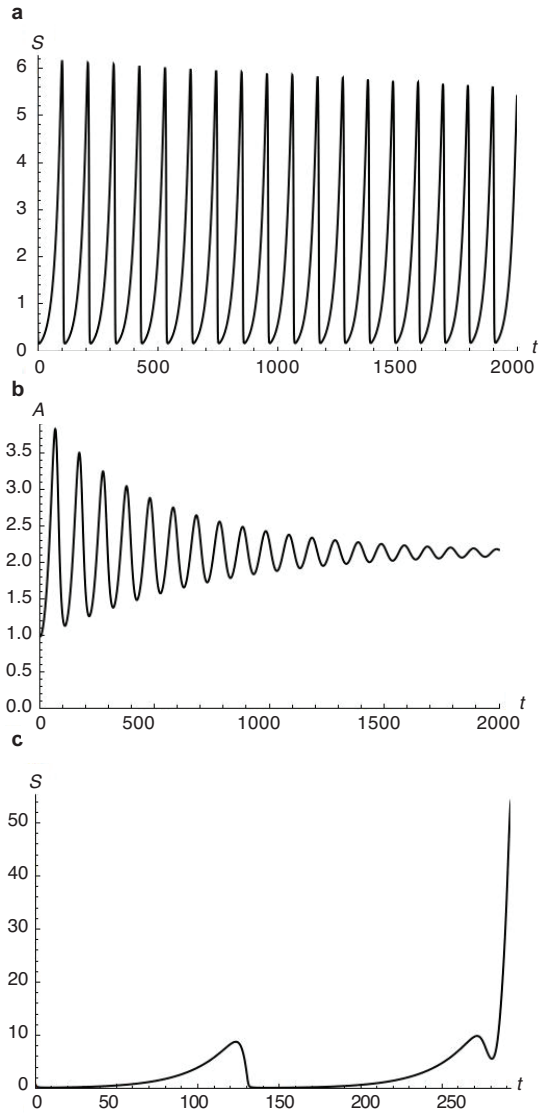

Figure S1.1 Taking stable conditions to unstable ones. Time series plots of pest populations (*S* and *A*) for **a**, parameters set such that subsystem 1 (pathogen-pest) and **b**, subsystem 2 (predator-pest) are stable limit cycles, the same parameters applied to **c**, system 3 (pathogen-predator-pest) produces unstable oscillations of increasing amplitude. The parameter

values are: r=0.04, α_1=0.92, α_2=0.05, β_1=1, β_2=0.01, m_1=0.459, m_2=0.1, K=20, ε=0.15, and the initial conditions are S_0=1, I_0=3, L_0= 1. Qualitative results are consistent after 10000 time steps for all possible permutations of S_0, I_0, L_0 each varied from 1-10. Where r is the per capita growth rate of the pest, α_1, α_2 is the attack rate of the pathogen and the predator, β_1, β_2 are the handling times of the pathogen and predator, m_1, m_2 are the mortality rates of the pathogen and predator, K is the carrying capacity of the predator, and ε is the conversion rate of infected prey consumed to predators produced.

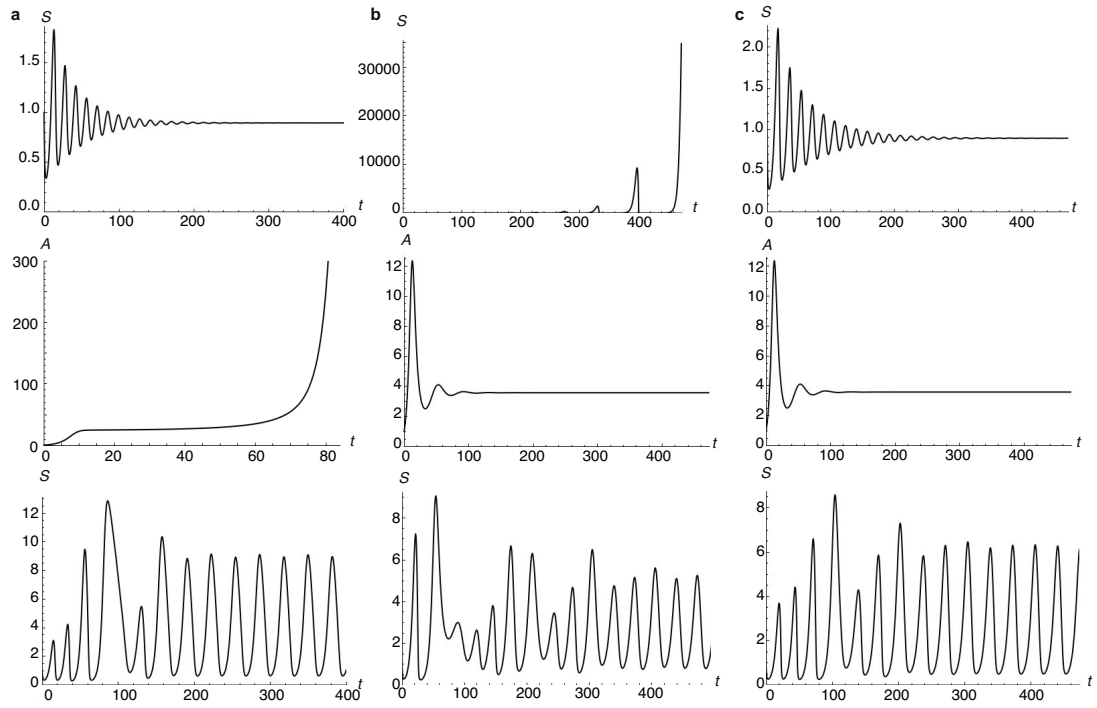

Figure S1.2 Stability arising from stable components. Exemplary time series plots for susceptible pest populations (*S* and *A)* of stable and unstable configurations of pathogen-pest subsystem 1 (top row), predator-pest subsystem 2 (middle row), and the result when combined into pathogen-predator-pest system 3 (bottom row). Columns are **a** model initialized with stable pathogen and unstable predator components; parameter values: r=0.44, α_1=0.9, α_2=0.06, β_1=1, β_2=0.01, m_1=0.40, m_2=0.1, K=10, ε=0.94, **b** model initialized with unstable pathogen and stable predator components; parameter values: r=0.30, α_1=0.9, α_2=0.06, β_1=1, β_2=0.01, m_1=0.47, m_2=0.1, K=10, ε=0.94, and **c** model initialized with stable pathogen and predator components; parameter values: r=0.30, α_1=0.9, α_2=0.06, β_1=1, β_2=0.01, m_1=0.40, m_2=0.1, K=10, ε=0.94. Initial conditions are S_0=1, I_0=3, L_0= 1. Qualitative results are consistent after 10000 time steps for all possible permutations of S_0, I_0, L_0 each varied from 1-10 excluding n=70 exceptions in **c** that are unstable. Where r is the per capita growth rate of the pest, α_1, α_2 is the attack rate of the pathogen and the predator, β_1, β_2 are the handling times of the pathogen and predator, m_1, m_2 are the mortality rates of the pathogen and predator, K is the carrying capacity of the predator, and ε is the conversion rate of infected prey consumed to predators produced.

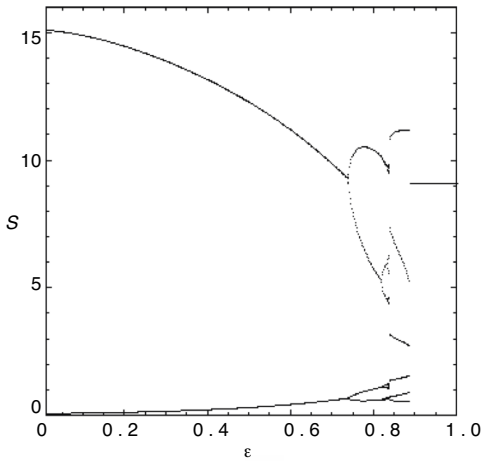

Figure S1.3 Reduced complexity when predator functional response is dependent on prey identity. When the functional response of the predator is altered to allow differences between consuming infected and healthy pests, we have the following system of equations (S1). Bifurcation diagram for conversion rate parameter ε, varied from 0 to 1.00 and evaluated for equilibrium values of the susceptible pest population *S.* Stability is still rescued from unstable component parts, but the chaotic window disappears. The parameter values are: r=0.44, α_1=0.9, α_2=0.06, β_1=1, β_2=0.01, m_1=0.47, m_2=0.1, K=10, and Initial conditions are S_0=1, I_0=3, L_0= 1. Where r is the per capita growth rate of the pest, α_1, α_2 is the attack rate of the pathogen and the predator, β_1, β_2 are the handling times of the pathogen and predator, m_1, m_2 are the mortality rates of the pathogen and predator, K is the carrying capacity of the predator, and ε is the conversion rate of infected prey consumed to predators produced.

$$\frac{dS}{dt} = rS - \alpha_1 SI\phi - \alpha_2 SL\theta_1 \quad \text{(S1a)}$$

$$\frac{dI}{dt} = \alpha_1 SI\phi - \varepsilon\alpha_2 IL\theta_2 - m_1 I \quad \text{(S1b)}$$

$$\frac{dL}{dt} = \alpha_2 (S\theta_1 + \varepsilon I\theta_2)L\left(\frac{K-L}{K}\right) - m_2 L \quad \text{(S1c)}$$

where $\phi = \frac{1}{1+\beta_1 S^2}$, $\theta_1 = \frac{1}{1+\beta_2 S}$ and $\theta_2 = \frac{1}{1+\beta_2 I}$.

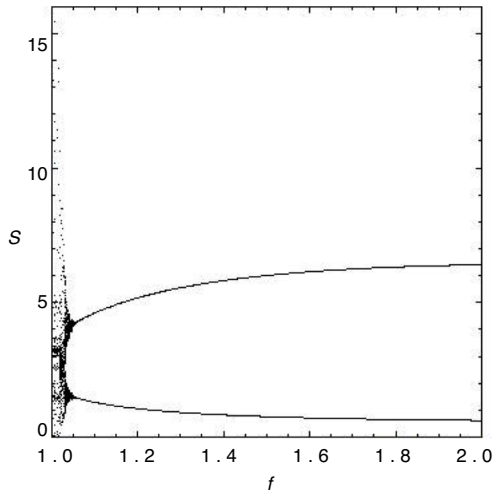

Figure S1.4 Moving from one predator to two. Bifurcating the functional response exponent, *f*, in $\phi = \frac{S^{(f-1)}}{1+\beta_1 S^f}$ from a pathogen-like control agent (*f*=2, Holling type III) to a predator-like control agent (*f*=1, Holling type II) in system 3 and evaluated for equilibrium values of the susceptible pest population *S*. The parameter values are: r=0.44, α_1=0.9, α_2=0.06, β_1=1, β_2=0.01, m_1=0.47, m_2=0.1, K=16, ε=0.49, and initial conditions are S_0=1, I_0=3, L_0= 1. Where r is the per capita growth rate of the pest, α_1, α_2 is the attack rate of the pathogen and the predator, β_1, β_2 are the handling times of the pathogen and predator, m_1, m_2 are the mortality rates of the pathogen and predator, K is the carrying capacity of the predator, and ε is the conversion rate of infected prey consumed to predators produced.

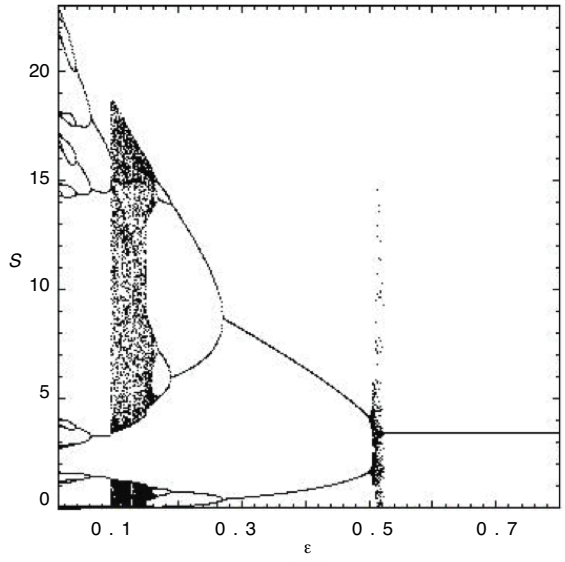

Figure S1.5 Complex behavior of double predator-pest system. Bifurcation of conversion rate, ε parameter evaluated for susceptible pest population (S) in system 3, altered so that there are two Holling type II predators. Stability is still rescued from unstable component parts, but behavior is more complex. The parameter values are: r=0.44, α_1=0.9, α_2=0.06, β_1=1, β_2=0.01, m_1=0.47, m_2=0.1, K=15, and initial conditions are S_0=1, I_0=3, L_0= 1. Where r is the per capita growth rate of the pest, α_1, α_2 is the attack rate of the pathogen and the predator, β_1, β_2 are the handling times of the pathogen and predator, m_1, m_2 are the mortality rates of the pathogen and predator, K is the carrying capacity of the predator, and ε is the conversion rate of infected prey consumed to predators produced.

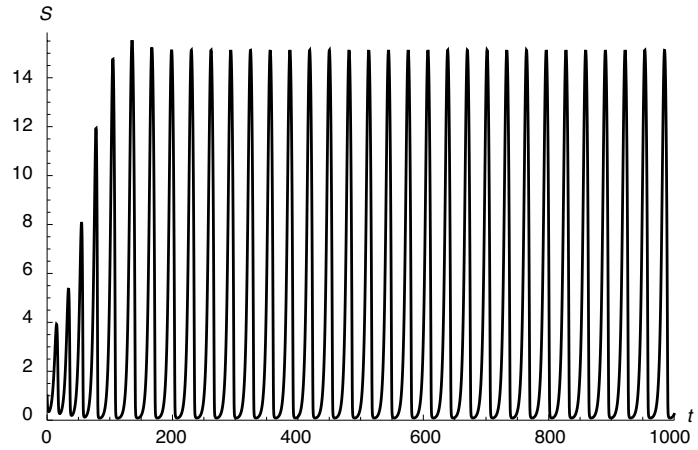

Figure S1.6 Stability rescued despite removal of intraguild predation. When intraguild predation is removed, we have the following system of equations (S2), which when set such that each subsystem is unstable alone (Fig. 1b, d-f), combining these two results in stability as pictured here in an exemplary time series plot of *S*, the susceptible pest population. Parameters set to r=0.44, α_1=0.9, α_2=0.06, β_1=1, β_2=0.01, m_1=0.47, m_2=0.1, K=10, and initial conditions: S_0=1, I_0=3, L_0= 1. Where r is the per capita growth rate of the pest, α_1, α_2 is the attack rate of the pathogen and the predator, β_1, β_2 are the handling times of the pathogen and predator, m_1, m_2 are the mortality rates of the pathogen and predator, K is the carrying capacity of the predator, and ε is the conversion rate of infected prey consumed to predators produced.

$$\frac{dS}{dt} = rS - \alpha_1 SI\phi - \alpha_2 SL\theta \quad \text{(S2a)}$$

$$\frac{dI}{dt} = \alpha_1 SI\phi - m_1 I \quad \text{(S2b)}$$

$$\frac{dL}{dt} = \alpha_2 SL\theta\left(\frac{K-L}{K}\right) - m_2 L \quad \text{(S2c)}$$

where $\phi = \frac{1}{1+\beta_1 S^2}$ and $\theta = \frac{1}{1+\beta_2 S}$.

CHAPTER II

Coupling unstable agents rescues biological control in a greenhouse experiment

Theresa Wei Ying Ong & John Vandermeer

In review, American Naturalist 2017

2.1 Abstract

Elementary theory suggests that persistent systems may arise from coupling unstable units via strong negative interactions. In a recent theoretical study mimicking the nature of complex biological control systems, two natural enemies were modeled so that they would fail to keep a pest from growing exponentially when alone, but when combined via strong negative interactions, they succeeded. While important in the practical question of pest control, this framework may also contribute to our understanding of diversity maintenance in natural systems. Here we test the theory using a predator-pathogen-pest system meant to mimic the original theoretical study. Our empirical results support theoretical predictions that when control agents are unable to control pests alone, competition between them can

stabilize the system and effectively rescue biological control of a pest. Results provide empirical support that stability can arise from coupling unstable units.

2.2 Introduction

To eliminate the need for costly off-farm inputs such as pesticides, one proposed solution is to mimic the complexity of "natural" ecosystems in agriculture such that autonomous biological control can be achieved (Lewis et al. 1997; Vandermeer et al. 2010*b*). In autonomous biological control, the goal is not to eliminate pests completely, but to maintain permanent yet small populations of pests (below levels that would cause economic loss) through complex interactions with permanent and diverse populations of natural enemies (Lewis et al. 1997; Vandermeer et al. 2010*b*). Charles Elton was the first to juxtapose the apparent instability of agro-ecosystems, which were often plagued by pest outbreaks, and the comparable stability of more diverse, "natural" ecosystems (Elton 1958). In an attempt to mimic natural systems, managers began to introduce natural enemies to control pest problems in agro-ecosystems. However, the inherent instability of biological control, both in theory and practice was dissuading (Murdoch 1975). Generalist control agents sometimes had negative effects on non-target beneficial organisms, whereas specialist control agents often failed to establish permanent populations thus requiring costly and continuous re-introductions (Howarth 1991; Roderick and Navajas 2003). Though these studies suggest that autonomous control is difficult to achieve, they were not specifically designed to test the potential of autonomous biological control to arise from complexity.

Using hybrid Lotka-Volterra, S-I predator-pathogen-prey models, we previously demonstrated that it is theoretically possible to combine two unstable two-dimensional systems (pest-predator and pest-pathogen) to produce a stable three-dimensional system (pest, predator, and pathogen) that is robust to perturbations in initial conditions (Ong and Vandermeer 2015). The more complex model where both enemies were combined was run under exactly the same parameters as the models where only one enemy was present. Where the simple models failed to control the pest, the complex model succeeded. In the model, a non-renewable carrying capacity limited the population size of the predator such that the number of pests overwhelmed the capacity to control them. Since the pathogen did not have this limitation, pest resources were overexploited, leading to boom-bust dynamics as the pathogen and pest decline and grow in cycles with ever-increasing magnitudes known in the literature as the paradox of biological control (Luck 1990). When combined, the predator consumed both healthy and pathogen-infected pests. This strong negative interaction, an example of intraguild predation, kept the pathogen from overexploiting the pest resources (ie. an epidemic) to the point where boom-bust pest dynamics would otherwise occur. Given that the parameters were kept constant across single and double enemy simulations, these results provided hope that an autonomous strategy of biological control that is maintained solely from the complexity of the agro-ecosystem rather than the addition of expensive, external inputs exists. Yet to arrive at practical solutions to real problems, empirical confirmation is necessary. Here we designed a greenhouse experiment that combined two separately unstable (in the sense that the pest escapes control) natural enemy-pest pairings to see whether autonomous control can arise from the emergent complexity of the combined system. Pest populations were simultaneously exposed to two control agents at levels previously determined to be ineffective singularly, and monitored over time to test if control was

rescued. Our results confirm theoretical predictions that unstable units can combine to rescue control. We argue that competitive interactions may in some cases drive system-level stability and that complexity does in fact contribute to the autonomous biological control we observe in natural systems.

2.3 Results and Discussion

To establish unstable conditions, populations of pea aphids (*Acyrthosiphon pisum*) were grown in the presence of natural enemies and monitored over time until populations exceeded a critical threshold beyond which the pest was considered an economic threat (here we chose a critical threshold of 100 aphids) (Stern 1973). For our purposes, stability is defined as effective biological control where pest populations are maintained at or below threshold levels. To mimic the theoretical framework of Ong and Vandermeer (Ong and Vandermeer 2015), both a predator control agent (*Hippodamia convergens*, the convergent ladybeetle) and a fungal pathogen (*Beauveria bassiana*) were separately tested (Fig. 2.1). Previous studies have documented strong negative effects of *B. bassiana* on ladybird beetle predators (Roy and Pell 2000; Roy and Cottrell 2008). Though *B. bassiana* is a used widely as a biological control agent of agricultural insect pests, many studies purport the presence of non-target effects on ladybird beetles including lethality, morbidity and reduced reproductive capacity either through direct exposure to the fungus or through the consumption of infected prey, a form of intraguild predation (Roy and Pell 2000; Roy and Cottrell 2008). In addition, field studies show that incidence of *H. convergens* are reduced between 75-93% for plants exposed to *B. bassiana* despite the presence of similar numbers of *A. pisum* prey (James et al. 1995). Evidence of these strong negative interactions, in addition to direct competition over shared resources, make the *A. pisum—B. bassiana—H.*

convergens system a strong empirical analogy of the Ong and Vandermeer theory (Ong and Vandermeer 2015).

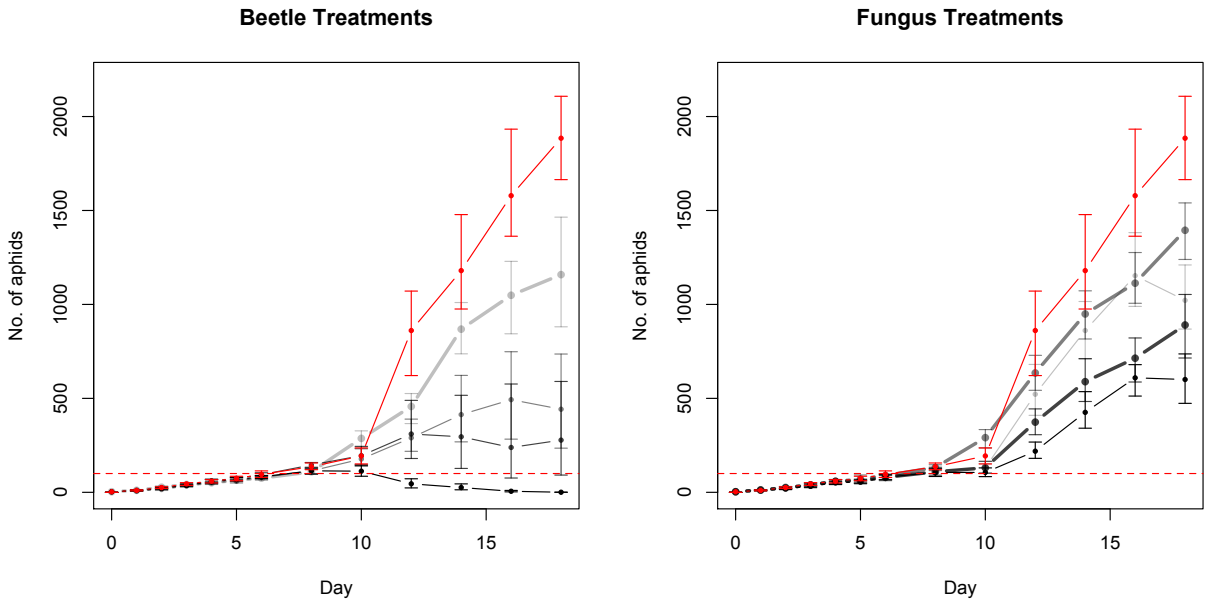

Figure 2.1 Establishing unstable conditions for each natural enemy. Red solid lines and points represent control curves (same curve plotted twice for clarity). Black and grey lines and points are beetle treatments (left plot) and fungal treatments (right plot). Treatments range from low (light grey) to high densities (black) of each type of control agent. Range for beetle treatments span from 2,4,8, and 16 individuals per enclosure. Aphids in fungal treatments were sprayed with a commercially available emulsion of *B. bassiana* known as Mycotrol-O diluted with dH_2O at a concentration of 4,8,16, and 32%. Bold lines indicate treatments chosen to represent unstable conditions. Confidence intervals are 95% confidence intervals based on bootstrapping (bca) with $N = 9999$ replicates. Dashed line represents experimental threshold of 100 aphids. When aphids crossed threshold natural enemies were introduced (day 8).

We applied four different densities of each natural enemy and monitored the trajectories of aphid populations post inoculation (Fig. 2.1). From this first set of results we chose one density of predator and two densities of pathogen where pest population growth continued to grow beyond the critical threshold and showed the least amount of saturation (Fig. 2.1). These densities were then combined to see how the presence of both enemies would influence pest growth rates (Fig. 2.2).

In treatments where pest populations were inoculated with two natural enemies simultaneously, growth was significantly reduced from controls (Fig. 2.2). After inoculation, pest population growth was reduced, bringing populations down to the critical threshold of 100 aphids for the remainder of the experiment. The result was consistent regardless of whether a low or high level of fungi was inoculated along with 2 ladybird beetle individuals. Coupling two ineffective control agents successfully maintained pest populations at threshold levels. Autonomous biological control asserts that pests are maintained at intermediate numbers so that populations are not reduced to the point of overexploitation followed by primary and secondary outbreaks (Luck 1990). Our results appear to mimic the structure of autonomous biological control since populations remained at threshold levels for a significant amount of time considering the rapid growth of aphids observed under control conditions.

Tolerance for threshold levels may outweigh the risks of a scenario where one or both natural enemies are absent. For treatments where only one natural enemy is present, aphid populations reached 6-150 times the threshold level in a matter of 10 days (Fig. 2.1). When all natural enemies were excluded, aphids reached 200-times threshold levels for the same time range (Figs. 2.1 and 2.2). Sampling was limited to 10-days post inoculation because the number and size of pea plants used for the experiment could not sustain the growth of aphid control populations much beyond this time frame. This is an important consideration because the model in which this experiment is based does not have a resource-based carrying capacity for the pest to account for the reality that pests are never allowed to reach carrying capacity in well-managed farmlands. Larger, more established plants are necessary to reveal whether the observed reductions in pest populations are maintained for longer time-scales.

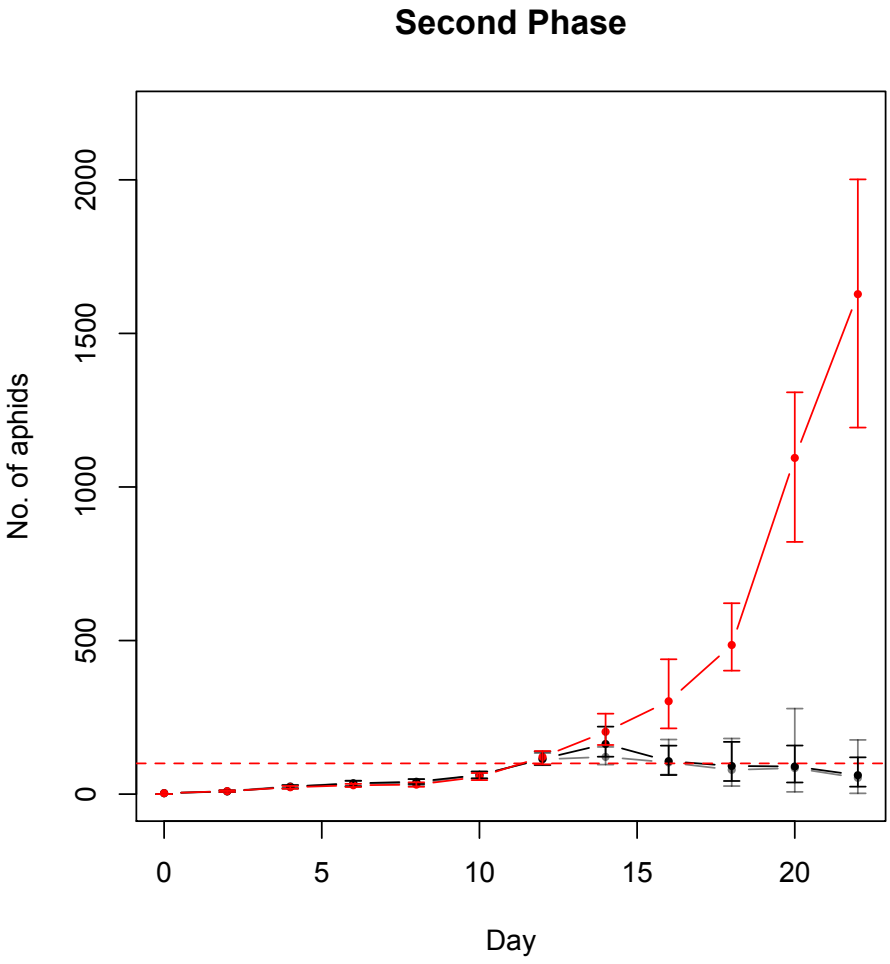

Figure 2.2 Coupling unstable agents to produce stability. Pea aphids (*Acyrthosiphon pisum*) were simultaneously exposed to ladybird beetles (*Hippodamia convergens*) and sprayed with a commercially available emulsion of *Beauveria bassiana* known as Mycotrol-O diluted with dH_2O at a concentration of 8 and 16%. Red solid line is control with no natural enemies. Black solid line= 2 beetles + 16 % fungal emulsion, grey solid line= 2 beetles + 8% fungal emulsion. Confidence intervals are 95% confidence intervals based on bootstrapping (bca) with N = 9999 replicates. Dashed red line represents experimental threshold of 100 aphids. When aphids crossed threshold natural enemies were introduced (day 13).

Our results provide empirical proof that consistently reduced populations of pests can result from the coupling of control agents that are alone, incapable of providing effective control. One of the greatest paradoxes in ecology is the question of how a diversity of organisms manage to coexist despite strong direct and indirect negative interactions (Gause 1934; Hutchinson 1961;

McCann 2000). Though the presence of weak negative interactions is thought to be responsible for the stability of complex systems, new theories suggest that this relies on the assumption that individual components of the system are stable in isolation (McCann et al. 1998; Ong and Vandermeer 2015). This study provides empirical validation of the theory that unstable units can combine to create stability, suggesting that the effects of component interactions (negative, positive or neutral) on whole-system stability are not readily interpretable. Though it is easy to presume that a predator-prey system that is stable when isolated may be destabilized by the addition of a competitor, there is no reason to expect that each component in a complex food web is capable of maintaining a key resource on its own. In fact, as complexity evolves, components in a system must continuously adapt to the arrival of new components. As this process continues, each component becomes dependent on its interactions with others in the network, feasibly continuing to the point where component units no longer function in isolation. Since complexity necessarily evolves from individual units, if we remove each unit from its place in the complex, we may find that the presence of single interactions that are unstable in isolation is a common phenomenon.

2.4 Materials and Methods

In the first phase of the experiment, populations of pea aphids (*Acyrthosiphon pisum*) were grown on pea seedlings and monitored over time until populations exceeded a critical threshold beyond which the pest was considered an economic threat (Stern 1973). Each enclosure included 9 one-week old *Pisum sativum* var. Dwarf grey seedlings and three aphids. We chose an arbitrary economic threshold of 100 aphids based on IPM recommendations for pea aphids (North Carolina State University IPM n.d.). Aphid populations were monitored every two

days until the average population exceeded 100 aphids. The next day (day 11), a single type of control agent was introduced to the pest population at a variety of densities.

To mimic the theoretical framework of Ong and Vandermeer (Ong and Vandermeer 2015), both a predator control agent (*Hippodamia convergens*, the convergent ladybeetle) and a fungal pathogen (*Beauveria bassiana*) were separately tested. Beetle treatments included 2,4,8, or 16 individuals per enclosure. Aphids in fungal treatments were sprayed with a commercially available emulsion of *B. bassiana* known as Mycotrol-O diluted with dH_2O at a concentration of 4,8,16, and 32%. Both of these are commonly used, publically available control agents of aphids.

We continued to monitor aphid populations every other day for eight days following enemy introduction and compared these to a control treatment where no control agents were introduced. Time series graphs were analyzed to determine what densities of control agents showed no evidence of declining aphid population growth, and these conditions selected for the second phase of the experiment.

In the second phase of the experiment, aphid populations were allowed to grow past a 100-aphid threshold then simultaneously exposed to both control agents at levels previously determined to be ineffective singularly. Populations were then monitored as in the first phase.

All experiments were conducted at the Matthaei Botanical Gardens in Ann Arbor, MI.

2.5 References

Elton, C. S. 1958. The ecology of invasions by plants and animals. Methuen, London 18.

Gause, G. F. 1934. The Struggle for Existence. Courier Dover Publications.

Howarth, F. G. 1991. Environmental Impacts of Classical Biological Control. Annual Review of Entomology 36:485–509.

Hutchinson, G. E. 1961. The Paradox of the Plankton. The American Naturalist 95:137–145.

James, R. R., B. T. Shaffer, B. Croft, and B. Lighthart. 1995. Field Evaluation of Beauveria bassiana: Its Persistence and Effects on the Pea Aphid and a Non-target Coccinellid in Alfalfa. Biocontrol Science and Technology 5:425–438.

Lewis, W. J., J. C. van Lenteren, S. C. Phatak, and J. H. Tumlinson. 1997. A total system approach to sustainable pest management. Proceedings of the National Academy of Sciences 94:12243–12248.

Luck, R. F. 1990. Evaluation of natural enemies for biological control: A behavioral approach. Trends in Ecology & Evolution 5:196–199.

McCann, K., A. Hastings, and G. R. Huxel. 1998. Weak trophic interactions and the balance of. Nature 395:794–798.

McCann, K. S. 2000. The diversity–stability debate. Nature 405:228–233.

Murdoch, W. W. 1975. Diversity, complexity, stability and pest control. J. appl. Ecol 12:795–807.

North Carolina State University IPM. n.d. *Pea Aphid*.

Ong, T. W., and J. H. Vandermeer. 2014. Antagonism between two natural enemies improves biological control of a coffee pest: The importance of dominance hierarchies. Biological Control 76:107–113.

Ong, T. W. Y., and J. H. Vandermeer. 2015. Coupling unstable agents in biological control. Nature Communications 6.

Roderick, G. K., and M. Navajas. 2003. Genes in new environments: genetics and evolution in biological control. Nature reviews. Genetics 4:889–899.

Roy, H. E., and T. E. Cottrell. 2008. Forgotten natural enemies: interactions between coccinellids and insect-parasitic fungi. European Journal of Entomology 105:391.

Roy, H. E., and J. K. Pell. 2000. Interactions Between Entomopathogenic Fungi and Other Natural Enemies: Implications for Biological Control. Biocontrol Science and Technology 10:737–752.

Stern, V. M. 1973. Economic Thresholds. Annual Review of Entomology 18:259–280.

Vandermeer, J., I. Perfecto, and S. Philpott. 2010*a*. Ecological Complexity and Pest Control in Organic Coffee Production: Uncovering an Autonomous Ecosystem Service. BioScience 60:527–537.

———. 2010*b*. Ecological Complexity and Pest Control in Organic Coffee Production: Uncovering an Autonomous Ecosystem Service. BioScience 60:527–537.

CHAPTER III

Huffaker revisited: spatial heterogeneity and the coupling of ineffective agents in biological control

In revisions, *Ecosphere* 2017

Theresa Wei Ying Ong, David Allen, and John Vandermeer

3.1 Abstract

Despite decades of research, much of our current understanding of predator-prey dynamics still draws on advances made in the early 20th century. In a classic ecological study, Huffaker demonstrated that spatial heterogeneity could induce stability in predator-prey interactions. Yet recent theories suggest that space can also act to destabilize predator-prey systems and that stability can arise from coupling of unstable units. Here we revisit Huffaker's classic experiment with modern empirical and statistical techniques to elucidate the effect of space on the coexistence of two natural enemies competing over a shared pest resource in a laboratory experiment. We find that while the application of two different control agents were ineffective at control pests in insolation, coupling them together not only improved control of the pest, but also reduced the occurrence of large spatially clustered pest outbreaks. These results

imply, more generally, that coexistence in diverse biological systems may arise through both the coupling of unstable interactions and the spatial heterogeneity induced by those interactions.

3.2 Introduction

In 1958, C. B. Huffaker conducted what would become a classic study on the role of dispersal in the coexistence of predators and prey (Huffaker 1958). At the time, the Lotka-Volterra equations were well-known to predict regular, repeatable cycles between predators and prey, yet empirical studies failed to reproduce these theoretical results (Gause 1934, Gause et al. 1936). These early empirical studies were done in well-mixed environments to mimic the assumptions of the Lotka-Voltera model. Predators had easy access to prey, but rather than decreasing in numbers before prey were completely exhausted, in most cases predators overexploited prey, leading to extinction of the whole system. Citing Nicholson's (1933, 1954) criticism of the early empirical studies being contained in microcosms that were "too small to even approximate a qualitative, to say nothing of a quantitative, conformity to theory," Huffaker designed experiments using a series of spatial arrays or "universes" composed of carefully arranged oranges (prey resources), while manipulating the dispersal abilities of predatory and prey mite species. He discovered that reducing the dispersal of predators by slowing them with petroleum jelly and encouraging dispersal in prey by providing wooden dowels for long distance migration introduced sufficient spatial heterogeneity to keep prey from going extinct immediately, allowing predator-prey cycles to be observed (Huffaker 1958). This early study established the importance of spatial heterogeneity in maintaining predator/prey cycles, providing one mechanism to explain the discordance between experimental evidence that

predator/prey pairs go extinct and the overwhelming evidence from nature that predators and their prey do indeed persist over many years.

In his conclusions, Huffaker cautioned that the use of spatially homogenous monocultures in agriculture could have unintended consequences for biological control, which are simply predator-prey systems where control agents are released to consume pest prey (Huffaker 1958, Huffaker et al. 1963). In fact, many biological control programs that sought to eliminate pest species with a single, highly efficient control agent found it similarly difficult to stabilize predator-prey dynamics (Nicholson and Bailey 1935, Murdoch 1975). Strong agents caused cycles of three repeating phases: 1) control agent overexploits pests 2) control agent declines due to lack of prey, and 3) pests resurge to outbreak levels under enemy-free conditions (Luck 1990, Arditi and Berryman 1991). Theory based on the Lotka-Volterra equations predicted that the magnitude of booms and busts would increase with every successive control agent-pest cycle until a stochastic event pushed the control agent to extinction (Luck 1990, Arditi and Berryman 1991). Using a diversity of control agents was one suggested solution (Murdoch 1975). Yet, in light of the then-popular competitive exclusion principle, incorporating more than one predator on a single prey (the pest) would be unlikely to work since only a single predator would survive, leading back to the same problem of prey overexploitation and extinction of the desired predator-prey control system (Denoth et al. 2002, Louda et al. 2003, Straub et al. 2008).

Huffaker's study moved in a different direction and sought to challenge the growing consensus that predator-prey systems are inherently unstable. Taking Nicholson's critique of previous empirical work, he sought to create background conditions that more closely reflected some key elements of the environments faced by real predator-prey systems in nature, effectively

removing the "mean-field" assumption of the well-mixed system and explicitly creating a spatially extended framework.

The prevalence of strong negative interactions in biological control, including intraguild predation where predators consume one another in addition to shared resources, dissuaded many from advocating multiple control agents to resolve pest problems (Rosenheim et al. 1995, McCann et al. 1998, Denoth et al. 2002, Straub et al. 2008). However, recent theoretical found that strong negative interactions between a predator control agent and a pathogen control agent can result in a system that is stable even when the agents are completely ineffective when alone (Ong and Vandermeer 2015). These strong negative interactions could be responsible for autonomous biological control—the observation that a diversity of natural enemies are able to keep levels of pests below economic thresholds, but above levels for natural enemies to persist without boom-bust dynamics (Lewis et al. 1997, Vandermeer et al. 2010, Ong and Vandermeer 2014).

Though Huffaker's study and many theoretical studies that followed established spatial prey refuges as a stabilizing force for consumer-resource dynamics, contemporary theoretical work has shown that space can also induce unstable dynamics, including chaos (Huffaker 1958, Folt and Schulze 1993, Pascual 1993, Petrovskii and Malchow 2001). Though the specific size of a pest population may become unpredictable, chaotic systems can still be considered "stable" in pest control if the range of pest population sizes possible is constrained to an envelope below economic thresholds (Ong and Vandermeer 2015). These are important considerations for diverse biological systems where large, unpredictable fluctuations in population sizes are a common phenomenon (Berryman 1982, Dwyer et al. 2004).

Here, we borrow Huffaker's classic framework to test how the coupling of competing pathogen and predator natural enemies improves or worsens control of pests when placed in a spatial context where dispersal is constrained or free. We ask if spatial heterogeneity rescued coexistence in Huffaker's original study, how might it unbalance an already stable system, or stabilize an unstable one? In accordance with results from both the current and classic literature, we expect dispersal to improve biological control through the maintenance of low, equilibrium pest densities when only one species of natural enemies is present. When two natural enemies are combined, competition may further increase spatial heterogeneity, resulting in better control. Alternatively, spatial heterogeneity itself may be so great as to induce outbreak conditions.

3.3 Methods Summary

Mimicking Huffaker's original study, we created "universes" composed of prey resources (*Pisum sativum* var. Dwarf Grey cuttings) arranged in a 4X5 array of isolated chambers connected via corridors of large or small dimension in order to control dispersal rates. We introduced pea aphids (*Acyrthosiphon pisum)* as prey, and the predatory ladybird beetle *Hippodamia convergens* and the entomopathogenic fungus *Beauveria bassiana* as competing natural enemies. For both dispersal conditions, we ran control treatments with no natural enemies, single enemy treatments, and a double enemy treatment (see Methods). Aphid population sizes and locations were surveyed for 28 time units, or until extinction, whichever was first. For each treatment, we fit a basic model of population growth via maximum likelihood, from which we estimated aphid growth rate, local and long-distance migration rates, and carrying capacity (r, m_1, m_2, K) for each treatment (Methods). To observe spatio-temporal dynamics beyond the timeframe and dimensions of the experiment (Appendix 1), we used parameter fits to project aphid population time series for 200 time units assuming a 30X30 spatial grid placed on a torus.

We assessed total aphid population sizes and clustering via Moran's I (Moran 1953) for each time step and treatment (see Methods).

3.4 Results and Discussion

Coexistence occurred only when aphids and natural enemies experienced high-dispersal conditions where they could move more easily through the array (Fig. 3.1). Fungus had consistent effects on migration rates for aphids regardless of the diameter of corridors between cells. In both high and low dispersal treatments, fungus caused aphids to reduce local migration rates and increase long-distance migration rates (Fig. 3.2). This may be an adaptation to avoid pathogen outbreaks that occur more easily with host clustering (Shah and Pell 2003). We see this play out in the spatial dynamics, where local clustering of aphids is significantly reduced when fungus is present (Fig. 3.3). We note that aphid growth rates actually increased relative to controls in low dispersal treatments with fungus (Fig. 3.2). Infection by the entomopathogenic fungus can cause a stress-response in aphids that encourages molting (quick progression to adulthood), and greater fecundity rates prior to death (Kim and Roberts 2012, Ortiz-Urquiza and Keyhani 2013). However, in high dispersal treatments where aphids survive long-term, the presence of fungus reduced growth rates in aphids, as expected. The effect of beetles on migration rates of aphids was dependent on whether the arrays allowed low or high dispersal. In low dispersal treatments, beetles mirrored fungus effects by causing local aphid migration rates to reduce and long-distance migration rates to increase (Fig. 3.2). Since aphids are already clustered in low dispersal treatments, beetles very easily discover and decimate local clusters of aphids, which are hindered from migrating due to the small diameter of the corridors between cells (Appendix 2, Fig. S3). This is evidenced by short aphid survival times and low aphid growth rates in the beetle only low-dispersal treatments (Figs. 3.1-3.2). Beetle movement is

highly constrained in the low dispersal treatments. Thus, aphids that are able to migrate longer distances survive, causing the increase in long-distance migration rates (Appendix 2, Fig. S3). However, in high dispersal treatments, beetles caused the reverse effect with local aphid migration rates increasing and long-distance migration rates decreasing (Fig. 3.2). Under conditions when aphids can easily move through the spatial array, beetle predation events disrupt clusters of aphid populations and cause short-distance migration to neighboring cells. Beetles can also move more easily in high dispersal arrays, though long predator search times appear to allow new, local clusters of aphids to build before re-discovery by the predator. This is evidenced by the increased aphid clustering that occurs with high dispersal-beetle only treatments (Fig. 3.3). When predator search times are sufficiently long, aphids are not consistently exposed to predation, and there may be less need for long-distance dispersal events.

Under low dispersal conditions, we could not estimate carrying capacities of aphids because of the large incidence of extinctions (Fig. 3.2, Methods). We did find that single natural enemy treatments increased local migration and reduced long-distance migration, but the combination of natural enemies eliminated effects on migration so that there were no differences from controls. Since aphids were a limiting resource in low dispersal treatments, competition between natural enemies in the combined natural enemy treatment may have reduced the effects of natural enemies on pest movement.

Under high dispersal conditions, the combination of both natural enemies best controlled aphids by reducing aphid clustering and equilibrium pest densities through a marked reduction in their carrying capacity (Fig. 3.1). This is a particularly surprising result since neither natural enemy alone reduced the carrying capacity of the pest (Fig. 3.2). In fact, the beetle significantly increased the carrying capacity of aphids (Fig. 3.1). Since no new food resources were made

available to aphids after they occupied a cell, aphid carrying capacity should increase only if aphids move to new cells and discover new food resources (Methods). Increases in local migration rates of aphids under the presence of beetles can explain the positive effect on aphid carrying capacity. Though the fungus alone reduced spatial clustering of aphids, carrying capacity was not reduced (Figs. 3.1-3.3). Increases in long-distance migration were canceled out by a reduction in aphid growth rates under fungus exposure to have no effect on carrying capacity (Fig. 3.1 and 3.2). Thus, equilibrium densities of aphids under the presence of fungus alone are no different than high dispersal controls (Fig. 3.1). However, when both natural enemies are combined, aphid populations are doubly threatened, reducing carrying capacities and increasing long-distance migration to a much larger extent than either enemy alone. This synergistic effect may result from combining intense predation by the beetle predator and the reduction in spatial clustering that occurs with the pathogen (Fig. 3.3). Much like in the original theoretical work that inspired our experiment (Ong and Vandermeer 2015), we find that a combination of two ineffective control agents can effectively rescue control, not only reducing equilibrium pest densities, but also reducing spatial clusters and limiting the carrying capacity of pests.

It is tempting to generalize these results. Allowing that all species on earth are faced with the combination of predators and pathogens acting simultaneously, we can envision the effects of spatial extent in a very simple dynamic. If the pathogen induces long-distance migration (as it here does), and if the predator is more effective at finding spatial clusters of prey (as it here is), then the pathogen, if its virulence is appropriately constrained, effectively causes the prey to "move" to "refuges." The refuges are the areas of recently migrated individuals that have not yet locally reproduced enough to form a cluster that is sufficiently attractive to the predator. The

stability condition (or persistence condition) is thus a critical combination of dispersal rates of all three elements, plus the nonlinear trait-mediated effects of the pathogen and predator on the dispersal of the prey. Generalizing to a system of two predators and a prey, the key nonlinearities (trait-mediated effects) of one predator increasing the migration rate of the prey, the other increasing the local cluster formation, creates the conditions for stabilizing the whole system (with appropriate parameter values). We summarize this speculative generalization in Figure 3.4.

3.5 Methods

Experimental Setup

Spatial arrays of 3'' pea plant cuttings (*P. sativum* var. Dwarf Grey) were set up under a 12hr-dark 12hr-light cycle. Each independent array (or "universe," as Huffaker referred to them) consisted of a 4X5 network of clear plastic chambers (3 ¾'' top diameter, 2 ½'' bottom diameter, 4 ¾'' height) that were sealed to prevent escape by arthropods, but not airtight. Each chamber included a test tube filled with dH_2O and a pea plant cutting inserted through a hole in the test tube top. The chambers were connected laterally using plastic corridors of two diameters: 0.219'' (small) and 0.47'' (large) cut to 2'' in length. A single universe consisted of all small or all large corridors to represent a low or high dispersal treatment, respectively. Chambers were connected using a von Neumann neighborhood design with edge effects. Both low (L) and high dispersal (H) universes were subjected to four treatments: 1) aphids (*A. pisum*) only, 2) aphids and beetles (*H. convergens*) (B), 3) aphids and fungus (*B. bassiana*) (F), 4) aphids, beetles, and fungus (FB). All units started with an initial population of 50 aphids, 25 in the (1,1) position and 25 in the (4,5) position of the spatial array (diagonal corners). Eight beetles were added to the (4,1)

position of the array for treatments including beetles. For our fungal treatments, the initial aphid populations were sprayed with 2 pumps of a *B. bassiana* emulsion made by vortexing 4 mL dH_2O and 1.28 mL *B. bassiana* obtained as the commercially available product "Mycotrol-O" with a concentration of 2 x 10^3 viable spores per quart. Universes were surveyed twice a week using direct counting methods. The number of healthy aphids was recorded for 28 time points or until extinction occurred. During census, pea cuttings were replaced as necessary so that fresh resources were always available in the array. Once a pea plant was colonized by one or more aphids, no new pea cuttings would be provided in that chamber until all aphids went locally extinct or moved to neighboring chambers. After every local extinction event, chambers were thoroughly cleansed with 70% ethanol and fresh pea cuttings provided. In total we ran 66 universes with 10 replicates of the L treatment, 5-H, 10-BL, 7-BH, 10-FL, 6-FH, 10-FBL, and 8-FBH. Given the available laboratory space, we were able to run 16 universes at a time, two replicates from each treatment were run simultaneously. Differences in times to extinction led to the different number of replicates per treatment we were able to achieve given constraints on funding and time.

Parameter Estimation

We modeled population dynamics using a coupled map lattice. The lattice was 4X5, the same as in the experimental setup. At each time step the entire lattice first experienced population dynamics, then local dispersal, and then long-distance dispersal.

At each site on the lattice population dynamics were determined by the Ricker function (Ricker 1954) with parameters *r* and *K*.

$$N_{ij}(t) = N_{ij}(t-1)e^{r\left(1-\frac{N_{ij}(t-1)}{K}\right)} \quad (1)$$

After local population dynamics a fraction, m_1, of individuals from each site migrated locally to neighboring sites. These migrating individuals were evenly distributed to the 2-4 sites in focal site's von Neumann neighborhood.

After local migration a fraction, m_2, of individuals migrated from each site migrated long-distance to all the sites in the lattice. These individuals were evenly distributed among the 19 other sites.

We ran these rules for 28 time steps from the same starting conditions as in the experiment. Population values were assumed to be Poisson distributed with mean given by the above model. For each treatment we estimated the maximum likelihood parameter values using simulated annealing. Model estimates converged for all parameters except for carrying capacities of aphids under low dispersal conditions. The large incidence of extinctions made carrying capacities irrelevant for these treatments because aphids had negative growth rates. Thus, populations never increased to the point where carrying capacities could be estimated. We calculated the 95% confidence intervals around parameter estimates using the likelihood ratio test.

Spatio-temporal projections

Our coupled map lattice model was then parameterized and used to project populations under each treatment for 200 time steps assuming both the original 4X5 experimental design with edge effects (Appendix 1) and a 30X30 spatial grid placed on a torus. We constructed confidence bands by simulating the model 1000 times for each treatment and taking the 95%

quantiles of the total aphid population size at each time step. For each simulation, spatial patterning was measured using Moran's I, where $I > 0$ implies clustered, and $I < 0$ implies dispersed patterns. We constructed 95% confidence bands for Moran's I using the same process as population size. Simulated and experimental results for aphid population size and spatial patterning are overlaid in Appendix 1. All analyses were conducted in R (Core R Team, 2016).

Acknowledgements

We would like to thank Damie Pak, Azucena Lucatero and Daniel Kowalski for assistance gathering experimental data. Thank you to Aaron King for advice in developing the coupled map lattice model and appropriate parameter estimating schemes.

3.6 References

Arditi, R., and A. A. Berryman. 1991. The biological control paradox. Trends in ecology & evolution 6:32.

Berryman, A. A. 1982. Biological Control, Thresholds, and Pest Outbreaks. Environmental Entomology 11:544–549.

Denoth, M., L. Frid, and J. H. Myers. 2002. Multiple agents in biological control: improving the odds? Biological Control 24:20–30.

Dwyer, G., J. Dushoff, and S. H. Yee. 2004. The combined effects of pathogens and predators on insect outbreaks. Nature 430:341–345.

Folt, C. L., and P. C. Schulze. 1993. Spatial Patchiness, Individual Performance and Predator Impacts. Oikos 68:560–566.

Gause, G. F. 1934. The Struggle for Existence. Courier Dover Publications.

Gause, G., N. Smaragdova, and A. Witt. 1936. Further studies of interaction between predators and prey. The Journal of Animal Ecology:1–18.

Huffaker, C. B. 1958. Experimental studies on predation: Dispersion factors and predator-prey oscillations. Hilgardia 27:343–383.

Huffaker, C. B., S. Herman, and K. Shea. 1963. Experimental studies on predation: complex dispersion and levels of food in an acarine predator-prey interaction. University of Calif.

Kim, J. J., and D. W. Roberts. 2012. The relationship between conidial dose, moulting and insect developmental stage on the susceptibility of cotton aphid, Aphis gossypii, to conidia of Lecanicillium attenuatum, an entomopathogenic fungus. Biocontrol Science and Technology 22:319–331.

Lewis, W. J., J. C. van Lenteren, S. C. Phatak, and J. H. Tumlinson. 1997. A total system approach to sustainable pest management. Proceedings of the National Academy of Sciences 94:12243–12248.

Louda, S. M., R. W. Pemberton, M. T. Johnson, and P. A. Follett. 2003. Nontarget effects- the Achilles' heel of biological control? Retrospective Analyses to Reduce Risk Associated with Biocontrol Introductions*. Annual Review of Entomology 48:365–396.

Luck, R. F. 1990. Evaluation of natural enemies for biological control: A behavioral approach. Trends in Ecology & Evolution 5:196–199.

McCann, K., A. Hastings, and G. R. Huxel. 1998. Weak trophic interactions and the balance of. Nature 395:794–798.

Moran, P. 1953. The statistical analysis of the Canadian Lynx cycle. Australian Journal of Zoology 1:291–298.

Murdoch, W. W. 1975. Diversity, complexity, stability and pest control. J. appl. Ecol 12:795–807.

Nicholson, A. J. 1933. Supplement: the balance of animal populations. The Journal of Animal Ecology:131–178.

Nicholson, A. J. 1954. An outline of the dynamics of animal populations. Australian journal of Zoology 2:9–65.

Nicholson, A. J., and V. A. Bailey. 1935. The Balance of Animal Populations.—Part I. Proceedings of the Zoological Society of London 105:551–598.

Ong, T. W., and J. H. Vandermeer. 2014. Antagonism between two natural enemies improves biological control of a coffee pest: The importance of dominance hierarchies. Biological Control 76:107–113.

Ong, T. W. Y., and J. H. Vandermeer. 2015. Coupling unstable agents in biological control. Nature Communications 6.

Ortiz-Urquiza, A., and N. O. Keyhani. 2013. Action on the Surface: Entomopathogenic Fungi versus the Insect Cuticle. Insects 4:357–374.

Pascual, M. 1993. Diffusion-Induced Chaos in a Spatial Predator--Prey System. Proceedings of the Royal Society of London B: Biological Sciences 251:1–7.

Petrovskii, S. V., and H. Malchow. 2001. Wave of Chaos: New Mechanism of Pattern Formation in Spatio-temporal Population Dynamics. Theoretical Population Biology 59:157–174.

Ricker, W. E. 1954. Stock and Recruitment. Journal of the Fisheries Research Board of Canada 11:559–623.

Rosenheim, J. A., H. K. Kaya, L. E. Ehler, J. J. Marois, and B. A. Jaffee. 1995. Intraguild Predation Among Biological-Control Agents: Theory and Evidence. Biological Control 5:303–335.

Shah, P. A., and J. K. Pell. 2003. Entomopathogenic fungi as biological control agents. Applied Microbiology and Biotechnology 61:413–423.

Straub, C. S., D. L. Finke, and W. E. Snyder. 2008. Are the conservation of natural enemy biodiversity and biological control compatible goals? Biological Control 45:225–237.

Vandermeer, J., I. Perfecto, and S. Philpott. 2010. Ecological Complexity and Pest Control in Organic Coffee Production: Uncovering an Autonomous Ecosystem Service. BioScience 60:527–537.

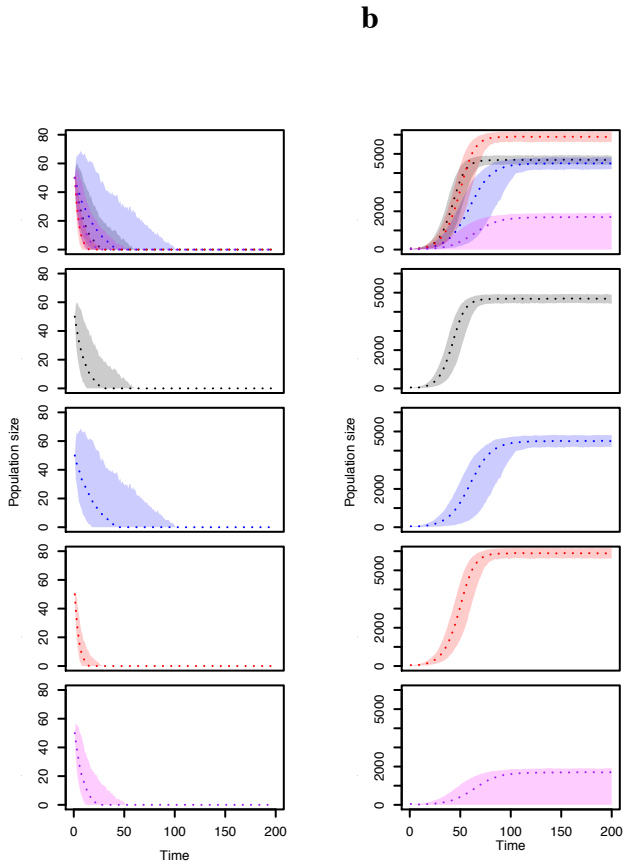

Fig. 3.1 Projected population time series. Total aphid population sizes are projected for 200 time units assuming a 30X30 spatial grid placed on a torus using parameters fit by maximum likelihood inference to the experimental data where aphids had **(a)** low dispersal and **(b)** high dispersal while alone (black) or in the presence of the following natural enemies: ladybird beetle only (red), entomopathogenic fungus only (blue), and fungus and beetle combined (purple). 95% confidence bands are plotted around mean model predictions (dotted lines) for n=1000 simulations. In top row, all low dispersal and all high dispersal plots are overlaid to show differences between treatments.

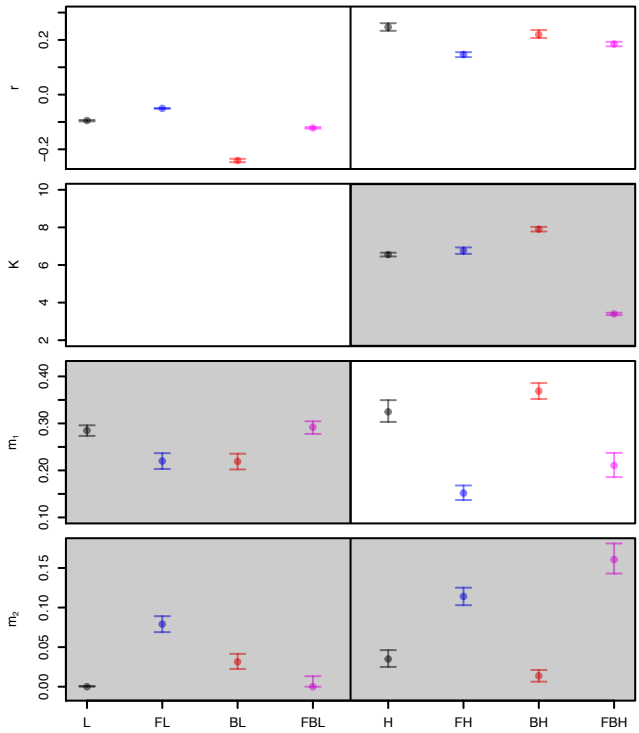

Fig. 3.2 Parameter estimates. Maximum likelihood fits to experimental data from treatments where aphids had L- low dispersal and H- high dispersal while in the presence of the following natural enemies: B- ladybird beetle only, F- entomopathogenic fungus only, and FB- fungus and beetle combined. Parameters include r, growth rate of aphids, K, carrying capacity of aphids, m_1, local migration rate, and m_2, long-distance migration rate. 95% confidence intervals using likelihood ratio test are plotted.

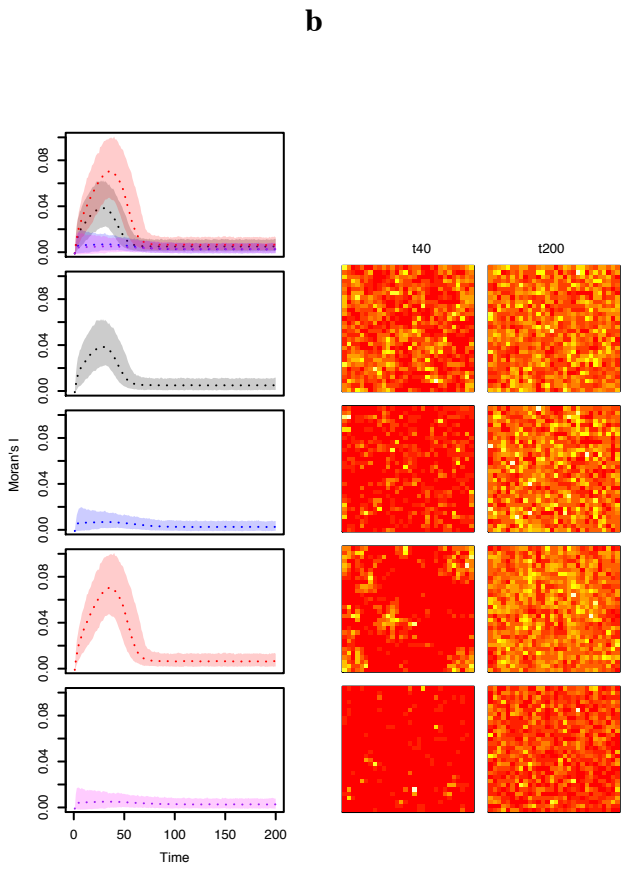

Fig. 3.3 Projected spatial clustering of aphids with high dispersal. (a) Plotted are the means (dotted line), and 95% quantile confidence bands of Moran's I for *n*=1000 simulations of the coupled lattice model assuming a 30X30 spatial grid on a torus using parameters estimated from treatments where aphids had high dispersal and no natural enemies (black), or while in the presence of the following natural enemies: ladybird beetle only (red), entomopathogenic fungus only (blue), and fungus and beetle combined (purple). **(b)** Example spatial plots show different levels of clustering for treatments (corresponding with rows in **a**) at time 40 when clustering peaks for beetle only treatment and equilibrium, time 200. White colors correspond to larger, and red to lower population sizes of aphids.

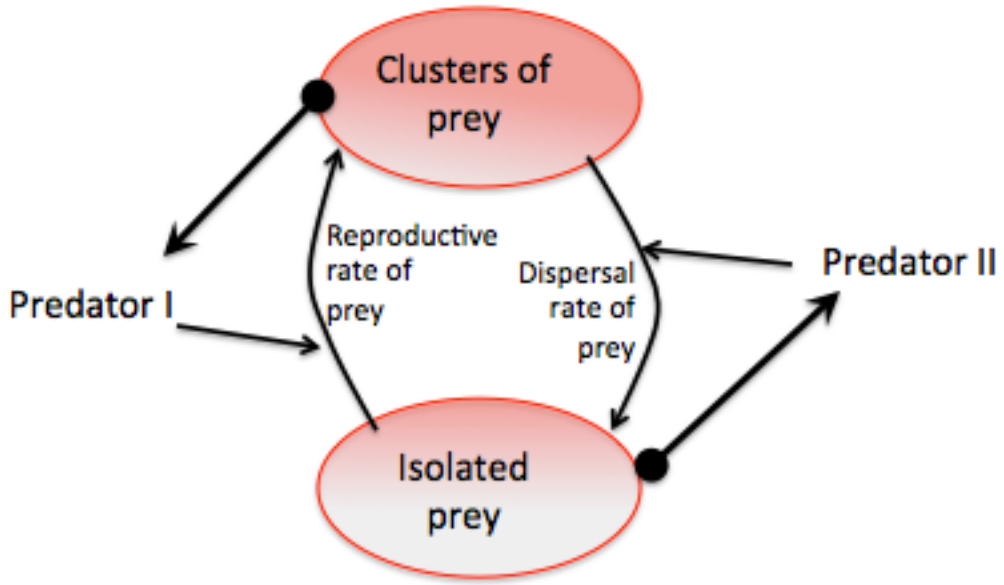

Fig. 3.4 Hypothesized generalization of coexistence of two competitors (the two predators) in a spatially extended system, where one of the predators has a trait-mediated effect in inducing the prey to disperse faster and the other has a trait-mediated effect in inducing the prey to form spatial clusters. In the absence of predator II, the prey will tend to occur as isolates, inducing extinction of predator I. In the absence of predator I, the prey will tend to occur in the clusters, inducing extinction of predator II.

APPENDIX 2

Supplementary Figures

a **b**

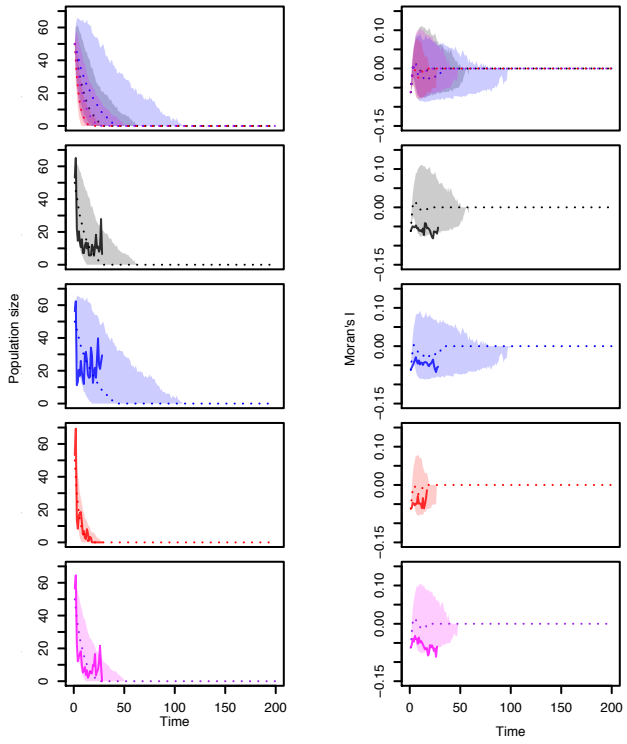

Fig. S3.1. Low dispersal model fits to data. Plots of total aphid population size and Moran's I for low dispersal treatments where aphids were alone (black) or under control by fungal pathogen (blue), beetle predator (red), or both (purple). Mean total population size **(a)** and Moran's I **(b)** across all repetitions from experiment are plotted as solid lines and overlaid on top of mean model predictions (dotted lines) and 95% confidence intervals constructed from 1000 simulations of the model assuming a 4X5 spatial grid with edge effects, projected to 200 time steps. All treatments are overlaid in top row.

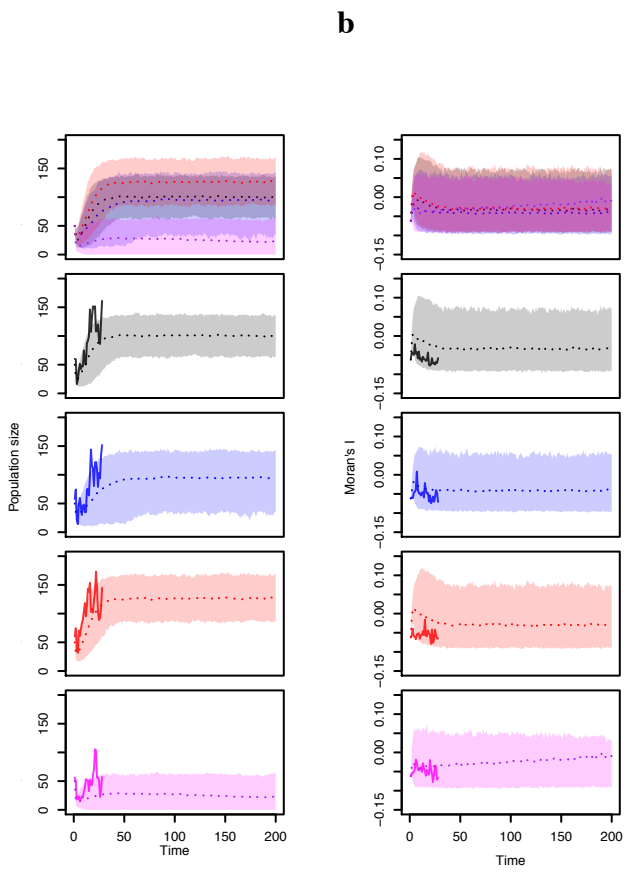

Fig. S3.2. High dispersal model fits to data. Plots of total aphid population size and Moran's I for high dispersal treatments where aphids were alone (black) or under control by fungal pathogen (blue), beetle predator (red), or both (purple). Mean total population size **(a)** and Moran's I **(b)** across all repetitions from experiment are plotted as solid lines and overlaid on top of mean model predictions (dotted lines) and 95% confidence intervals constructed from 1000 simulations of the model assuming a 4X5 spatial grid with edge effects, projected to 200 time steps. All treatments are overlaid in top row.

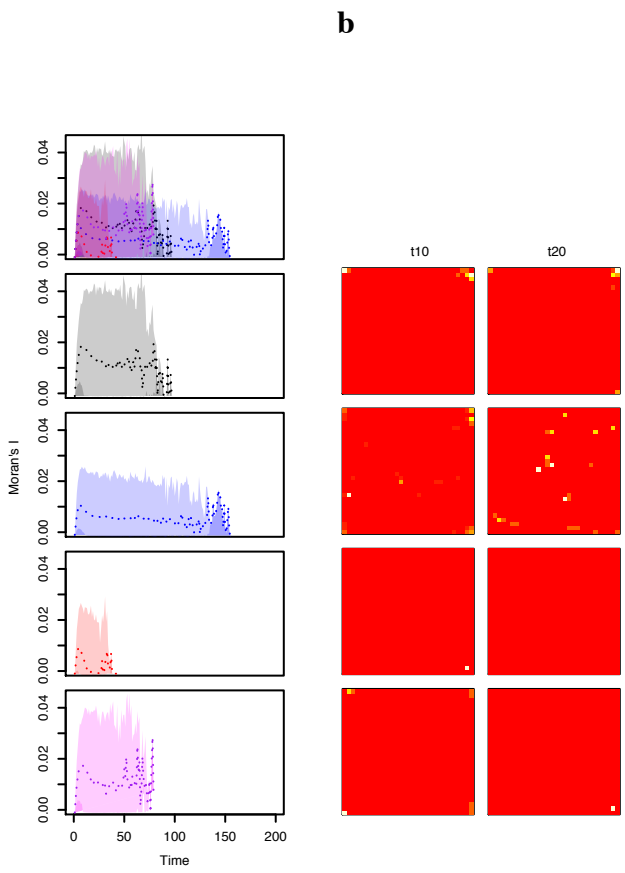

Fig. S3.3. Projected spatial clustering of aphids with low dispersal. (a) Plotted are the means (dotted line), and 95% quantile confidence bands of Moran's I for *n*=1000 simulations of the larger spatial-scale model assuming a 30x30 spatial grid on a torus using parameters estimated from treatments where aphids had low dispersal and no natural enemies (black), or while in the presence of the following natural enemies: ladybird beetle only (red), entomopathogenic fungus only (blue), and fungus and beetle combined (purple). **(b)** Example spatial plots show different levels of clustering for treatments (corresponding with rows in **a**) at time 10 and 20. White colors correspond to larger, and red to lower population sizes of aphids.

CHAPTER IV

Taylor made landscapes: using Taylor's law to scale between metapopulations and source-sinks in urban garden space

Theresa W. Ong, Kevin Li, Azucena Lucatero, Damie Pak, L'Oreal Hawkes, MaryCarol Hunter, John Vandermeer

4.1 Abstract

The structure of terrestrial landscapes is commonly viewed as a problem of statistical description defined by the number, size and distance between habitat patches. Yet, for organisms living in that landscape, structure may be perceived very differently depending on the dispersal capacity of the organism of concern. We assert that as dispersal across fragmented habitats increases, subpopulations are forced to overlap in space and synchronize in time, effectively shifting population structure from metapopulations to source-sinks. Taylor's law, a universal scaling law denoting a power law relationship between population size and variance, is used to indicate the synchrony of arthropod populations sampled across time in a fragmented urban landscape. Regardless of the fragmentation pattern existing in the landscape, short-ranged species are isolated to small, independent habitat patches (metapopulation-like) with subpopulations that oscillate out of sync, while long-ranged species traverse greater distances, synchronizing subpopulations across large, shared spaces (source sink-like). These results

suggest an inherent link between Taylor's temporal law and metapopulation theory, providing a potential mechanism to explain species-specific slopes of Taylor's law as arising from the ability of organisms to differentially experience fragmented space along the continuum between metapopulation and source-sink.

4.2 Introduction

Biological populations inevitably exist in a spatially extended context. The traditional view of exploring population dynamics locally is thus inevitably compromised by dispersal, which is to say, population dynamics regionally. This fact has led researchers to develop framings that take into account dynamics in both space and time, leading to conceptual skeletons such as metapopulations or source-sink populations, on which the flesh of dynamic complexity can be visualized [1–3]. In particular, the same spatial distribution of suitable habitat "islands" may present itself to a population as either a metapopulation-producing background, or a source-sink producing background, depending on the details of dispersal of the organisms comprising the population. Observables such as type and characteristics of the spatial distribution, including cross correlations among sites and the apparent noise exhibited from point to point in space [4], are both consequences and potential causes of the spatio-temporal population dynamics. Here we use the well-known relationship between mean and variance formulated as Taylor's law [5,6] to produce a cohesive theoretical framework that combines the observables of skewed frequency distributions, environmental versus demographic stochasticity, and population synchrony, so as to query the issue of whether populations are metapopulations or source/sink populations. We suggest that divergent dispersal ranges cause shifts in the frequency distributions of organisms across habitat patches, providing a biological mechanism for skewed distributions [7] that logically connects ideas of metapopulation and source/sink theory with population synchrony [8].

Furthermore, this mechanism is modified by the balance between demographic versus environmental forces to predictably constrain Taylor's temporal law [9]. With this framework we are able to integrate elements of landscape ecology, metapopulation theory, and Taylor's law under a shared notion of scale. We posit that temporal population fluctuations will be more synchronous across space in source-sink landscapes than in metapopulation landscapes, and, furthermore, we derive the potentially practical conclusion that populations closer to a source-sink state will have slopes of Taylor's temporal law near 2.0, and those closer to metapopulations near 1.0.

Applying this theoretical framework to a real life situation of three groups of arthropods in an urban garden setting, we examine how "perceptions" of landscape structure (i.e., on the part of the arthropods) influence the synchrony of populations and consequently the slope of Taylor's temporal law. Using populations of aphids, ladybird beetles, and parasitoid wasps sampled regularly across an entire city landscape over three time periods, we determine if and at what spatial scale abundance and temporal variability are influenced by the size of urban garden patches. This allows us to posit where along the continuum from metapopulation to source-sink each member of this real community of arthropods, coexisting in the same physical space may deferentially perceive urban garden patches as habitat.

4.3 Theoretical Framework

Taylor's law: The law has been described as one of the few unifying laws in ecology, with many case studies in support of its claims [5,6,10]. It arises from the seemingly ubiquitous power law relationship between population sizes and their variances, which has been applied broadly to a great diversity of disciplines ranging from physics to economics [6]. There are two

forms of the law, one spatial and one temporal. Taylor's law for temporal fluctuations states that the variance (V) of population numbers over time will follow a power function relationship to the mean (M) of that population over the same time frame, i.e., $V = aM^b$ [5]. The exponent b of Taylor's temporal law, the slope of the linear regression on the log-scale, indicates whether temporal population fluctuations are invariant to population size (slope = 2), or whether larger populations are less variable than expected by chance (2 > slope > 1). Particular focus has been directed towards providing mechanisms that explain slopes below 2 because they imply unusually high levels of stability (defined here as low variance) of large populations, an oft-sought goal for conservation [10–12]. The breadth of disciplines in which Taylor's law has been applied suggests that there may be some unifying mechanism to explain particular slope values. Yet the mechanisms proposed to explain the large incidence of intermediate values in empirical studies (e.g., interspecific competition, demographic stochasticity, measurement error) are either case specific or only apply when populations are sufficiently small [6].

When applied to the effect of mean population size on the variance of populations across space, slopes of 1 correspond to random spatial distributions, and larger slopes correspond to clustered distributions [5]. Although the spatial form is well studied, the connection between the spatial and temporal forms of Taylor's law is vague. The few studies that have examined connections between the spatial and temporal form of the law find no relationship [6,13,14]. Although most interest in this dilemma focuses on the direct relationship between the temporal and spatial form of the model, there is a related but distinct question that emerges directly from attempts at creating a useful framework for landscape structure, namely, the influence of landscape structure, a fundamentally spatial factor, on the temporal form of Taylor's law.

Here, we focus on the temporal form of Taylor's law because it has been used to indicate the synchrony of temporal oscillations for populations sampled across space [6,8,15]. If populations across a landscape grow and decline in complete synchrony, variance over time becomes independent of population identity [6]. Theoretical and empirical studies have confirmed this by showing that the slope of Taylor's temporal law switches from 1 to 2 exactly at the point of synchrony where trees began to exhibit masting behavior [6,8,15,16]. In fact, the synchrony of temporal population fluctuations across space has been associated with both forms of Taylor's laws. Theoretical work examining Taylor's spatial law in metapopulations showed that as temporal synchrony from patch to patch increases, the slope of Taylor's spatial law increases. This indicates that populations that oscillate in sync are also spatially clustered [4]. Though Hanski did not explicitly test the effect of spatial clustering on the temporal form of Taylor's law, an abundance of theoretical work shows that increasing dispersal rates and reducing inter-patch distance in metapopulations (methods to increase spatial clustering) can increase the synchrony of temporal population fluctuations across patches [17–22]. This would suggest a basic contradiction: on the one hand, dispersal is key for maintaining persistence of metapopulations, yet, on the other hand, isolation with attendant reduced dispersal, is expected to increase asynchrony in metapopulations, improving long term population persistence [23]. Indeed in at least one case, increased isolation increased asynchrony of populations when placed within the context of complex communities [24]. Here we attempt to resolve this contradiction by considering the effects of dispersal on population synchrony when the habitat patches of each population are isolated versus when the habitat space is shared.

Yet another factor known to influence population synchrony and the slope of Taylor's temporal law is the balance between demographic and environmental stochasticity. Stochasticity

can reduce variance in large populations, while strong environmental forcing can induce temporal synchrony, known as Moran effects [9,25–28]. However, it is also known that any random process producing a skewed distribution can also result in an apparent Taylor's law [7].

A model system: To test the effect of landscape structure on the synchrony of populations and Taylor's law, we adapt a Ricker model (1) [29] to include two main components: deterministic demographic forces and stochastic migration events. We consider n populations, where the density x of population i at time $t + 1$, is given by:

$$x_i(t+1) = x_i(t)e^{\left(\frac{r(1-x_i(t))}{k_i}\right)} + M \qquad (1)$$

The first term we take to represent the demographic forces; where k_i is the carrying capacity for population i, and r is the intrinsic rate of increase for all populations. We take advantage of the well-behaved nature of the Ricker model to control deterministic population dynamics via r, which bifurcates from point, periodic, and finally chaotic dynamics as r transitions from 0-2, 2-2.6924, and > 2.6924 respectively [29].

We model migration (M) in a spatially implicit form such that it follows a seasonal trend via a noisy sine curve. Seasonal forcing is a common and well-explored topic, yet models typically force birth rates or carrying capacities, not migration. Aphids for example, have two general peaks in migration; one in the early spring when overwintering eggs emerge from the soil as alates equipped with wings, and again in the fall when shortening day lengths signal the production of reproductives capable of flight [30]. Most organisms have peak migratory seasons so it stands to reason that many populations would be regulated as such. In a purely mixed population, we expect that such a stochastic, seasonal trend could synchronize subpopulations

across a landscape similar to the way the Moran effect is known to sync independent populations via shared external noise from a common environment [28]. We argue that this is particularly true in source-sink landscapes where unidirectional dispersal from source to sink patches should further strengthen the synchrony of population fluctuations across the landscape.

Yet it seems reasonable to assume that subpopulations having common shared habitat are much different than subpopulations that are completely isolated in space. These isolated patches become metapopulations, but rather than separation by physical barriers, they are separated by constrained home ranges. We argue that as populations become increasingly isolated, seasonal migratory signals become obscured by noise. Island effects such as increased extinction risks and stochastic long-distance emigration and immigration events may muddle the signal. Much like traditional metapopulations, isolated patches experience multi-directional dispersal events that can add asynchrony to population dynamics. We model this in a spatially implicit form by relaxing the seasonal signal of migration to complete randomness as the amount of shared habitat decreases (Fig S1, Appendix 3).

Specifically, the carrying capacity of each population is quantified in terms of the amount of habitat (ie. the number of urban gardens) within the dispersal range of an organism. We determine how much habitat space is shared on average in a landscape by calculating the Gini coefficient across k in all n populations for a single landscape simulation. A Gini coefficient of 0 indicates that patch size (k) is equal across all n samples, 1 indicates complete inequality (31). When the dispersal range is large enough, all populations should have the same k, causing $G_{k_1}^{k_n} \to 0$. Thus, $G_{k_1}^{k_n}$ depends on the distribution of habitats in the landscape, the n population locations, and the dispersal range of the focal species. The amplitude (A) of the migratory effect

is kept constant, but synchrony increases as dispersal range increases, $G_{k_1}^{k_n} \to 0$ and the noise collapses around a strong, seasonal cycle. This is achieved by constraining migration to values between 0 and 2*A* for all values of $G_{k_1}^{k_n}$. To do this,

$$M = A\left[1 + \delta Sin(\alpha t)(1 - G_{k_1}^{k_n})\right] + \varepsilon \qquad (2)$$

The number of migrants is determined by two main components that scale with $G_{k_1}^{k_n}$: 1) a simple random variable, $\varepsilon \sim unif(-AG_{k_1}^{k_n}, AG_{k_1}^{k_n})$, and 2) a seasonal signal modeled with a Sine function having period = $\frac{2\pi}{\alpha}$, and amplitude *A*. The seasonal trend is modified by its own stochastic term $\delta \sim unif(0,1)$ and $(1 - G_{k_1}^{k_n})$. This is done so that when $G_{k_1}^{k_n} = 1$, or the landscape is composed of completely isolated populations, the Sine function becomes 0 and

$$M = A + \varepsilon . \qquad (2a)$$

Since $\varepsilon \sim unif(-A, A)$ when $G_{k_1}^{k_n} = 1$, *M* remains constrained between 0 and 2*A*. When $G_{k_1}^{k_n} = 0$ all populations overlap meaning they all have the same *k*, and the first stochastic term ε drops out of the equation to give:

$$M = A[1 + \delta Sin(\alpha t)] \qquad (2b)$$

The Sine function has its own stochastic term, δ to allow some variation around the seasonal signal even for landscapes with populations that completely overlap.

This model allows us to test how the seasonality of stochastic migration events, determined by degree of habitat overlap, impacts the synchrony of populations across a landscape. Rather than explicitly model migration between specific habitat patches, we use this highly generalized spatially implicit mean-field approach. However, it is important to remember that despite this, the model does take into account space by including the $G_{k_1}^{k_n}$ parameter, which measures how much habitat space is shared on average in a landscape. The idea is to assess how a group of organisms experiences the landscape as a whole; is it split into many asynchronous metapopulations or does it function as a source-sink landscape where clear migratory pathways lead to synchrony? To measure synchrony in temporal population oscillations across a landscape, we calculate Pearson's correlation coefficient for all unique combinations of population time series within a single landscape simulation, and average them to give a mean cross-correlation value following historical approaches [4,11,18]. For a landscape simulation composed of *N* populations, the mean-cross correlation is the mean over all Pearson's correlation coefficients resulting from the lower half of the orthogonal *N* x *N* matrix of population time series crosses, excluding the identity line. This allows us to assess the synchrony of population oscillations across a landscape, which we then compare to calculations of Taylor's temporal law, discussed in Full Methods (ESM 4).

In reality, landscapes almost always result in populations that exist somewhere between metapopulations and source-sinks [31]. We note that in the classic metapopulation definition,

sinks have $k = 0$ [1]. In our model, the deterministic component disappears when all $k = 0$ such that dynamics are determined only by the stochastic migration term, indicating a pure sink patch. In contrast, large carrying capacities increase the effect of deterministic demographic processes relative to stochastic migration events.

4.4 Methods Summary

Full, detailed methods are available in electronic supplementary materials (Appendix 3). In summary, model was simulated for hypothetical landscapes parameterized to represent source-sink or metapopulations depending on degree of habitat overlap. Taylor's law was calculated, and population synchrony measured using cross-correlation coefficients. Then, at N=100 local and N=28 landscape sampling points taken across the city of Ann Arbor, MI, urban garden patch size was calculated for a range of hypothetical dispersal distances and used to parameterize the carrying capacities, k for each of the N sampling point populations. The model was used to project population changes at each sampling point, Taylor's law was calculated, and population synchrony was measured. These simulated population dynamics were compared to empirical calculations of dispersal distance (see Full Methods, ESM 4), Taylor's law and population synchrony for real population time series data of aphids, ladybird beetles, and parasitoid wasps taken at each of the N=128 sampling points across three sampling times.

4.5 Results and Discussion

Model results. Solutions of (1) are presented in Fig. 4.1 for three different Gini coefficients calculated over a collection of 100 habitat patches, illustrating the application of Taylor's law. The model behaves such that populations existing in landscapes composed of small, distinct patches (metapopulation-like) exhibit asynchronous dynamics with slopes of Taylor's

temporal law close to 1, in contrast to populations existing in landscapes composed of large, similar patches (source-sink-like), which exhibit large-magnitude, highly synchronous oscillations with slopes of Taylor's temporal law near 2 (Fig. 4.1).

Previous studies have been unable to produce realistic ranges for the slope of Taylor's law for large populations, but our model reproduces this range for any set of k depending on the relative balance between the effects of demography, migration and seasonality (Fig. 4.2) [6]. Each dashed line in Figure 4.2 is a null condition where only demography, migration or seasonally forced migration is in effect (see Full Methods, Appendix 3). The effects of demography (black dashed lines, $r = 2$, $G_{k_1}^{k_n} = 0.72$, $A = 0$), migration (red dashed lines, $r = 0$, $G_{k_1}^{k_n} = 0$, $A = 1$ to 100) and seasonally forced migration (blue dashed lines, $r = 0$ and $G_{k_1}^{k_n} = 1$, $A = 1$ to 100) alone all have slopes of Taylor's temporal law approaching 2, but different y-intercepts. When simulating using the full model (1), the dynamics are clearly stretched between the dashed reference lines (2a-4), resulting in a range of slope values falling between 1 and 2. The fit and slope of Taylor's law depends on how population means and variances are pulled between the effects of demography, migration, and seasonality (Fig. 4.2). By increasing A, the effects of migration are heightened, shifting dynamics diagonally upwards along the blue and red migration reference lines, reducing the slope (Fig. 4.2a). This makes sense, since stochastic migration events necessarily increase the mean and variance of populations. Increased seasonality, achieved by forcing the Gini coefficient to 1 while keeping all other parameters constant, causes declines in population variances and steeper Taylor's temporal law slopes (Fig. 4.2b). In our model, migration events are constrained around a seasonal signal when habitats overlap and $G_{k_1}^{k_n}$ approaches 1, accounting for the decrease in population variance. Demographic

effects are easily controlled in our model by varying the per-capita growth rate parameter r, which is well-known to transition from chaotic, cyclic and stable point dynamics as r decreases (the Ricker map) (Fig. 4.2c). The y-intercept of the demographic reference line (black dashed line) shifts upward with increases in r, causing slopes for Taylor's temporal law to increase. Population dynamics become chaotic as r increases, accounting for the increase in population variances that leads to higher Taylor's law slopes. In summary, stochastic migration events decrease Taylor's law slopes towards 1, while seasonality ($G_{k_1}^{k_n}=1$) and demographic effects (large r) increase Taylor's law slopes towards 2. The balance between these forces is consistent with the preponderance of intermediate slope values found in empirical studies [10–12].

Spatial distribution of urban gardens. Using urban gardens in Ann Arbor, MI as an example, we show that sub-sampling the same clustered habitat distribution at different spatial scales can result in dramatically different interpretations of landscape structure (Fig. 4.3) [32]. For 128 sample points positioned at regular intervals across the landscape at two spatial scales, we analyzed habitat patch size by summing the number of gardens falling within a certain radius of each sample location (Fig. 4.3b). As the radius used to measure patch size increases, samples transition from being composed of mostly small and a few large patches into being composed of mostly large and a few small patches (Fig. 4.3c and 4.4a). This is because at large radii, habitat regions in adjacent sample locations overlap (Fig. 4.3c). Thus, dispersal-range influences the skewness of the habitat size frequency distribution. To study this effect we calculate the Gini coefficient, over all sampled patch sizes measured for radii between 100 and 2000m. As expected, Gini coefficients move towards unity (total equivalence) at a rate dependent on the distance between samples and the overall dimensions of the sample area (Fig. 4.4b). Since our local scale plot (N = 100) is much more dense and smaller in area than the landscape scale plot

($N = 28$), samples become more similar at shorter sampling radii than the landscape plot alone or the landscape and local plots combined (Fig. 4.4b). Traditionally, sample independence is thought necessary for assessing the effect of landscape structure on populations. However, the correct distance to space samples for independence is difficult if not impossible to ascertain apriori and choice of sampling sites is often limited to practical realities [37,38]. We argue that eliminating potential overlap obscures important effects of the landscape, since sample independence is as much a result of sample design as the dispersal capacity of the focal organism. Increased dispersal capacity can also mitigate the effects of a fragmented landscape if long-range species can effectively traverse fragmented space [39]. Here we demonstrate how degree of sample dependence may help in understanding how a species perceives a fragmented landscape on a continuum from highly independent, small, isolated patches (metapopulation-like) to highly dependent, large, shared patches (source-sink like).

Using garden data to parameterize the model. For simulated populations (1) parameterized using actual garden data (from Fig. 4.3) as carrying capacities, the slope of Taylor's temporal law increases from 1 to 2 as the sampling radius increases, which also corresponds to an increase in mean cross-correlation (Fig. 4.5a). This occurs due to the synchronizing effect of seasonal migration events, which increases as habitat patches are shared by populations at large sample radii ($G_{k_1}^{k_n} \to 0$). At small radii, habitat patches are largely independent and skewed towards smaller sink patches. The population dynamics of these sinks are driven primarily by random migration events that increase the asynchrony of populations, causing the slope of Taylor's law to decline towards 1 and mean cross-correlation to move towards 0. We ran the model using carrying capacities derived from garden patch size at the local-level only, landscape-level only, and the full dataset including all combined samples (Fig.

3a). The results are strikingly similar regardless of what spatial-level patch size distribution data is taken, all of which effectively reproduce a realistic range of Taylor's temporal law slopes between 1 and 2 as documented by many empirical studies [6]. As expected, the spatial sampling-level influences the rate at which synchrony ($\text{slope} \to 2$) is achieved, since the distribution of patch size becomes homogenous ($G_{k_1}^{k_n} \to 0$) at smaller radii if the sample points are closer together (Fig. 4.4). Our theoretical framework may settle the dispute over whether dispersal increases or decreases synchrony by specifying the conditions under which dispersal occurs [17,18,21,23,24]. When populations share habitat space due to long dispersal ranges, the shared environment can induce a strong synchronizing effect on those populations. Even patches on the outskirts are synchronized to larger, source populations if dispersal is unidirectional from source to sinks. However, when populations have highly constrained ranges as in metapopulations, random long-distance colonization and extinction events between patches can induce asynchrony.

Deduced population structure of aphids, beetles and parasitoids. Calculating the slope of Taylor's temporal law and mean cross-correlation for actual populations of aphids, ladybird beetles and parasitoid wasps, we find that aphids had a slope approaching 2 and a large mean cross-correlation while ladybird beetles and parasitoid wasps had slopes closer to 1 and lower mean cross-correlations (Fig. 4.5b). Based on our theoretical findings, these slopes indicate that aphids should have long dispersal ranges and exist in source-sink habitats with synchronous population dynamics, while ladybird beetles and parasitoid wasps should exist as metapopulations with asynchronous population dynamics and short-range dispersal. To test these predictions we approximated dispersal range by comparing linear models predicting the coefficient of variation (*CV*) for abundance of each taxa across time as a function of patch size

for a range of radii (Full Methods, Table S1, Appendix 3). Empirical results largely confirmed theoretical predictions with aphids responding to gardens at much larger radii (2000m) than parasitoid wasps (150m) (Fig. 4.5a, Fig. S2). Our estimates of dispersal range are consistent across local, landscape and combined sampling areas. The best-fit models across all three sampling units vary a maximum of 50m for each taxa, giving us confidence in our method for determining dispersal range (Table S1, Appendix 3). Ladybird beetles did not respond to gardens at any of the radii examined; however, the low slope of Taylor's law and mean cross-correlation suggests that their populations are highly asynchronous and that dispersal in the city is constrained. Proclivity to utilize urban spaces as nesting habitat may explain why ladybird beetle population dynamics are not associated with urban garden patch size. Our empirical results both satisfy theoretical predictions and are biologically reasonable. Aphids are known to have long-dispersal ranges [30] and large, synchronized population booms and busts are typical of agricultural pests [40]. In contrast, natural enemies like ladybird beetles and parasitoid wasps are highly sensitive to local-factors associated with habitat quality, and may find navigating through highly disturbed landscapes like cities difficult [41–44].

Concluding remarks. It is not unusual to note that different organisms may perceive the same fragmented landscape differently depending on their dispersal range. Here we show that these perceptions may be inherently linked to the slope of Taylor's temporal law and the fundamental structure of populations. Not only do organisms respond to landscapes forming a continuum from metapopulation to source-sink population, but a single landscape may fall anywhere along this continuum simultaneously and differentially for each organism that exists within it. Though found to apply almost ubiquitously to a variety of systems, the mechanism behind Taylor's temporal law, its associated slope and connection to space are still debated. By

combining ideas from landscape ecology, metapopulation theory, and population and community ecology we provide a highly generalizable explanation for slopes of Taylor's temporal law between 1 and 2 that incorporates space and applies to both large and small populations. Using theory backed up with empirical results, we show that species-specific perceptions of landscape structure can cause skewed habitat-size frequency distributions that are responsible for the fit to Taylor's law. When dispersal range is short, organisms exist as isolated metapopulations, which experience a large degree of environmental perturbations and random migration events that cause asynchrony and slopes of Taylor's law closer to 1. In contrast, when dispersal range is long, organisms share habitat in the landscape and experience it as a source-sink with unidirectional dispersal events that cause synchrony and slopes of Taylor's law closer to 2. The results of this work imply that we may no longer be able to simplify landscapes to their obvious physical features such as size and distance between habitat patches. In the context of trophic interactions, other questions arise. Is biological control best achieved when organisms experience the landscape similarly, or does a disjunction between perceptions keep the system in a state of persistence that may be impossible to maintain otherwise? Is there a way of maximizing long-distance dispersal events in organisms of conservation concern while maintaining asynchrony of their populations across the landscape? The answers to such questions requires further study, but future studies testing the effects of fragmentation patterns on Taylor's temporal law across multiple landscapes and organisms may help untangle the complex relationship between population and landscape structures. Practical applications including the planning of urban landscapes that can maximize natural enemy persistence, while reducing synchronous dynamics in long-range pest species is just one example.

Authors' contributions

T.W.O. and J.V. conceived and developed the study. T.W.O, L.H., A.L. jointly designed and carried out field surveys. D.P and L.H. identified field specimens. T.W.O., K.L., D.P, and A.L. analyzed field data. M.H. provided original garden data. T.W.O. developed and analyzed the model. T.W.O. and J.V. drafted the manuscript, and all authors contributed revisions.

Competing interests

The authors declare no competing interests.

Funding

This research was supported by the Department of Ecology and Evolutionary Biology and the Rackham Graduate School at the University of Michigan.

Acknowledgments

Thank you to Ivette Perfecto and Stacy Philpott for comments on an early version of this manuscript. The University of Michigan Rackham Graduate School provided financial support.

4.6 References

1. Pulliam, H. R. 1988 Sources, Sinks, and Population Regulation. *Am. Nat.* **132**, 652–661.

2. Levins, R. 1969 Some Demographic and Genetic Consequences of Environmental Heterogeneity for Biological Control. *Bull. Entomol. Soc. Am.* **15**, 237–240. (doi:10.1093/besa/15.3.237)

3. Hanski, I. & Gilpin, M. 1991 Metapopulation dynamics: brief history and conceptual domain. *Biol. J. Linn. Soc.* **42**, 3–16. (doi:10.1111/j.1095-8312.1991.tb00548.x)

4. Hanski, I. 1987 Cross-correlation in population dynamics and the slope of spatial variance: mean regressions. *Oikos* , 148–151.

5. Taylor, L. 1961 Aggregation, variance and the mean.

6. Eisler, Z., Bartos, I. & Kertesz, J. 2008 Fluctuation scaling in complex systems: Taylor's law and beyond 1. *Adv. Phys.* **57**, 89–142.

7. Cohen, J. E. & Xu, M. 2015 Random sampling of skewed distributions implies Taylor's power law of fluctuation scaling. *Proc. Natl. Acad. Sci.* **112**, 7749–7754. (doi:10.1073/pnas.1503824112)

8. Ballantyne IV, F. & Kerkhoff, A. J. 2005 Reproductive correlation and mean–variance scaling of reproductive output for a forest model. *J. Theor. Biol.* **235**, 373–380. (doi:10.1016/j.jtbi.2005.01.017)

9. Lande, R. 1998 Demographic Stochasticity and Allee Effect on a Scale with Isotropic Noise. *Oikos* **83**, 353–358. (doi:10.2307/3546849)

10. Kilpatrick, A. M. & Ives, A. R. 2003 Species interactions can explain Taylor's power law for ecological time series. *Nature* **422**, 65–68. (doi:10.1038/nature01471)

11. Anderson, R. M., Gordon, D. M., Crawley, M. J. & Hassell, M. P. 1982 Variability in the abundance of animal and plant species. *Nature* **296**, 245–248. (doi:10.1038/296245a0)

12. Titmus, G. 1983 Are animal populations really aggregated. *Oikos* **40**, 64–68. (doi:10.2307/3544199)

13. Taylor, L. & Woiwod, I. 1982 Comparative synoptic dynamics. I. Relationships between inter-and intra-specific spatial and temporal variance/mean population parameters. *J. Anim. Ecol.* , 879–906.

14. McArdle, B., Gaston, K. & Lawton, J. 1990 Variation in the size of animal populations: patterns, problems and artefacts. *J. Anim. Ecol.* , 439–454.

15. Ballantyne, I. & J Kerkhoff, A. 2007 The observed range for temporal mean-variance scaling exponents can be explained by reproductive correlation. *Oikos* **116**, 174–180.

16. Satake, A. & Iwasa, Y. 2000 Pollen coupling of forest trees: forming synchronized and periodic reproduction out of chaos. *J. Theor. Biol.* **203**, 63–84.

17. Hastings, A. 1993 Complex interactions between dispersal and dynamics: lessons from coupled logistic equations. *Ecology* , 1362–1372.

18. Ranta, E., Kaitala, V., Lindstrom, J. & Linden, H. 1995 Synchrony in population dynamics. *Proc. R. Soc. Lond. B Biol. Sci.* **262**, 113–118.

19. Ranta, E., Kaitala, V. & Lundberg, P. 1997 The spatial dimension in population fluctuations. *Science* **278**, 1621–1623.

20. Ranta, E., Kaitala, V. & Lundberg, P. 1998 Population variability in space and time: the dynamics of synchronous population fluctuations. *Oikos* , 376–382.

21. Ruxton, G. D. & Rohani, P. 1999 Fitness-dependent dispersal in metapopulations and its consequences for persistence and synchrony. *J. Anim. Ecol.* **68**, 530–539.

22. Earn, D. J. D., Levin, S. A. & Rohani, P. 2000 Coherence and Conservation. *Science* **290**, 1360–1364. (doi:10.1126/science.290.5495.1360)

23. Hassell, M. P., Comins, H. N. & May, R. M. 1994 Species coexistence and self-organizing spatial dynamics. *Nature* **370**, 290–292. (doi:10.1038/370290a0)

24. Koelle, K. & Vandermeer, J. 2005 Dispersal-induced desynchronization: from metapopulations to metacommunities. *Ecol. Lett.* **8**, 167–175.

25. Grenfell, B. T., Wilson, K., Finkenstädt, B. F., Coulson, T. N., Murray, S., Albon, S. D., Pemberton, J. M., Clutton-Brock, T. H. & Crawley, M. J. 1998 Noise and determinism in synchronized sheep dynamics. *Nature* **394**, 674–677. (doi:10.1038/29291)

26. Bjørnstad, O. N. & Grenfell, B. T. 2001 Noisy Clockwork: Time Series Analysis of Population Fluctuations in Animals. *Science* **293**, 638–643. (doi:10.1126/science.1062226)

27. Sæther, B.-E., Tufto, J., Engen, S., Jerstad, K., Røstad, O. W. & Skåtan, J. E. 2000 Population Dynamical Consequences of Climate Change for a Small Temperate Songbird. *Science* **287**, 854–856. (doi:10.1126/science.287.5454.854)

28. Moran, P. 1953 The statistical analysis of the Canadian Lynx cycle. *Aust. J. Zool.* **1**, 291–298.

29. Ricker, W. E. 1954 Stock and Recruitment. *J. Fish. Res. Board Can.* **11**, 559–623. (doi:10.1139/f54-039)

30. Kring, J. B. 1972 Flight Behavior of Aphids. *Annu. Rev. Entomol.* **17**, 461–492. (doi:10.1146/annurev.en.17.010172.002333)

31. Jackson, D., Allen, D., Perfecto, I. & Vandermeer, J. 2014 Self-organization of background habitat determines the nature of population spatial structure. *Oikos* **123**, 751–761. (doi:10.1111/j.1600-0706.2013.00827.x)

32. Hunter, M. C. R. & Brown, D. G. 2012 Spatial contagion: Gardening along the street in residential neighborhoods. *Landsc. Urban Plan.* **105**, 407–416. (doi:10.1016/j.landurbplan.2012.01.013)

33. Lin, B. B., Philpott, S. M. & Jha, S. 2015 The future of urban agriculture and biodiversity-ecosystem services: Challenges and next steps. *Basic Appl. Ecol.* **16**, 189–201. (doi:10.1016/j.baae.2015.01.005)

34. Tilman, D., Knops, J., Wedin, D., Reich, P., Ritchie, M. & Siemann, E. 1997 The Influence of Functional Diversity and Composition on Ecosystem Processes. *Science* **277**, 1300–1302. (doi:10.1126/science.277.5330.1300)

35. Tilman, D. 1999 The ecological consequences of changes in biodiversity: a search for general principles. *Ecology* **80**, 1455–1474. (doi:10.1890/0012-9658(1999)080[1455:TECOCI]2.0.CO;2)

36. Cardinale, B. J., Srivastava, D. S., Emmett Duffy, J., Wright, J. P., Downing, A. L., Sankaran, M. & Jouseau, C. 2006 Effects of biodiversity on the functioning of trophic groups and ecosystems. *Nature* **443**, 989–992. (doi:10.1038/nature05202)

37. Legendre, P. 1993 Spatial Autocorrelation: Trouble or New Paradigm? *Ecology* **74**, 1659–1673. (doi:10.2307/1939924)

38. Zuckerberg, B., Desrochers, A., Hochachka, W. M., Fink, D., Koenig, W. D. & Dickinson, J. L. 2012 Overlapping landscapes: A persistent, but misdirected concern when collecting and analyzing ecological data. *J. Wildl. Manag.* **76**, 1072–1080. (doi:10.1002/jwmg.326)

39. Taylor, P. D., Fahrig, L., Henein, K. & Merriam, G. 1993 Connectivity Is a Vital Element of Landscape Structure. *Oikos* **68**, 571–573. (doi:10.2307/3544927)

40. Wallner, W. E. 1987 Factors Affecting Insect Population Dynamics: Differences Between Outbreak and Non-Outbreak Species. *Annu. Rev. Entomol.* **32**, 317–340. (doi:10.1146/annurev.en.32.010187.001533)

41. Bennett, A. B. & Gratton, C. 2012 Local and landscape scale variables impact parasitoid assemblages across an urbanization gradient. *Landsc. Urban Plan.* **104**, 26–33. (doi:10.1016/j.landurbplan.2011.09.007)

42. Langellotto, G. & Denno, R. 2004 Responses of invertebrate natural enemies to complex-structured habitats: a meta-analytical synthesis. *Oecologia* **139**, 1–10. (doi:10.1007/s00442-004-1497-3)

43. Jha, S. & Kremen, C. 2013 Resource diversity and landscape-level homogeneity drive native bee foraging. *Proc. Natl. Acad. Sci.* **110**, 555–558. (doi:10.1073/pnas.1208682110)

44. O'Rourke, M. E., Rienzo-Stack, K. & Power, A. G. 2011 A multi-scale, landscape approach to predicting insect populations in agroecosystems. *Ecol. Appl.* **21**, 1782–1791.

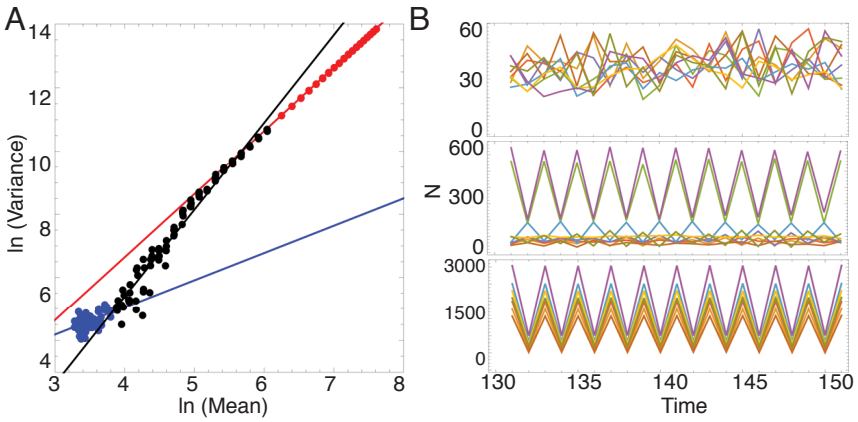

Fig. 4.1 Effect of landscape structure on Taylor's temporal law and population synchrony. Taylor's temporal law calculated for sets of N =100 simulated populations (**A**) selected to include mainly sink patches (small, dissimilar carrying capacities, k) in blue with Gini coefficient (G) = 0.43 and slope = 0.86 ($P < 0.001$, $R^2 = 0.26$), mainly source patches (large, similar k) in red with G = 0.15 and slope = 2.0 ($P < 0.001$, $R^2 = 0.99$), and both source and sink patches in black with G = 0.39 and slope = 2.75 ($P < 0.001$, $R^2 = 0.97$). Time series plots (**B**) of N =10 random populations pulled from blue sink simulations (top), black source-sink simulations (center) and red source simulations (bottom) showing the increasing degree of temporal synchrony. Each color represents a different population. For these plots, the intrinsic growth rate r = 2.2, the period for the stochastic seasonal forcing θ = 20 and the amplitude of stochastic effects A= 30.

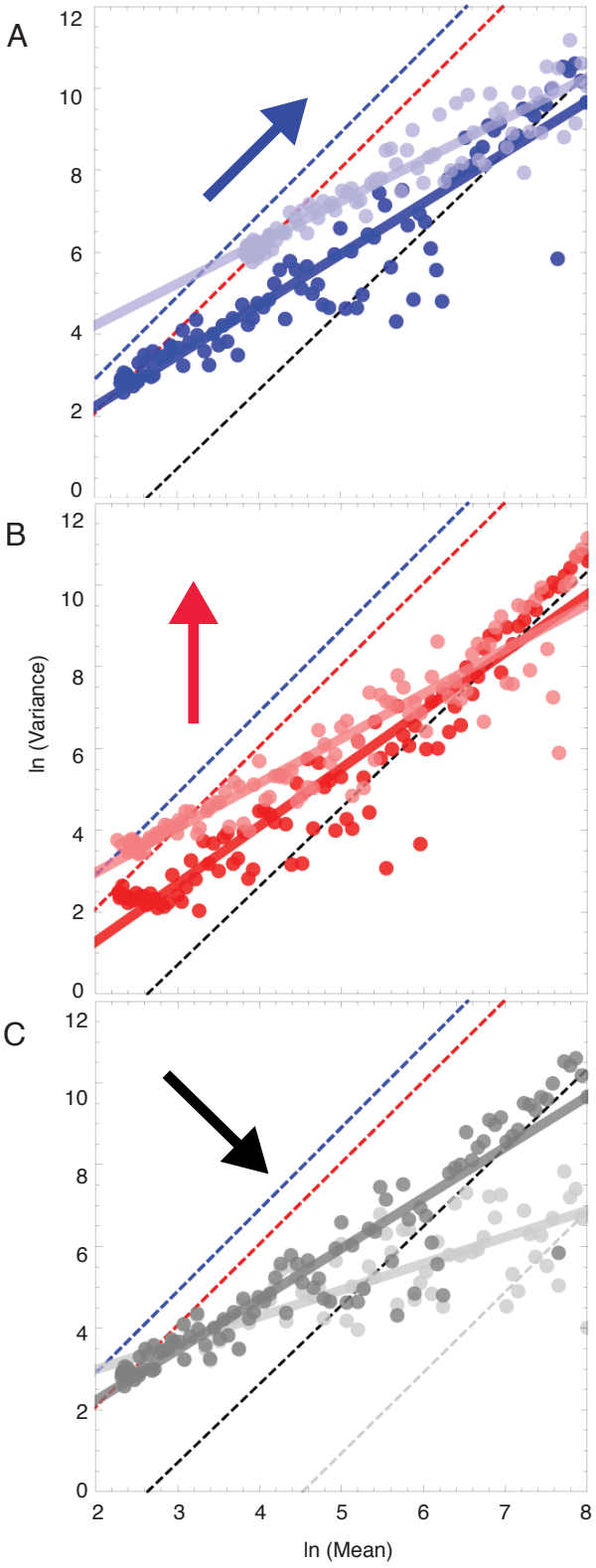

Fig. 4.2 Balance between demographics, migration and seasonality produces intermediate Taylor's law slopes. Reference Taylor's temporal slope lines for the effects of demography (black dashed lines, $r = 2$, $G = 0.72$, $A = 0$), random dispersal (red dashed lines, $r = 0$, $G = 0$, $A =$

1 to 100) and seasonally forced dispersal processes (blue dashed lines, $r = 0$ and $G = 1$, $A = 1$ to 100) alone (only linear regressions plotted, points for reference lines not shown). Reference lines are graphically compared to sets of n =100 populations simulated using full model and parameterized to have strong and weak migration **(A)**, seasonality **(B)** and demographics **(C)** effects. All points are populations simulated using full model and k values uniformly distributed between e^1-8. Simulations were run for 150 time steps and the last 100 used to calculate the means and variances plotted. High slopes with weak migration effects ($r = 2$, $G = 0.72$, $A = 10$, dark blue points) and low slopes with strong migration effects ($A = 50$, light blue points) in (**A**). Corresponding regressions plotted using thick lines with slopes = 1.24, 1.00; $R^2 = 0.89, 0.90$; $P < 0.001$ both. High slopes with strong seasonality (G forced to 1, dark red points) and low slopes with no seasonality (G forced to 0, light red points), while keeping $r = 2$, $A = 10$ and k values between e^1-8 in (**B**). Linear regressions plotted with thick lines have slopes = 1.41, 1.10; $R^2 = 0.91, 0.88$; $P < 0.001$ both, respectively. In (**C**), two demographic-only reference curves are plotted ($G = 0.72$, $A = 0$) and $r = 2$ (black dashed line), $r = 1.98$ (grey dashed line). High slopes with strong demographic effects ($G = 0.72$, $A = 10$, $r = 2$, dark grey points) and low slopes with weaker demographic effects ($G = 0.72$, $A = 10$, $r = 1.98$, light grey points). Corresponding regressions with slopes = 1.24, 0.65; $R^2 = 0.89, 0.73$; $P < 0.001$ both, respectively plotted with thick lines of corresponding color.

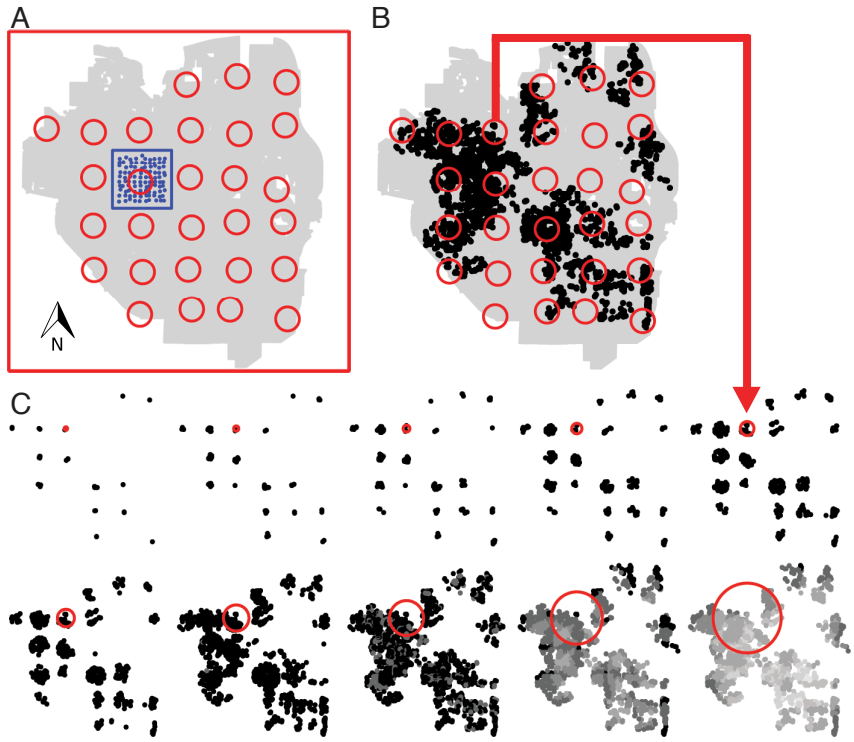

Fig. 4.3 Scaling between a metapopulation and source-sink landscape. (**A**) Sampling scheme of gardens in the area of Ann Arbor, MI (grey background). Sampling of arthropods was conducted regularly across the entire landscape at two spatial scales (red box: landscape-level and blue box: local-level) and three time points (June, July and August 2013). A total of $N = 28$ samples were conducted at the landscape-level (open red circles), and $N = 100$ at the local-level (blue circles). Landscape-level samples are drawn in (**B**) at a radius of 400m on top of actual distribution of urban gardens (closed black circles). Patch size was equal to number of gardens falling within the radius of a single sampling circle, visualized in (**C**) by plotting only the gardens (black/gray points) falling within radii of 100, 150, 200, 300, 400m (top row), and 500, 750, 1000, 1500, 2000m (bottom row) for landscape-level sampling points only. One patch is highlighted for each radius (open red circles) to show scale, with a red arrow connecting this point to its location among all landscape-level sample points plotted at the same 400m radius in (**B**). At a radius of 1000m and beyond, neighboring landscape-level samples begin to overlap; degree of overlap is indicated by the darkness of garden points with lightest points having the greatest overlap. The same patch size analysis was done for local-level samples, but not shown here.

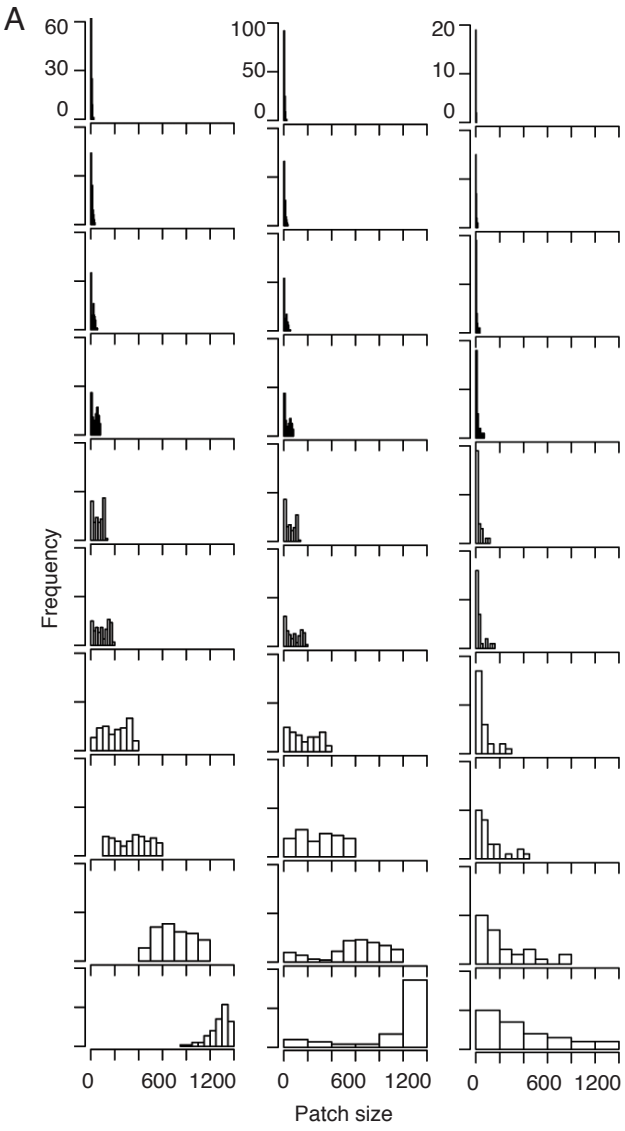
A
60
30
0
100
50
0
20
10
0
Frequency
0
600
1200
Patch size

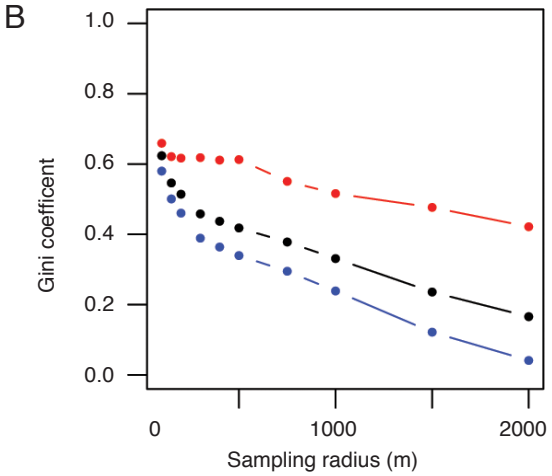
B
1.0
0.8
0.6
0.4
0.2
0.0
Gini coefficent
0
1000
2000
Sampling radius (m)

Fig. 4.4 Scale-dependent patch size distributions. (**A**) Histograms of patch size at each sampling radius of 100, 150, 200, 300, 400, 500, 750, 1000, 1500, 2000m (from top to bottom rows) are plotted for local-level samples (left column), local and landscape-level samples combined (middle column), and landscape-level samples only (right column). (**B**) Gini coefficients calculated over all patch sizes at each sampling radius for landscape-level samples (red), local-level samples (blue) and all sample points combined (black). A Gini coefficient of 0 indicates that patch size is equal across all samples, 1 indicates complete inequality.

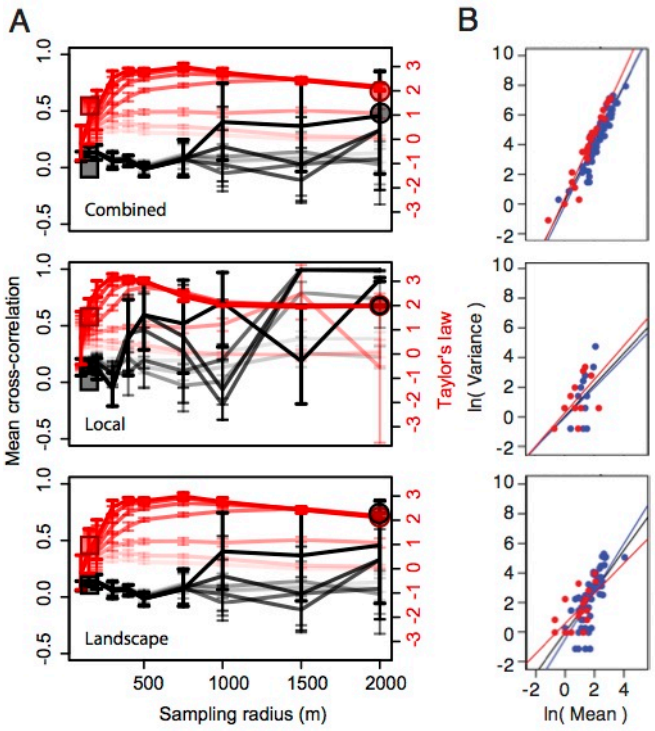

Fig. 4.5 Model predictions and empirical estimates of Taylor's law slopes and population synchrony of arthropods. The mean and 95% confidence intervals (resampling with replacement *N*=10000 replicates) for the slope of Taylor's temporal law (red) and mean cross-correlation (black) calculated across sets of 10 simulated populations, replicated 10 times, discarding the first 50 of 150 iterations (**A**). Population sets were parameterized using real garden patch size data as carrying capacities. Carrying capacities were randomly pulled from patch sizes calculated by counting the number of gardens falling within each sampling radius for combined, local, and landscape-level sample points (top to bottom panels). The Gini coefficient was calculated across carrying capacities in each set of 10 populations. In each panel, per capita growth rate r was varied from 1.6 (lightest) to 2.8 (darkest) in intervals of 0.2, progressing through stable point, periodic and chaotic population dynamics. For all simulations, $A = 30$ and $\theta = 20$. Actual survey results of arthropods were used to calculate slopes of Taylor's temporal law, mean cross-correlation and dispersal ranges, significant results were overlaid onto simulations for parasitoid wasps (square points) and aphids (circular points). Populations of ladybird beetles did not respond to gardens at any spatial scale so are not plotted. Linear regressions of Taylor's temporal law calculated for real populations (**B**) of aphids (top), ladybird beetles (middle), and parasitoid wasps (bottom) at landscape-level (red), local-level (blue) and all sample points combined (black). For aphids, slopes = 2.1581, 2.01165, 1.96036, $R^2 = 0.92, 0.89, 0.88$, $P < 0.001$ for all; ladybird beetles, slopes = 1.1406, 1.0173, 1.0668, $R^2 = 0.52, 0.39, 0.44$, $P < 0.001$ for all; and parasitoid wasps, slopes = 1.0081, 1.5955, 1.372548, $R^2 = 0.40, 0.56, 0.53$, $P = 0.003$, < 0.001, < 0.001 for landscape-level, local-level and combined sample points, respectively.

APPENDIX 3

Supplementary Table for **Taylor made landscapes: using Taylor's law to scale between metapopulations and source-sinks in urban garden space**

Organism	Sample Level	Null	100m	150m	200m	300m	400m	500m	750m	1000m	1500m	2000m
Aphids	Local	**48.72**	48.85	48.75	49.20	49.99	50.65	50.70	50.69	50.63	50.64	50.62
	Landscape	4.10	3.86	4.76	4.88	4.58	4.72	4.75	4.57	4.41	3.88	**3.71**
	Combined	61.66	59.19	59.18	59.56	60.44	61.87	62.43	62.09	61.79	60.15	**58.97***
Ladybird beetles	Local	**103.79**	105.40	105.11	104.79	104.63	105.45	105.30	105.57	105.72	105.20	105.77
	Landscape	**36.35**	38.35	38.08	38.22	38.33	38.28	38.31	38.34	38.34	38.25	38.01
	Combined	**136.61**	138.49	138.48	138.36	138.33	138.60	138.58	138.61	138.55	138.61	138.52
Parasitoid wasps	Local	102.93	102.07	**99.36***	101.38	102.65	103.19	103.33	104.62	104.87	104.49	104.87
	Landscape	27.96	**27.81**	29.01	28.81	29.16	29.14	29.09	29.02	28.96	29.00	29.47
	Combined	127.40	127.39	**125.46**	127.26	128.23	128.60	128.72	129.35	129.40	129.39	129.33

Table S4.1. Determining dispersal-range of arthropods. Akaike Information Criterion (*AIC*) values for linear models predicting organism coefficient of variation (*CV*) as a function of patch size calculated at various radii (column headers) for samples at the local-level, landscape-level, and combined levels. To determine if and at what radius organism coefficient of variation was sensitive to garden patch size, models for each radius were compared along with a null model across rows, bold type indicates the best-fit model with lowest *AIC*. *indicates significant ($P \leq 0.05$) regressions.

Supplementary Figures for **Taylor made landscapes: using Taylor's law to scale between metapopulations and source-sinks in urban garden space**

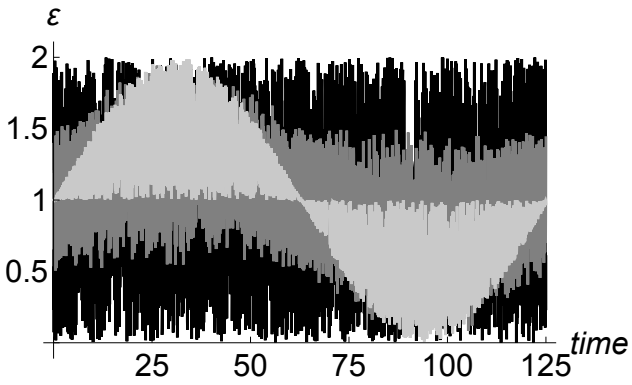

Fig. S4.1. Stochasticity driven by dispersal and the shared environment. Stochastic terms were modeled so that they transition from dispersal driven to environment driven as the Gini coefficient across all carrying capacities/patch sizes, G is varied from 0 to 1. Stochasticity is plotted for amplitude $A = 1$, θ (period)= 20, and $G = 1$ (black), 0.5 (dark gray) and 0 (light gray).

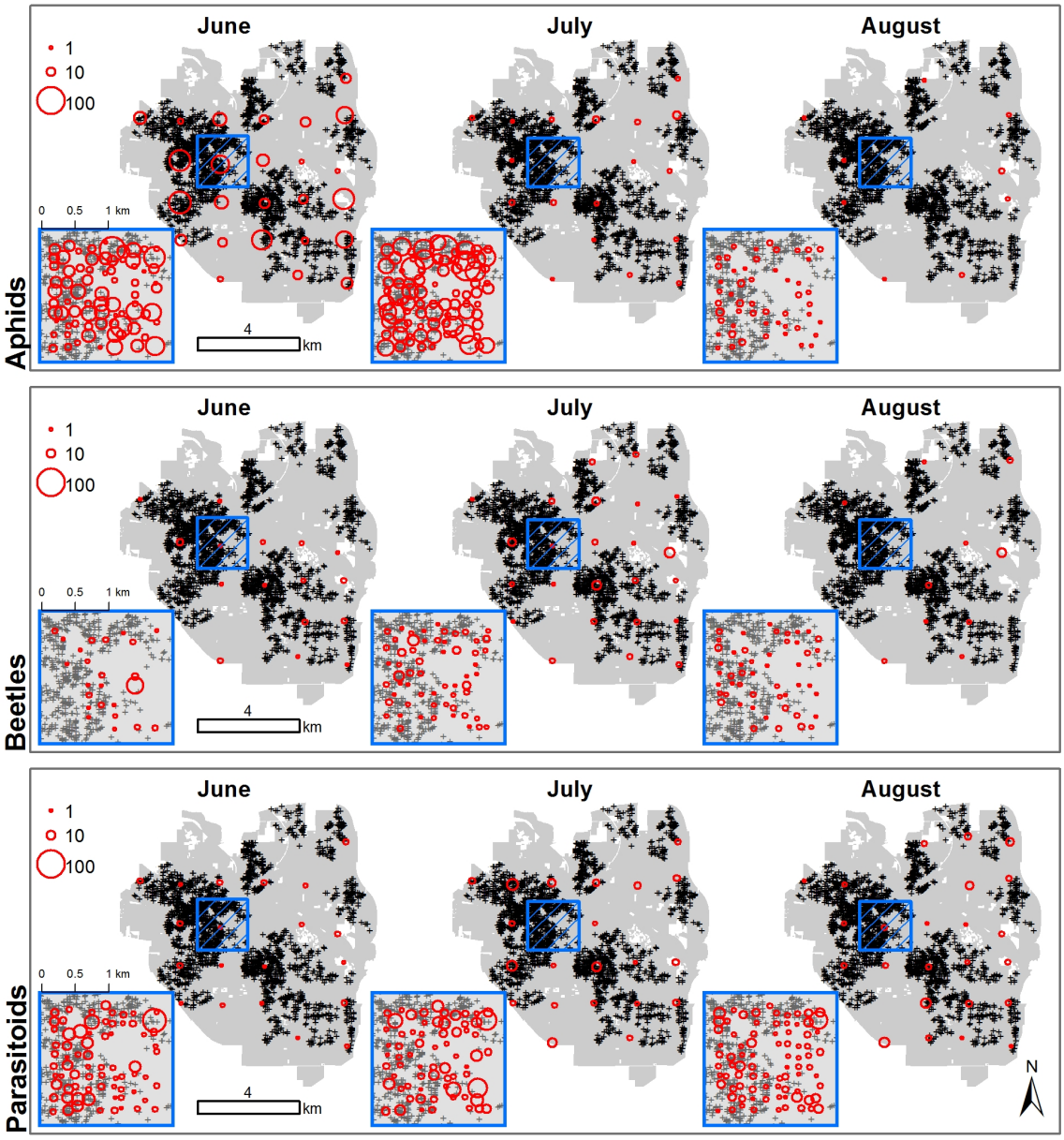

Fig. S4.2. Arthropods are sensitive to urban gardens at different spatio-temporal scales. The size of red, open circles indicate the abundance of aphids (top row), ladybird beetles (middle row), and parasitoid wasps (bottom row) in June (first column), July (second column) and August (third column) 2013. Small blue box indicates position of local-scale sampling area, which covers downtown Ann Arbor, MI and adjacent neighborhoods with 100 points placed an average of 128m apart. Larger blue box is an enlarged view of local-scale samples. Landscape-scale sampling covers the entire city landscape with 28 points placed an average of 1470m apart. Easement gardens are indicated by black and grey plus signs.

Full Methods for **Taylor made landscapes: using Taylor's law to scale between metapopulations and source-sinks in urban garden space**

Theory: The model was parameterized using different sets of k values, representing different perceptions of landscape structures both theoretical and actual. Slopes for Taylor's temporal law were determined by regressing the mean and variance of each set of simulations on a log-scale. To remove transience, simulations were run for 150 time steps and only the last 100 time steps used to calculate Taylor's temporal law. After removing transience, mean cross-correlation was calculated for each simulated landscape to measure population synchrony.

To graphically assess how simulation results for Taylor's law are influenced by demography, migration, and seasonality, we examine results of the full model (1) with respect to deterministic demography, stochastic migration, and stochastic seasonal migration only reference lines.

By setting $A = 0$, only demography is in effect, reducing (1) to the classic Ricker model [29]:

$$x_i(t+1) = x_i(t)e^{\left(\frac{r(1-x_i(t))}{k_i}\right)} \quad (3)$$

To look at effects of migration in isolation, we set $r = 0$, reducing (1) to

$$x_i(t+1) = x_i(t) + M \quad (4)$$

When $G_{k_1}^{k_n} = 0$ in (4), population dynamics arise from completely random migration events (2a). When $G_{k_1}^{k_n} = 1$ in (4), population dynamics arise from random migration events with a strong seasonal trend (2b, Fig S1).

To create the demography only reference line, we use (3) to simulate 100 populations with *k* values set to range uniformly between e^1-8, so that the log of simulated population sizes fall between 1-8, representing a range from very small to very large populations. The demography reference line is the linear regression of population size versus variance for these 100 simulations. For the null conditions where only migration is in effect (4), *k* does not affect population size. Thus to create migration only reference lines, we simulated 100 populations with the amplitude of migration events *A* ranging from 0 to 100 in order to achieve a range of population sizes for which we can apply linear regressions of size versus variance. For stochastic migration $G_{k_1}^{k_n} = 0$, and for stochastic, seasonal migration $G_{k_1}^{k_n} = 1$. When the *k* values in a landscape simulation are all different, $G_{k_1}^{k_n} = 0$, and when they are all the same $G_{k_1}^{k_n} = 1$. Thus $G_{k_1}^{k_n}$ depends on the distribution of *k* values used in a landscape simulation. However, for our migration only reference lines we wanted to isolate the effect of the $G_{k_1}^{k_n}$ term from *k*. Thus for these reference lines, we removed the effect of *k* on $G_{k_1}^{k_n}$ by turning $G_{k_1}^{k_n}$ into a constant of 0 and 1 to represent the effect of stochastic migration and stochastic, seasonal migration only, while keeping the range of *k* values the same as those used in the demographic only reference line. Please note that this was done only for the migration reference lines. In all other simulations $G_{k_1}^{k_n}$ is dependent on the *k* distribution of the landscape simulation.

Arthropod census. Glue-based, yellow sticky card traps were used to monitor aphid, ladybird beetle, and parasitoid wasp populations in Ann Arbor, MI during the months of June, July and August 2013. The sticky traps were placed at mapped grid points regularly across the landscape at two spatial scales. One set of map points corresponded to a grid over the total area of the city of Ann Arbor (landscape-scale), and the second set covered the area of downtown Ann Arbor and adjacent neighborhoods (local-scale). The finer, local-scale grid had 100 points spread an average of 128m apart. The coarser, landscape-scale grid had 28 points, spread an average of 1470m apart. At each point, a sticky trap was either taped to a metal street pole or stapled to a tree or wooden post at breast height. Every 5 weeks for 15 weeks (3-months), the sticky traps were collected and sampled for abundance. Each sticky trap location represents an individual replicate. Characteristic morphological features were used to identify each aphid, ladybird beetle and parasitoid wasp individual. While we did not identify individuals into families or assign them into morpho-species (due to degraded sticky trap samples), we did exclude predatory wasps, specifically those from the family Vespidae. Though Vespid wasps are important for controlling garden pests, we were more interested in parasitoid wasps due to their reliance on floral resources and potential to be natural enemies of aphids. The mean and variance for each group of organisms was plotted on a log-scale and regressed for local samples, landscape samples and both local and landscape samples combined. The slopes of these regressions are the slopes of Taylor's temporal law for each organism and each set of sample points. We calculated mean cross-correlation for the time series data of each taxa at local, landscape and combined scales.

Garden census. Garden census data was taken from [32], in which all private properties within the entire Ann Arbor, MI municipal region ($N > 20000$) were surveyed in person,

recording the location and presence of easement gardens (municipally owned green space that falls between the sidewalk and the road) [33]. In Ann Arbor, homeowners are required to care and manage these city-owned parcels. The universal tranverse mercator (*UTM*) coordinates of any parcel showing signs of horticulture (other than mowed lawn) was recorded as an easement garden. Both primarily aesthetic and food-related gardens were recorded since both are important for insect populations. Further details are available from the original source [32]. Although the use of easement gardens in this study excludes other examples of urban agriculture in Ann Arbor (public gardens, community gardens, backyard gardens, etc.), it is a consistent census tool that has been extensively ground-truthed in the study area. Results from the original mapping study showed that easement gardens are significantly clustered in space, which the authors argued is a result of a spatial-contagion effect [32]. Visual access to the nearest neighbor's easement garden increased the intensity of garden clustering so that homeowners were more than twice as likely to have an easement garden if one existed within 30m. Due to this spatial-contagion effect, we expect areas with many easement gardens to contain other kinds of urban agriculture in the region as well. Thus in this study, we use easement gardens as a proxy for urban gardens, generally. Garden patch size was calculated at each sampling point where arthropod data was taken by summing the number of gardens falling within a radius of 100, 150, 200, 300, 400, 500, 750, 1000, 1500, and 2000m from the sampling location. This range of radii was chosen so that samples go from independent to overlapping, as the sampling radius increases and $G_{k_1}^{k_n} \to 0$.

Determining dispersal range. In order to determine dispersal range for each sampled organism we compared several linear models predicting the coefficient of variation (*CV*) for abundance across time as a function of patch size at a particular sampling radius. The *CV* is equal to the standard deviation divided by the mean of the three abundances sampled in June, July and

August 2013. The *CV* was chosen as the predictor variable since it is directly related to Taylor's temporal law, which compares the mean and variance across several populations on a log-scale. In addition, *CV* is a statistic used to quantify population dynamics in many empirical studies. Because *CV* values indicate the degree of population variability over time, conservation practitioners use this statistic as a proxy for population persistence and stability [34–36]. The Akaike Information Criterion (*AIC*) for each radius was compared to a null model to determine if and at which radius patch size predicts organism *CV*. This approach tests at what distance, patch size best predicts the population dynamics of each organism. We define dispersal range as this distance at which population dynamics are most sensitive to underlying habitat features. Thus, the radius with the lowest *AIC* is the dispersal range of the organism. To test for consistency, we determined radius of influence for local-scale, landscape-scale and combined datasets separately. If the distance at which organism *CV* is most sensitive to garden patch size is a good definition of dispersal range, this range should remain fairly consistent across local-scale, landscape-scale and combined datasets.

Empirical Taylor's law and cross-correlation coefficients. Using data from the arthropod census, we calculated Taylor's temporal law for sampled populations of aphids, parasitoid wasps and ladybird beetles at the landscape, local, and combined spatial scales. The slope of Taylor's law was calculated by regressing means and variance of populations across the three sampled times on a log-scale. Significance of regressions was assessed using *F*-tests. To assess population synchrony, mean cross-correlation was calculated for each arthropod type by taking the mean of Pearson's correlation coefficient for all 3-pt empirical time series in the lower half of the orthogonal N x N matrix of all unique population crosses, excluding the identity line for local (N=100), landscape (N=28), and combined (N=128) spatial scale sampling points.

Comparing model predictions and empirical results. To assess how well the model (1) predicts data on how organisms respond to gardens as habitat in Ann Arbor, we simulated populations using garden patch size data as carrying capacities, *k*. Recall that patch size was calculated at different radii for local, landscape, and combined spatial scale sample points using the methods described earlier. Each radius represents a different perception of the urban gardens in Ann Arbor, ranging from small, isolated patches to large overlapping patches as the radius increases. To understand how perceptions of the landscape would influence Taylor's law and population synchrony, we simulated sets of 10 populations at each sampling radius and dataset of interest. These sets of 10 populations were used to calculate Taylor's temporal law and mean cross-correlation after discarding the first 50 of 150 time step iterations. Each set of 10 populations is considered a landscape simulation since $G_{k_1}^{k_n}$ for each individual simulation is calculated across the 10 *k* values in a set. The 10 *k* values were pulled from garden patch size data at random, but were specific to the sampling radius and dataset of sampling points used. For each sampling radius and dataset of sampling points, we varied *r* values from 1.6 to 2.8 in intervals of 0.2 so that we could assess the effects of progressing through stable point, periodic and chaotic population dynamics. Each landscape simulation was replicated 10 times. For all simulations, $A = 30$ and $\theta = 20$.

For example, to predict the population synchrony of local-scale samples, we simulated 10 populations (a single landscape simulation) for 150 time steps with their *k* values randomly pulled from the dataset of garden patch sizes for the local-scale sampling points we have in downtown Ann Arbor (N=100). We measured population synchrony in the simulated time series, excluding the first 50 time steps, by calculating mean-cross correlation. In this case there are 10 populations in a landscape simulation, so the mean-cross correlation is the mean of Pearson's

correlation coefficient for the lower half of the orthogonal 10x10 matrix of all unique population crosses, excluding the identity line (4900 crosses total).

We repeated this analysis 10 times for each sampling radius (100, 150, 200, 300, 400, 500, 750, 1000, 1500, and 2000m), each sampling dataset (local, landscape, combined), and each *r* value (1.6 to 2.8 in intervals of 0.2), then calculated 95% confidence intervals for simulations of Taylor's law and mean cross-correlation using resampling with *N*=10000 replicates and replacement. Finally, empirical values for the slope of Taylor's law and mean cross-correlation for each taxa and spatial scale were overlaid onto simulation results at the sampling radius determined to be the dispersal range to test for consistency. If the empirical values of Taylor's law and mean cross-correlation fall within the 95% confidence intervals of the simulations, the model significantly predicts the empirical data.

CHAPTER V

Cities as sinks: population structure in pea aphids across an urban landscape

Ong, T. W., J. H. Vandermeer, and T. Y. James.

5.1 Abstract

Urban gardens are increasingly recognized for their potential to preserve biodiversity in harsh urban environments. Yet little is known about whether the biodiversity observed in gardens are long-term residents or short-term visitors. The ability of populations to persist in small, isolated habitat patches depends on adequate dispersal across the landscape. Using microsatellite markers we examine how urbanity influences the dispersal and population structure of pea aphids found in urban gardens. We find significant population structure across space and time, with evidence that genetic diversity decreases with increasing urbanity. Genetic diversity appears to source from the least urban sites, suggesting that cities as a whole may act as population sinks. These results suggest that populations persisting in urban garden patches are isolated and likely to experience significant population drift resulting from isolating effects of the urban environment. Conservation of biodiversity in urban gardens may require improving the permeability of urban landscapes for dispersing organisms.

5.2 Introduction

With more than 54% of the human population residing in urban areas, urban agriculture is emerging as an alternative food movement that eliminates the rural-urban divide between food production and consumption, improves food security, builds community, and provides green space for people and wildlife in urban areas (Brown and Jameton 2000, McClintock 2010, Goddard et al. 2010, Barthel et al. 2014, Lin et al. 2015, WHO 2016). Urban agriculture has gained a recent foothold in ecology with many studies showing concrete evidence that gardens can provide substantial resources to support a diversity of organisms that contribute to ecosystem services like biological control. Since urban agriculture is often small-scale, plots can be very carefully managed to include a surprising amount of biodiversity in terms of crops, ornamentals and their associated wildlife (pollinators, natural enemies, birds, etc.) (Akinnifesi et al. 2009, Lin et al. 2015). Resurgence of interest in urban agriculture in the United States and other parts of the world suggest a real potential to utilize urban spaces for the triple benefit of food production, community building, and conservation of biodiversity.

However, the long-term viability of biodiversity in urban areas is still in question (Douglas 1983, MacDougall et al. 2013, Beninde et al. 2015). Studies have shown that impervious surface, heat island effects, and pollution in urban areas may present critical obstacles for the dispersal and maintenance of populations persisting in urban garden refuges (Goddard et al. 2010, Beninde et al. 2015). Many species of conservation concern survive in small pockets of habitat in fragmented landscapes, however lack of dispersal between isolated populations significantly increases extinction risks (Perfecto et al. 2009, Vandermeer et al. 2010). Climate change further exacerbates problems as species distributions shift northwards, but landscapes remain fragmented (Sæther et al. 2000). Thus, improving the matrix between habitat

fragments is key for increasing the resilience of threatened populations to environmental perturbations (McClintock 2010, Goddard et al. 2010, Gardiner et al. 2013, Lin et al. 2015).

From a meta-population perspective, we can envision each garden as a habitat patch interspersed within a matrix of inhospitable urban space (Hanski and Gilpin 1991, Parris 2006, Johnson et al. 2013). Yet the degree to which organisms perceive urbanity as an obstacle for dispersal between gardens is difficult to assess in ecology, especially for small organisms where mark and recapture techniques are largely unreliable (Nathan 2001). Here we borrow techniques from molecular ecology to explore the dispersion and population structure of pea aphids sampled across an urban landscape in a single growing season. A variety of organisms inhabit urban gardens, but those of particular ease to study are also those of most concern to gardeners: agricultural pests. Pea aphids are specific to legumes including important agricultural crops like peas, greenbeans and soybean. They are long-distance dispersers and are sensitive to broad scale changes in percentage of non-crop habitat within agricultural landscape structure (Werling and Gratton 2010). Thus, aphids are an ideal study organism to address questions of how urbanity influences dispersal and persistence of populations.

Pea aphids are model organisms with a large number of pre-existing microsatellite markers in the literature (Caillaud et al. 2004, Wilson et al. 2004). They are parthenogenic, with alternating clonal and sexual reproductive phases. Sexual reproduction occurs only in the fall, when reproductive females mate with males to produce eggs that overwinter and hatch the following spring (Sack and Stern 2007). Due to this parthenogenic life cycle, all aphids sampled in a single growing season arise through asexual reproduction. We take advantage of this life cycle pattern to address questions of aphid dispersal. Since no genetic information is exchanged via sexual reproduction within a single growing season, any changes in genetic population

structure must arise through dispersal and competition. By tracking changes in population structure across space and time we can address how urbanity influences aphid dispersal patterns and overall genetic diversity. We predict that if urbanity presents a significant obstacle to aphid dispersal, we will find significant population structure through space and time, as well as decreasing genetic diversity with urbanity.

5.3 Methods

Aphid sampling and study sites

Five potted pea plants (*Pisum sativum* var. dwarf grey) were placed in urban gardens across the city of Ann Arbor, MI. Once a week from April 30 - August 13, 2013, all plants were surveyed for pea aphids (*Acrythosiphon pisum*). Every adult individual was typed as apterous (non-winged) or alateous (winged), collected, and stored in 95% ethanol. We then searched the plants exhaustively and destroyed all juveniles and other species of aphids. This was done to prevent oversampling of genetic clones, and so that any aphids sampled in the following week would be new migrants. Our sampling period was split evenly into 3 seasons: spring (weeks 1-6), summer (weeks 7-10), and fall (weeks 11-16). In addition to collections on our sentinel plants, we also searched adjacent vegetation for adult pea aphids in a sweep net using 30 full sweeps at each site, once per week.

In total we surveyed 11 urban gardens ranging in urbanity from 3.6 – 65% urban. We measured urbanity at each site by computing the % impervious surface within a 1000ft radius from the center of each garden. This was the maximum radius for sample site independence. Data on impervious surface was taken from the Ann Arbor municipal GIS database. All except the most urban site (To) belonged to the community garden organization Project Grow. Project Grow leases public and private land in the city of Ann Arbor to community gardeners. The plots

are split into small adjacent parcels that are managed individually by community members. However, all gardens adhere to strict rules regarding organic management. No synthetic pesticides or fertilizers are allowed. The most urban site was a private backyard garden in downtown Ann Arbor. This site was also under organic management.

DNA extraction and genotyping

DNA from whole aphids was extracted using a 10% Chelex solution following the methods in (Casquet et al. 2012). Samples were then subjected to multiplex PCR using 6 microsatellite markers split into two sets. The first set included the markers: ApH 10M, AlB07M and AlB08M. The second set included ApH 08M, S3.43 and A1A09M. All loci were taken from (Caillaud et al. 2004, Wilson et al. 2004). Markers of similar size ranges were tagged with different colored fluorescent dyes (HEX, TET, and FAM) in order to differentiate alleles in chromatograms. We conducted 8ul PCR reactions including 0.04ul exTaq DNA polymerase, 0.8ul 10X buffer, 0.9ul $MgCl_2$, 1.2ul dNTPs, 0.8ul BSA, and1ul ¼ dilution Chelex extracted DNA. Reverse and forward primers for microsatellite markers were added in the following amounts: ApH 10M (0.6ul), AlB07M (0.3ul), AlB08M (0.3ul), ApH 08M (0.5ul), S3.43 (0.3ul), A1A09M (0.3ul). Finally dH_20 was added to reach a total volume of 8ul per reaction. PCR involved 2m at 94°, followed by 40 cycles of 94° (20s), 50° (20s), and 72° (2m). Following PCR, samples were genotyped at the University of Michigan's sequencing core on a 3730XL Genetic Analyzer using ROX 500 as a size standard.

Alleles were called using the program GeneMarker. After the first round of multiplex PCR, we ran single locus PCR reactions for all loci where data was missing. Single locus reactions were run using the same concentrations of reagents and final reaction volume as our multiplex reactions except for microsatellite primers, which were added at 0.3ul per 8ul reaction

for all markers. Following the second round of allele calls, all individuals with >2 missing loci were excluded from the analysis. This process left us with $N = 129$ final genotyped samples.

Data analysis

We measured genetic diversity across all samples by calculating mean number of alleles, the Simpson Index, Hexp (Nei's 1978 gene diversity), and evenness across all 6 microsatellite loci. We tabulated all genotypes in order to determine the number of clones.

To assess population structure, samples were the split into 3 strata: site (11 total), season (3), and type (2). We used AMOVA (analysis of molecular variance) to compare genetic variation within and between samples and also between each strata. Significance was calculated using randomization tests with $N = 999$ repeats (Excoffier et al. 1992).We visualized population structure for site and season using DAPC (discriminant analysis of principal components) (Jombart et al. 2010). For all DAPCs we ran cross validations to choose the appropriate number of PCs to retain in the analysis.

We also conducted K-means hierarchical clustering to determine the number of unique genetic clusters across our entire dataset regardless of sampling site and visualized results with DAPC. Since pea aphids should only show signatures of clonal growth during our sampling period, we can track the movement of these apriori genetic clusters across site and season.

To assess the effects of urbanity, we measured genetic diversity within sites by calculating mean number of alleles, the Simpson Index, Hexp (Nei's 1978 gene diversity), and evenness across all 6 microsatellite loci per site. We ran linear regressions of each diversity metric as a function of % impervious surface to test for a relationship between urbanity and genetic diversity. To remove potential confounding effects of space, we first tested for isolation by distance by regressing Bruvo's distance (for microsatellite data with missing data) as our

measure of genetic distance against the Euclidean distance between the locations of each sample in space (Bruvo et al. 2004). This was followed by a partial mantel test to assess Pearson's correlation between genetic distance and distance in impervious surface (also Euclidian) while controlling for actual physical distance between samples.

5.4 Results

We found that pea aphids sampled across an urban area in a single clonal growing season had significant population structure across site (AMOVA, $p = 0.003$) and season ($p = 0.024$) but not type (apterous versus alateous) ($p = 0.190$) (Fig 5.1, Fig S1). Samples fell into seven distinct clusters (Fig. 5.2a), three of which were present throughout the sampling time period (Fig. 5.2b-d). Genetic diversity measured as mean H_{exp}, Simpson Index, and the number of alleles across loci per site significantly decreased with urbanity (Fig. 5.3). Evenness may increase with urbanity, though this relationship was only partially significant (Fig. 5.3, $p = 0.06$). When examining the distribution of genetic clusters across the sampled sites, we note that uncommon clusters occurred only in the least urban sites (Fig. 5.2).

Our samples ($N = 129$) had no genetic clones and high allelic diversity (Table 1). Low within sample (AMOVA, $p = 0.001$) and high between sample variation ($p= 0.001$) are consistent with the clonal reproduction of pea aphids that is expected to occur throughout the sampled period (Fig. S1). Our samples also displayed a significant isolation by distance relationship (Fig S2, $p = 0.004$). When distance was taken into account, there was still a significant relationship between genetic distance and urbanity, such that individuals from sites that were similar in urbanity were also more genetically similar (partial mantel test, $r = 0.078$ $p = 0.05$).

Loci	Alleles	1-D	H_{exp}	Evenness
A1A09M	8	0.75	0.76	0.79
D	16	0.80	0.81	0.62
S343	7	0.73	0.74	0.86
E	11	0.78	0.79	0.71
A	16	0.50	0.50	0.38
B	17	0.88	0.88	0.75
mean	12.5	0.74	0.74	0.68

Table 5.1. Summary of genetic diversity metrics for 6 microsatellite loci across all samples. Alleles = Number of observed alleles, 1-D = Simpson index, Hexp = Nei's 1978 gene diversity.

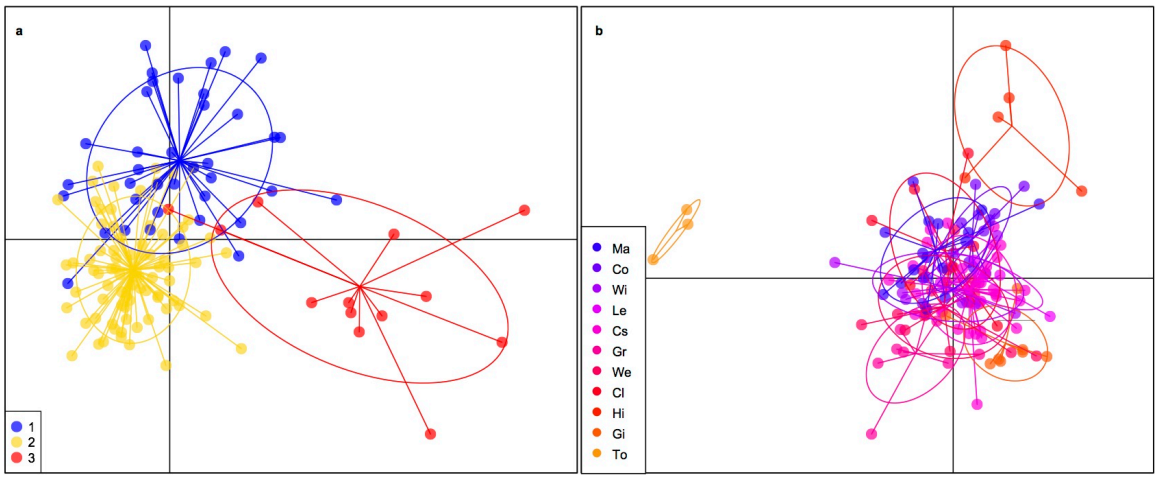

Fig. 5.1. Population structure across time and space. DAPCs showing segregation in alleles for pea aphids sampled across **a)** time (1= spring, 2= summer, 3= fall) and **b)** space. Sites are arranged from least to most urban (cool to warm colors).

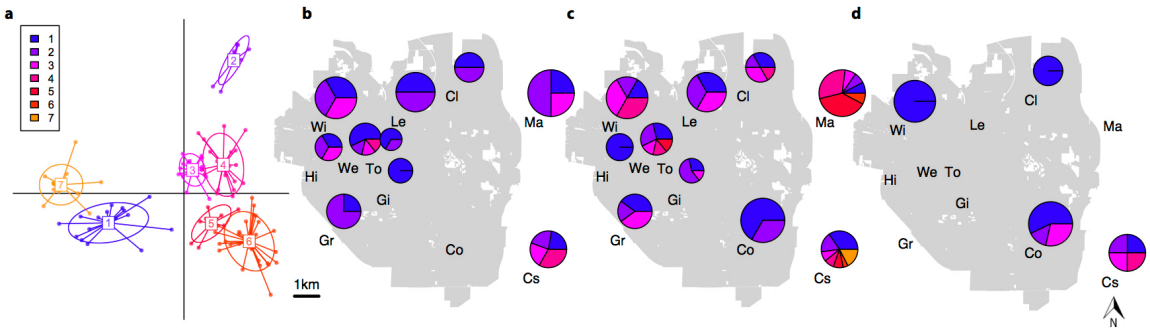

Fig. 5.2. Genetic clusters of pea aphid over space and time. a) DAPC showing seven distinct genetic clusters. **b)** Fractions of sampled populations in from each genetic cluster in spring, **c)** summer, and **d)** fall. Size of pie graphs correspond to rank from least (smallest) to most rural (largest) site. Grey polygon outlines the city limits of the study site (Ann Arbor, MI). 1km scale bar is included for reference. Sites are labeled with names. Labels with no pie indicate no aphids were found or successfully genotyped at that site and season.

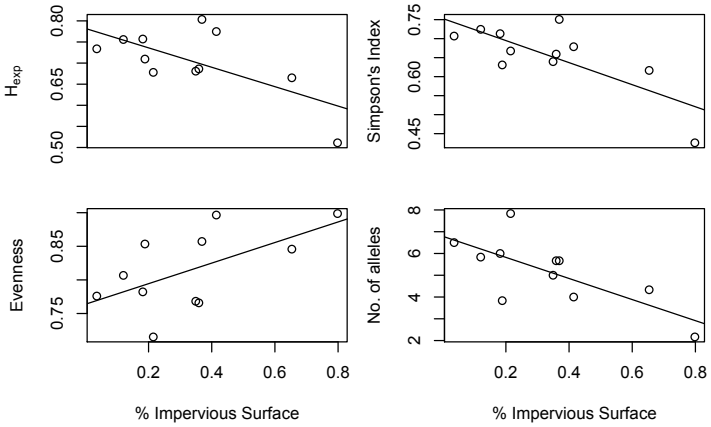

Fig. 5.3. Genetic diversity decreases with urbanity. Genetic diversity measured in mean H_{exp} (Nei's 1978 gene diversity) (adjusted $R^2 = 0.38$, $p = 0.025$), Simpson's Index (adjusted $R^2 = 0.53$, $p = 0.0065$), evenness (adjusted $R^2 = 0.27$, $p = 0.057$), and the number of alleles (adjusted $R^2 = 0.47$, $p = 0.012$) across all 6 microsatellite loci per site as a function of urbanity (% impervious surface) in each site. All linear regressions are significant, except for evenness.

5.5 Discussion

Population structure through time

Our results are consistent with previous studies that show evidence of high genetic diversity in parthenogenic aphid species despite the fact that we sampled aphids strictly within time periods associated with their clonal reproductive phase (Barro et al. 1995, Sunnucks et al. 1997, Sack and Stern 2007). The genetic divergence we observed occurred in a single growing season, suggesting that this divergence must result from either or a combination of competition between dominant genetic clusters and dispersal from surrounding areas not sampled in the study (Fig 1a). Pea aphids are specialists on legumes, and changes in population structure could potentially correlate with changes in crop type and abundance in the surrounding agricultural area as the weather warms and the growing season progresses (S R Singh and Emden 1979, Via 1999).

Population structure through space

Genetic similarity across sampled sites suggests that dispersal is indeed high for pea aphids across the city of Ann Arbor (Fig 1b). Aphids are known to be capable of flying long-distances, yet little is known about their dynamics across urban space (Halbert et al. 1981, Dixon 1998). Despite evidence of high dispersal across the study area, urbanity does appear to constrain movement such that aphids in more urban areas are less genetically diverse and more closely related to individuals from sites with similar levels of urbanity regardless of distance.

Source-sink structure

These results imply that though dispersal occurs across the city of Ann Arbor, urbanity does constrain movement. Due to the clonal nature of aphids during the sample period, increases in genetic diversity sampled across the growing season likely resulted from dispersal of aphids

from surrounding agricultural areas to the sampled urban gardens. In a metapopulation framework, surrounding agriculture sites may be envisioned as source populations, supplying urban gardens within cities with long distance migrants adding genetic diversity to isolated, low diversity populations. Cities as a whole may represent sinks, with the harshness of the surrounding habitat significantly hindering both the dispersal and survival of rare genotypes that are sourced from surrounding agricultural areas. This would explain the decrease in genetic diversity with urbanity and the fact that rare genetic clusters only occurred in the least urban sites (Figs. 2 and 3). Future studies could sample aphids in both urban gardens within the city and putative sources in surrounding farmland to confirm the hypothesized source-sink population structure. Regardless, our results indicate that urbanity does indeed constrain the dispersal and population structure of aphids, organisms that are capable of very long-distance dispersal. These results suggest that improving the permeability of urban landscapes may be essential to insure the long-term survival of the biodiversity that currently persists in small, isolated urban garden patches.

Acknowledgements:

We would like to thank L'Oreal Hawkes, Kerrel Spivey, Anderson Shu, and Azucena Lucatero for assistance collecting samples, extracting DNA and genotyping samples. Thank you to Project Grow and the University of Michigan Matthaei Botanical Gardens for hosting the study. The University of Michigan Rackham Graduate School and Department of Ecology and Evolutionary Biology provided funding.

5.6 Literature Cited

Akinnifesi, F. K., G. W. Sileshi, O. C. Ajayi, A. I. Akinnifesi, E. G. de Moura, J. F. P. Linhares, and I. Rodrigues. 2009. Biodiversity of the urban homegardens of São Luís city, Northeastern Brazil. Urban Ecosystems 13:129–146.

Barro, P. J. D., T. N. Sherratt, C. P. Brookes, O. David, and N. Maclean. 1995. Spatial and Temporal Genetic Variation in British Field Populations of the Grain Aphid Sitobion avenae (F.) (Hemiptera: Aphididae) Studied Using RAPD-PCR. Proceedings of the Royal Society of London B: Biological Sciences 262:321–327.

Barthel, S., J. Parker, C. Folke, and J. Colding. 2014. Urban Gardens: Pockets of Social-Ecological Memory. Pages 145–158 *in* K. G. Tidball and M. E. Krasny, editors. Greening in the Red Zone. Springer Netherlands.

Beninde, J., M. Veith, and A. Hochkirch. 2015. Biodiversity in cities needs space: a meta-analysis of factors determining intra-urban biodiversity variation. Ecology Letters 18:581–592.

Brown, K. H., and A. L. Jameton. 2000. Public Health Implications of Urban Agriculture. Journal of Public Health Policy 21:20–39.

Bruvo, R., N. K. Michiels, T. G. D'souza, and H. Schulenburg. 2004. A simple method for the calculation of microsatellite genotype distances irrespective of ploidy level. Molecular Ecology 13:2101–2106.

Caillaud, M. C., G. Mondor-Genson, S. Levine-Wilkinson, L. Mieuzet, A. Frantz, J. C. Simon, and A. Coeur D'acier. 2004. Microsatellite DNA markers for the pea aphid Acyrthosiphon pisum. Molecular Ecology Notes 4:446–448.

Casquet, J., C. Thebaud, and R. G. Gillespie. 2012. Chelex without boiling, a rapid and easy technique to obtain stable amplifiable DNA from small amounts of ethanol-stored spiders. Molecular Ecology Resources 12:136–141.

Dixon, A. F. G. 1998. Aphid Ecology: An Optimization Approach. Springer.

Douglas, I. 1983. The urban environment.

Excoffier, L., P. E. Smouse, and J. M. Quattro. 1992. Analysis of molecular variance inferred from metric distances among DNA haplotypes: application to human mitochondrial DNA restriction data. Genetics 131:479–491.

Gardiner, M. M., C. E. Burkman, and S. P. Prajzner. 2013. The Value of Urban Vacant Land to Support Arthropod Biodiversity and Ecosystem Services. Environmental Entomology 42:1123–1136.

Goddard, M. A., A. J. Dougill, and T. G. Benton. 2010. Scaling up from gardens: biodiversity conservation in urban environments. Trends in Ecology & Evolution 25:90–98.

Halbert, S. E., M. E. Irwin, and R. M. Goodman. 1981. Alate aphid (Homoptera: Aphididae) species and their relative importance as field vectors of soybean mosaic virus. Annals of Applied Biology 97:1–9.

Hanski, I., and M. Gilpin. 1991. Metapopulation dynamics: brief history and conceptual domain. Biological Journal of the Linnean Society 42:3–16.

Johnson, P. T. J., J. T. Hoverman, V. J. McKenzie, A. R. Blaustein, and K. L. D. Richgels. 2013. Urbanization and wetland communities: applying metacommunity theory to understand the local and landscape effects. Journal of Applied Ecology 50:34–42.

Jombart, T., S. Devillard, and F. Balloux. 2010. Discriminant analysis of principal components: a new method for the analysis of genetically structured populations. BMC genetics 11:94.

Lin, B. B., S. M. Philpott, and S. Jha. 2015. The future of urban agriculture and biodiversity-ecosystem services: Challenges and next steps. Basic and Applied Ecology 16:189–201.

MacDougall, A. S., K. S. McCann, G. Gellner, and R. Turkington. 2013. Diversity loss with persistent human disturbance increases vulnerability to ecosystem collapse. Nature 494:86–89.

McClintock, N. 2010. Why farm the city? Theorizing urban agriculture through a lens of metabolic rift. Cambridge Journal of Regions, Economy and Society:rsq005.

Nathan, R. 2001. The challenges of studying dispersal. Trends in Ecology & Evolution 16:481–483.

Parris, K. M. 2006. Urban amphibian assemblages as metacommunities. Journal of Animal Ecology 75:757–764.

Perfecto, I., J. H. Vandermeer, and A. L. Wright. 2009. Nature's Matrix: Linking Agriculture, Conservation and Food Sovereignty. Earthscan.

S R Singh, and and H. F. V. Emden. 1979. Insect Pests of Grain Legumes. Annual Review of Entomology 24:255–278.

Sack, C., and D. L. Stern. 2007. Sex and Death in the Male Pea Aphid, Acyrthosiphon pisum: The Life-History Effects of a Wing Dimorphism. Journal of Insect Science 7.

Sæther, B.-E., J. Tufto, S. Engen, K. Jerstad, O. W. Røstad, and J. E. Skåtan. 2000. Population Dynamical Consequences of Climate Change for a Small Temperate Songbird. Science 287:854–856.

Sunnucks, P., P. J. De Barro, G. Lushai, N. MacLean, and D. Hales. 1997. Genetic structure of an aphid studied using microsatellites: cyclic parthenogenesis, differentiated lineages and host specialization. Molecular Ecology 6:1059–1073.

Vandermeer, J., I. Perfecto, and S. Philpott. 2010. Ecological Complexity and Pest Control in Organic Coffee Production: Uncovering an Autonomous Ecosystem Service. BioScience 60:527–537.

Via, S. 1999. Reproductive Isolation between Sympatric Races of Pea Aphids. I. Gene Flow Restriction and Habitat Choice. Evolution 53:1446–1457.

Werling, B. P., and C. Gratton. 2010. Local and broadscale landscape structure differentially impact predation of two potato pests. Ecological Applications 20:1114–1125.

WHO, U. H. 2016. Global Report on Urban Health.

Wilson, A. C. C., B. Massonnet, J.-C. Simon, N. Prunier-Leterme, L. Dolatti, K. S. Llewellyn, C. C. Figueroa, C. C. Ramirez, R. L. Blackman, A. Estoup, and P. Sunnucks. 2004. Cross-species amplification of microsatellite loci in aphids: assessment and application. Molecular Ecology Notes 4:104–109.

APPENDIX 4

Supplementary Information:

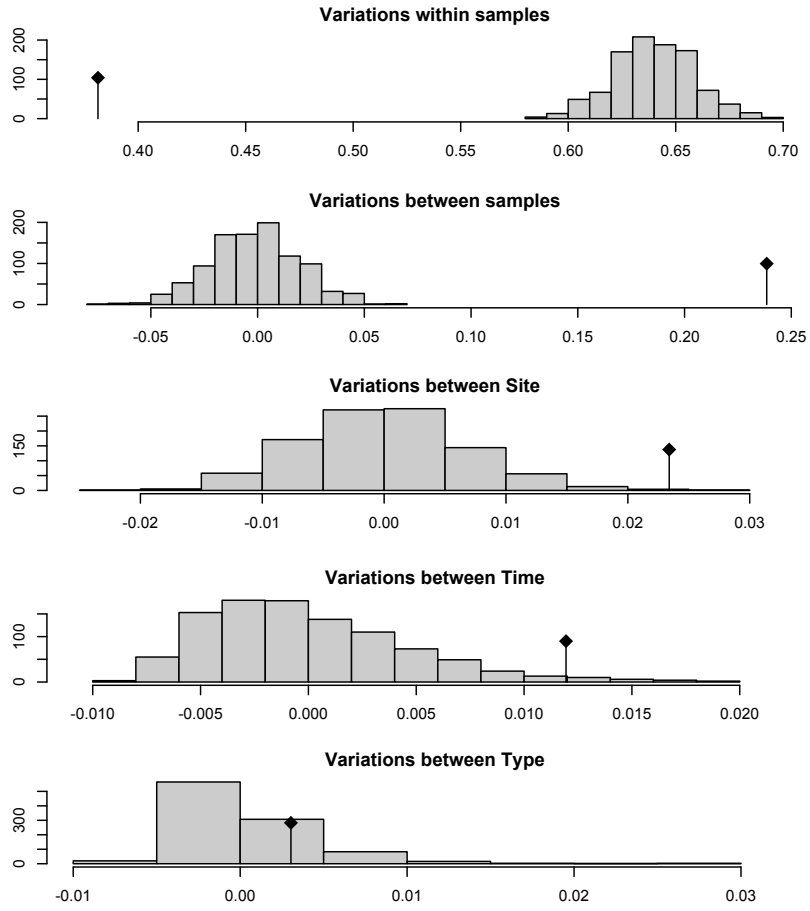

Fig. S5.1. AMOVA results showing population structure. From top to bottom: variation within, between samples, and between site, time (spring, summer, fall), and type (apterous and alateous). Histograms are the results of $N = 999$ random permutations compared to actual results marked by line with diamond marker. Separate models were run for each strata.

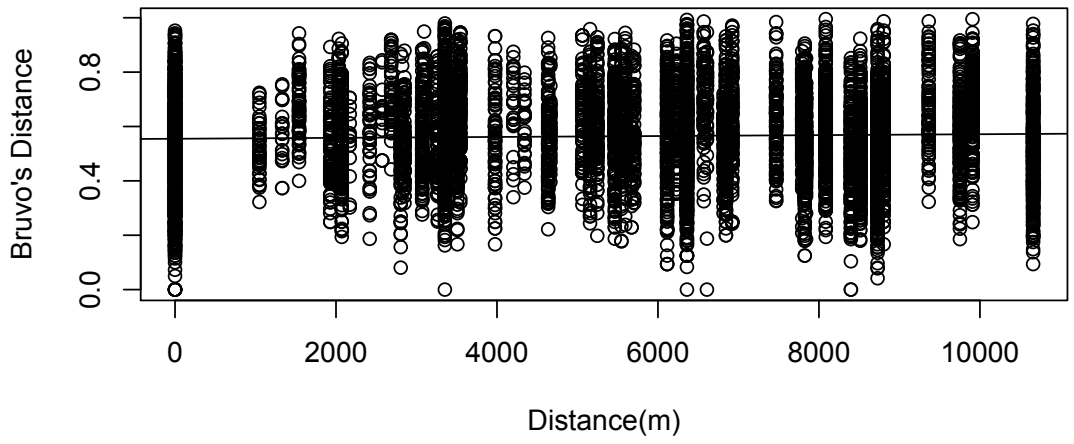

Fig. S5.2. Isolation by distance. Linear regression of physical distance and genetic distance (Bruvo's) between every possible pair of samples. (adjusted $R^2 = 0.00087$, $p = 0.0042$)

CHAPTER VI

Multiple hysteretic patterns from elementary population models

Theresa Ong and John Vandermeer

6.1 Abstract

Critical transitions whereby small changes in conditions can cause large and irreversible changes in ecosystem states are of cause of increasing concern in ecology. Here we focus on the irreversibility of these transitions, formally known as hysteresis. We explore how simple correlations between parameters in Lotkva-Volterra equations result in a variety of complicated hysteretic patterns. These patterns include "unattainable" stable states that once lost may never be recovered. We suspect these patterns to be common in natural systems, where interactions between diverse assemblages are unavoidable. Thus, understanding underlying hysteretic structures may be necessary for rescuing lost ecosystem states and avoiding future losses.

6.2 Introduction

Tipping points, also called critical transitions, are increasingly acknowledged as important elements of ecological systems (Scheffer 2009, Scheffer et al. 2012). They emerge in popular perception as potential doomsday behemoths in the context of climate change research

(Lenton 2011) where multiple tipping points may form a perfect doomsday storm -- e.g., Arctic ice melts to a point that the previous moderating albido effect is lost, while tipping atmospheric heat rises suddenly above the point where methane hydrate currently sequestered in permafrost begins runaway melting leading to a sudden drop in the Atlantic thermohaline circulation (Kvenvolden 1988). Many other examples could be cited (May 1977, Scheffer 2009) Vandermeer et al., 2004. An associated structure that has received less attention is hysteresis, in which movement of a control parameter in one direction generates a tipping point that is distinct from a tipping point when the control parameter is moved in the opposite direction. Thus, reducing rainfall in the Amazon may very well generate, at some critical threshold of rainfall, a dramatic switch from forest to savannah, but having undergone that switch, increasing the rainfall to where it had been before, will not necessarily result in regeneration of the forest (Hirota et al. 2011, Staver et al. 2011).

The importance of hysteresis is evident in many practical situations (fisheries management, pest management, forestry) and we suggest that it is a form worthy of incorporating into our toolbox of theoretical ecology. While we commonly acknowledge a variety of dynamical concepts potentially involved in community structure (e.g., stable/unstable points and cycles, chaos, deterministic versus stochastic forces, time lags, etc.), the possibility that ecological communities are also strongly affected by hysteresis is less frequently acknowledged and, we argue, worthy of consideration. Pursuant to this goal, the nature of such dynamical behavior in the elementary mathematical forms of population interactions is an obvious starting point.

It has long been known that classical models of population interactions are capable of generating catastrophic transitions (May 1977, Scheffer 2009), frequently presenting hysteretic

patterns, as has been noted in the past. For example, the cod fishery of the North Sea has been reported as an example of hysteresis (De Roos and Persson 2002, Fauchald 2010). Codfish (*Gadus morhua*) are predators on herring (*Clupea harengus*), although the latter is a predator on the larvae and eggs of the former. It is thought that increasing the population density of herring causes an eventual tipping point where the predation of herring on early stages of codfish causes herring populations to dominate the ecosystem. Reversal of that population density need not result in revitalization of the cod industry because of an evident hysteretic effect. We can see this structure if we simply model the codfish/herring system as one of competition (larvae of codfish and herring overlap considerably in their food choices), where fishing pressure is modeled as reducing the effective carrying capacity of the codfish. Simple Lotka-Volterra competition equations produce an evident hysteretic effect (Fig. 6.1).

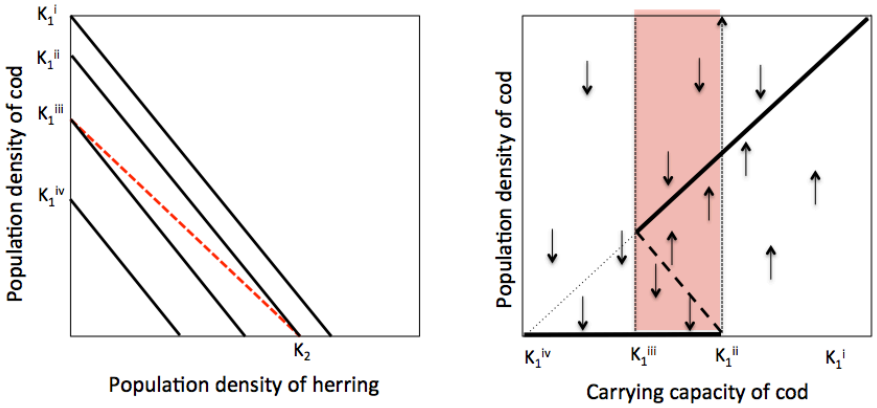

Fig. 6.1 Construction of hysteretic zone in classic competition, using the carrying capacity of codfish as a tuning parameter. **(a)** classic isocline analysis of competition between two species with an unstable (indeterminate) equilibrium. **(b)** resulting tipping point graph from changing the carrying capacity of species 2 (codfish).

In more general ecological applications the idea is not unusual, effectively recognized since the recognition of alternative stable equilibria in, for example, the Gaussian concept of indeterminate competition or many other classical ecological applications (May 1977). We here

extend some of the insights of the past (particularly, May 1977) and examine the basic ecological process of consumption from the point of view of the category of tipping points that carry with them associated hysteresis. We demonstrate that the hysteretic patterns of a common form of the Lotka-Volterra predator prey equations can be diverse and complicated.

6.3 Theoretical Approach

We begin with the classic equations and then add two popular nonlinearities. The key nonlinearities normally added are 1) density dependence on the prey (resource, host) element and 2) a functional response (satiation) on the predatory element, either analytically or with simple graphical reasoning as pioneered by Rosenzweig and MacArthur (1963). Adding density dependence to the prey, the resultant equations are:

$$\frac{dV}{dt} = rV(1-V) - \frac{\alpha VP}{1+\beta V} \qquad 1a$$

$$\frac{dP}{dt} = \frac{\delta VP}{1+\beta V} - mP \qquad 1b$$

The classic picture in phase space is illustrated in Figure 6.2.

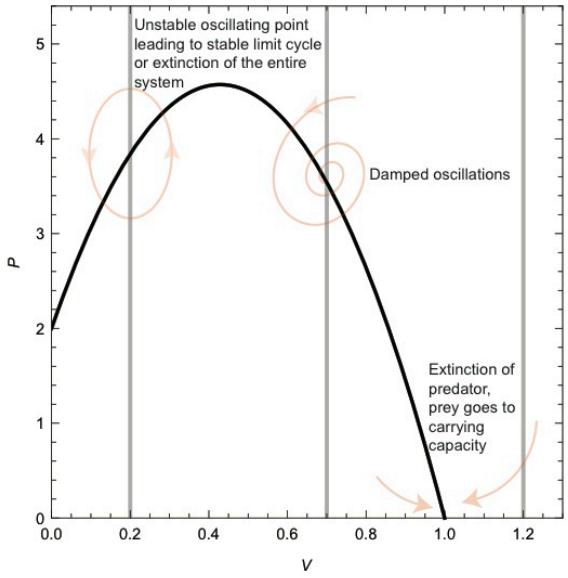

Fig. 6.2 Classic phase space representation of a predator/prey situation, from system 1, illustrating the two zero growth isoclines. The placement of the predator isocline stipulates which of the three outcomes results.

Relaxing the assumption that the predator is limited only by its prey (i.e., allowing for there to be density dependent control on the predator as well as the prey), several authors have analyzed the more complicated possibilities that may emerge (Noy-Meir 1975, Vandermeer and King 2010). For example, adding a carrying capacity to the predator transforms system 2 into:

$$\frac{dV}{dt} = rV(1-V) - \frac{\alpha VP}{1+\beta V} \qquad 2a$$

$$\frac{dP}{dt} = \frac{\delta VP}{1+\beta V}\left(1-\frac{P}{k}\right) - mP \qquad 2b$$

with zero growth isoclines:

$$P = \frac{r(1-V)(1+\beta V)}{\alpha} \qquad 3a$$

$$P = \frac{k(\delta V - \beta m V - m)}{\delta V} \qquad 3b$$

Here, as proposed qualitatively by Noy-Meir in 1975 and Rosenzweig and MacArthur in 1963, if the predator has an independent source of control, this places a cap on the predator isocline and creates conditions for alternative equilibrium points, including bifurcation patterns that suggest the system may respond in a critical transition fashion to a variety of parameter manipulations, as demonstrated in Figure 6.3. Most notable is the zone of hysteresis, suggesting different meta-behavior of the system as the parameter is varied (indicated by dashed arrows). If the predator carrying capacity is high (say around 7 in Figure 6.2), the equilibrium of the prey is low. As we reduce the carrying capacity of the predator, the equilibrium of the prey remains relatively low, until we decrease the carrying capacity to the critical point (about 4.6 in Figure 6.2a), and the prey equilibrium density jumps up dramatically. Reversing the tuning of k, the prey equilibrium begins to decline, but reaches a critical point at a value of k that is larger than the original critical point, thus creating a zone of hysteresis, within which alternative stable situations coexist.

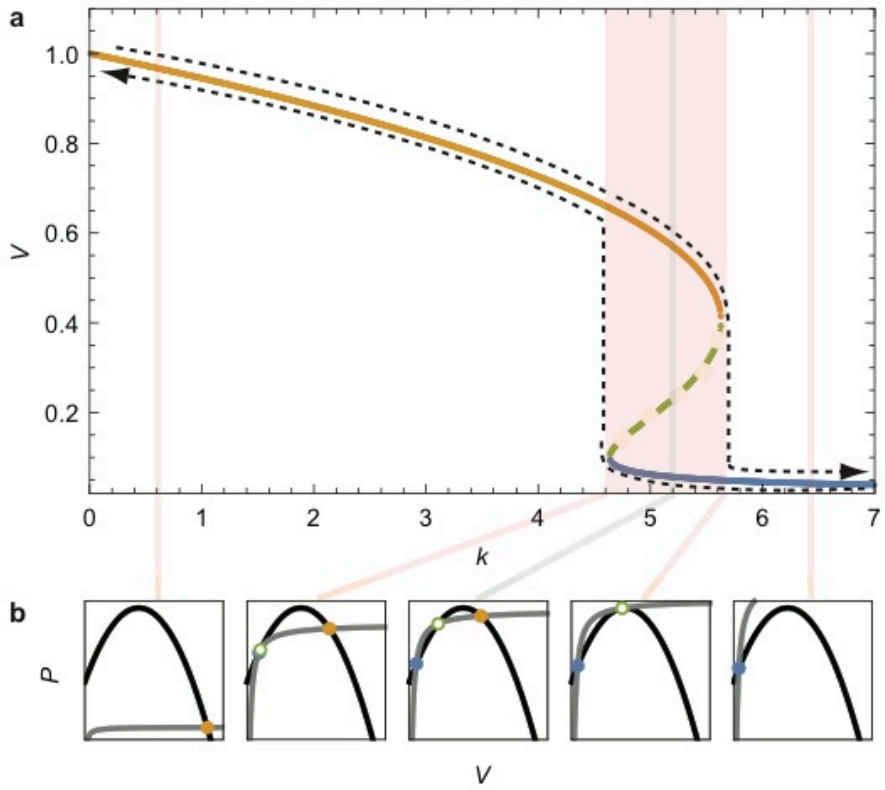

Fig. 6.3 Changing upper-limited predator isocline in (b), illustrating tipping point behavior and zone of hysteresis in (a). Dashed arrows in a indicate distinct behavior associated with reducing k from high to low versus increasing k from low to high. Shaded area is zone of hysteresis.

The equilibrium points are given as the roots to the equation,

$$\frac{r(1-V)(1+\beta V)}{\alpha} = \frac{k(\delta V - \beta m V - m)}{\delta V}$$

or

$$\alpha k m + (r\delta - \alpha k\delta + \alpha k\beta m)V + r\delta(\beta - 1)V^2 - r\delta\beta V^3 = 0$$

which has roots λ_1, λ_2, and λ_3 (in order of size). The points of critical transition are then [$\lambda_3 > \lambda_1 = \lambda_2$] and [$\lambda_1 < \lambda_2 = \lambda_3$], as illustrated in panels 2 and 4 of Figure 3b.

6.4 Results

In reality it is unlikely that effects of an environmental change will be restricted to a single parameter (as in Figures 6.1 and 6.3, where the carrying capacity of the predator is the only change resulting from change in a postulated environmental driver). Most frequently parameters are likely to change in a correlated fashion. In particular, we focus on the simultaneous transformation of the predator attack rate (α) and the predator carrying capacity (k), a combination that generates a rich diversity of critical transition behaviors. While other parameters are likely to exhibit correlated changes also, our intent in this article is simply to illustrate the qualitatively rich hysteretic behavior of this elementary pair of equations.

In Figure 6.4 we illustrate the situation in which the variation in k and α is such that they are positively correlated. Qualitatively, the tipping point behavior is identical to the previous example (Fig. 6.3), although the details are distinct (note that both isoclines change along with simultaneous changes in k and α.

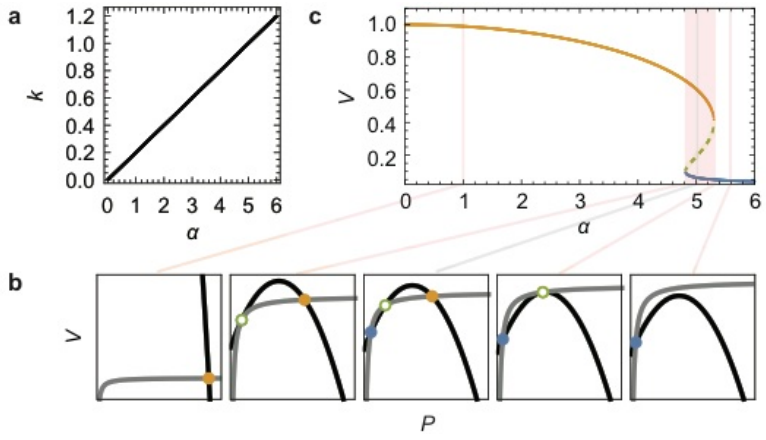

Fig. 6.4 Expected pattern of critical transitions and hysteretic zone when predator attack rate (α) and carrying capacity (k) are positively correlated. a) Plot of variable α against variable k for the values used in the calculations. **b)** Four exemplary isocline arrangements as k and α are varied. **c)** Resulting critical transition and hysteretic zone (shaded) for the system (qualitatively the same as Figure 2).

In Figure 6.5 we illustrate four other potential correlations in the simultaneous response of k and α to some environmental driver. Note how the patterns of hysteresis can become quite complicated. In particular, in Figure 6.5a and b we show the mirror results of an environmental change that changes k and α proportionally (linearly) (Fig. 6.5a is a repeat of Fig. 6.4). In Figure 6.5c the relationship between α and k is somewhat more complicated, but the resulting hysteretic zones can be easily predicted from the hysteretic patterns of Figure 6.5a and b separately. Yet the pattern itself suggests the existence of a complicated relationship between the tuning variable and the resulting equilibrium points. Sudden loss of the prey population is eventually replaced with sudden gain, even as the tuning parameter is changed in the same direction. For example, if the classic enrichment approach were to be applied to a predator destined to be a biological control agent, initially we might imagine an increase in both k and α as the enrichment program favored many aspects of the predator's niche. However, it is conceivable that as the program moves forward, the connection between the carrying capacity and the consumption efficiency may break down. So if the initial arrangement stipulates $k = \alpha$, we can imagine the α decreasing as the consumption efficiency (β) rises, or $k = (\alpha - \alpha\beta)\alpha$, whence the hysteresis pattern of Figure 6.5c emerges. The prey item thus would go from very high (which, if a potential pest species, for example, would be negative) to virtual extinction in response to the enrichment program. Yet further enrichment would surprisingly produce yet again a burgeoning prey population. At any time reversing course would result in tipping points again, but at relatively unpredictable points in the enrichment program.

The example in Figure 6.5d presents a qualitatively distinct picture, in which a locus of stable points may be unreachable. Once the system is at the lower equilibrium point, there is no

way to reach the stable locus through the tuning parameter. If the system starts within the stable set it will remain there, but only through a narrow range of tuning parameter values. Once it reaches a tipping point, the prey population descends to almost zero and is unable to reach the stable situation ever again. The conservation implications here are evident. If the prey species is of conservation concern, and efforts are made to either decrease or increase the predatory influence on it, the result could be a critical transition to a very low population density, which may become stagnated at that point no matter what future manipulations may be undertaken.

In Figure 5e we illustrate what is effectively a combination of the situations in Figure 6.5c and d. Again, there is an "unattainable" locus of equilibrium points. But here we have three distinct hysteretic zones, from very high prey at one end of the tuning parameter to very high at the other end, with two hysteretic zones in between, but also including a hysteretic zone at the locus of the "unattainable" points. If, for whatever reason, the intermediate density is the desired one, as in the example in Figure 6.5d, it could easily be lost to the larger densities at either low or high tuning parameter values, never to return again because of the nature of the intermediate hysteretic zone.

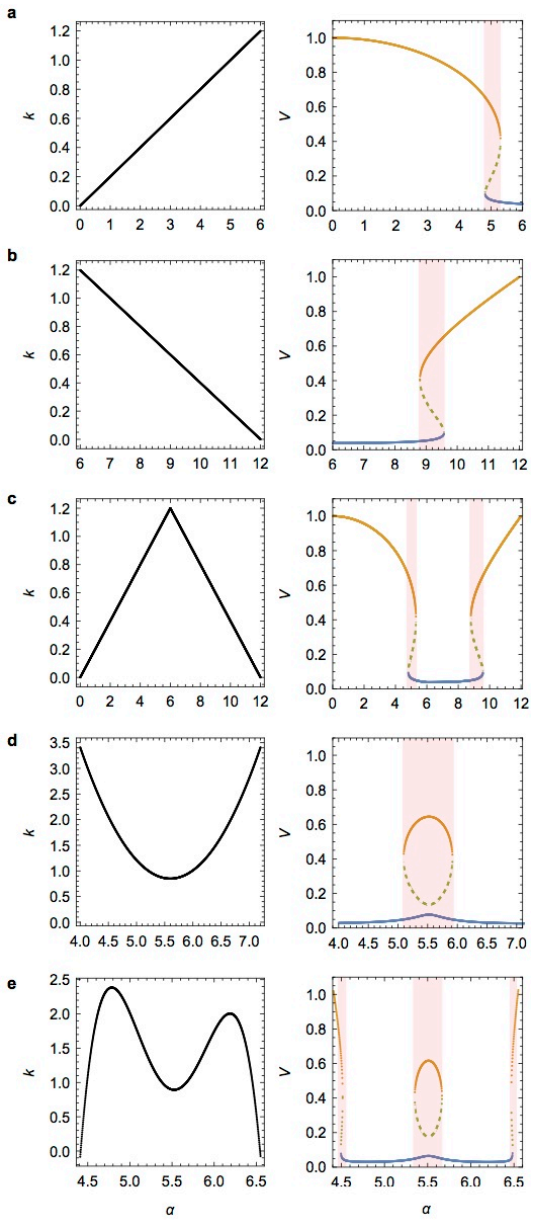

Fig. 6.5 A menagerie of hysteretic patterns. Examples of **(a-b)** linear, parabolic **(c-d)** and **(e)** polynomial correlations between the tuning parameter α and k, and resulting hysteretic patterns. Equations for correlations between α and k are: **(a)** $k = 0.2\alpha$, **(b)** $k = -0.2\alpha + 2.4$, **(c)** $k = -(\alpha - 5.6)^2 + 1.6$, **(d)** $k = (\alpha - 5.6)^2 + 0.85$, **(e)** $k = -5.3335\alpha^4 + 117.331\alpha^3 - 962.671\alpha^2 + 3490.77\alpha - 4718$, and critical transition points for hysteretic regions are: α_c = **(a)** 4.81, 5.31, **(b)** 8.80, 9.58, **(c)** 4.80, 4.93, 6.45, 6.55, **(d)** 5.10, 5.92, and **(e)** 4.49, 4.51, 5.35, 5.67, 6.47, 6.48. Stable equilibrium points plotted in orange and blue, along with unstable green points (dotted line). Red shaded region is zone of hysteresis.

6.5 Discussion

The literature on tipping points in ecology is very large (see reviews in Schröder et al. 2005, Scheffer 2009, Scheffer et al. 2012), but the associated issue of hysteresis is frequently dealt with only in passing. Yet, from both a basic structural phenomenon and a practical standpoint it could be an important force. Especially in any form of environmental management it is perhaps disheartening to learn that facing an error in a management decision may not be easily reversible. Historical examples abound. For example, a change in fishing technology that increases harvesting of the top predator, cod, can switch the ecosystem to one dominated by herring (Fauchald 2010), but a subsequent reversal of that change will not necessarily result in the reversion to a healthy cod population. A decision to eliminate shade trees from a coffee plantation encourages weedy growth and the inevitable competition from weeds, yet returning to shade is impossible since those weeds compete with newly planted tree seedlings (Perfecto and Vandermeer 2015). Beyond management considerations, tipping points are well known to contextualize larger ecosystems, at least theoretically (Vandermeer and Yodzis 1999, Schreiber 2003, Scheffer et al. 2012). Since it is frequently the case that tipping points carry with them hysteresis, it would be prudent to ask what effect such behavior will have when embedded in larger systems (Giller et al. 1997, Merton 1998, van Nes and Scheffer 2004).

We have shown that complex hysteretic patterns very easily emerge from simple correlations between parameters in classic population models. These complexities are likely the rule, not exception, for larger systems, where higher order interactions much exceeding the simple correlations explored here, abound. In basic hysteresis, changes to the state of an ecosystem are merely difficult to reverse; decreases in global precipitation may transform forests into savannahs, and if the rain were to suddenly increase, forests may still not return for many

years (Staver et al. 2011). But if the hysteretic patterns are such that the forest state is "unattainable", reversion to forests may be impossible once a transition to savannahs has occurred. Yet all is not lost. Reversion to the pre-transition state is indeed impossible if management focuses only on the drivers of change (in our last example, precipitation or for management purposes, irrigation). It is however, conceivable to reach the "unattainable" state through an external perturbation that shifts the ecosystem state itself. In the last example, precipitation may drive changes in the ecosystem state, but rather than adding water to the system, managers could instead restore forest plants to artificially shift the ecosystem state while precipitation remains constant. Yet restoring the forest would in theory be unsuccessful if the system was not situated at the precipitation level where the "unattainable" forest state could be achieved by a vertical shift in the ecosystem state. In such cases, successful reversion to ideal states depends strongly on how well the underlying hysteretic nature of the system is understood. Since complex hysteretic patterns are likely commonplace in nature, we suggest that studies focused on characterizing patterns of hysteresis are essential for both rescuing systems that have transitioned to undesirable states and preventing unwanted transitions from occurring in the first place.

6.6 Methods Summary

To observe hysteretic patterns resulting from Eq. 2a-b, we analytically calculated three unique equilibrium points from the intersection of predator and prey isoclines. Equilibrium points were plotted as a function of driver variables α and k using the variety of theoretical correlations between the two parameters in Figure 5. Analytical solutions for critical points were impossible because of the higher order nature of equilibrium point equations, thus critical points

in Figure 5 were determined using a numerical approach, testing for equality in equilibrium points as a function of 0.01 intervals changes in the driver variable α.

Acknowledgements

We would like to thank Gyuri Barabas for help with numerical approximations of critical transition points. Thank you to the Ecology and Evolutionary Biology Department and the Rackham Graduate School at the University of Michigan for funding.

6.7 Literature Cited

De Roos, A. M., and L. Persson. 2002. Size-dependent life-history traits promote catastrophic collapses of top predators. Proceedings of the National Academy of Sciences 99:12907–12912.

Fauchald, P. 2010. Predator–prey reversal: A possible mechanism for ecosystem hysteresis in the North Sea? Ecology 91:2191–2197.

Giller, K. E., M. H. Beare, P. Lavelle, A.-M. N. Izac, and M. J. Swift. 1997. Agricultural intensification, soil biodiversity and agroecosystem function. Applied Soil Ecology 6:3–16.

Hirota, M., M. Holmgren, E. H. Van Nes, and M. Scheffer. 2011. Global resilience of tropical forest and savanna to critical transitions. Science 334:232–235.

Kvenvolden, K. A. 1988. Methane hydrate—a major reservoir of carbon in the shallow geosphere? Chemical geology 71:41–51.

Lenton, T. M. 2011. Early warning of climate tipping points. Nature Climate Change 1:201–209.

May, R. M. 1977. Thresholds and breakpoints in ecosystems with a multiplicity of stable states. Nature 269:471–477.

Merton, R. 1998. Monitoring community hysteresis using spectral shift analysis and the red-edge vegetation stress index. Pages 12–16.

van Nes, E. H., and M. Scheffer. 2004. Large Species Shifts Triggered by Small Forces. The American Naturalist 164:255–266.

Noy-Meir, I. 1975. Stability of Grazing Systems: An Application of Predator-Prey Graphs. Journal of Ecology 63:459–481.

Perfecto, I., and J. Vandermeer. 2015. Coffee Agroecology: A new approach to understanding agricultural biodiversity, ecosystem services and sustainable development. Routledge.

Rosenzweig, M. L., and R. H. MacArthur. 1963. Graphical Representation and Stability Conditions of Predator-Prey Interactions. The American Naturalist 97:209–223.

Scheffer, M. 2009. Critical transitions in nature and society. Princeton University Press.

Scheffer, M., S. R. Carpenter, T. M. Lenton, J. Bascompte, W. Brock, V. Dakos, J. van de Koppel, I. A. van de Leemput, S. A. Levin, E. H. van Nes, M. Pascual, and J. Vandermeer. 2012. Anticipating Critical Transitions. Science 338:344–348.

Schreiber, S. J. 2003. Allee effects, extinctions, and chaotic transients in simple population models. Theoretical Population Biology 64:201–209.

Schröder, A., L. Persson, and A. M. De Roos. 2005. Direct experimental evidence for alternative stable states: a review. Oikos 110:3–19.

Staver, A. C., S. Archibald, and S. A. Levin. 2011. The global extent and determinants of savanna and forest as alternative biome states. Science 334:230–232.

Vandermeer, J., and A. King. 2010. Consequential classes of resources: Subtle global bifurcation with dramatic ecological consequences in a simple population model. Journal of Theoretical Biology 263:237–241.

Vandermeer, J., and P. Yodzis. 1999. Basin Boundary Collision as a Model of Discontinuous Change in Ecosystems. Ecology 80:1817–1827.

CHAPTER VII

Past management regimes constrain future returns in agriculture: an experimental demonstration of complex hysteretic patterns

Theresa Wei Ying Ong & John Vandermeer

7.1 Abstract

Hysteresis is a mathematical phenomenon that occurs when transformation of a system as a parameter changes in one direction does not produce the same effect when the parameter changes in the reverse direction. This is a common phenomenon in soils, where nutrient uptake has long been known to exhibit sensitivity to initial conditions [1–3]. Yet despite this deep knowledge base, the question of how hysteresis impacts the success of agriculture practices with different historical land-use has not been addressed. Here we show empirical evidence that transitions in agricultural management can result in complex hysteretic patterns including some with hidden stable states that qualitatively resemble those that emerge when parameters of a well-known model of nutrient-soil feedbacks [4] are correlated. Soil beds were slowly transitioned from conventional to organic regimes by manipulating the proportion of chemical ($CaNO_3$) to organic (earthworm castings) nitrogen sources while measuring effects on nitrogen flux, water

retention and yield quality. Build up of organic matter and nutrients caused the transition from a conventional to organic agriculture regime to be sharp and irreversible. This experimentally derived exhibition of hysteresis could explain why less intensive agriculture models are difficult to maintain with little financial support.

7.2 Main Text

Hysteresis is often discussed within the context of critical transitions, with a focus on the sudden and often dramatic changes between two alternative stable states: forest and savannah, oligotrophic and eutrophic lakes, sustainable fisheries and collapse, to name a few [5–8]. Though it is a necessary component of critical transitions, hysteresis, where the state of the system depends not only on current but also past drivers of the system, receives far less attention (Ong and Vandermeer, in prep). Here we argue that when the system is a human-managed system, in particular agriculture, hysteresis may have far-reaching policy implications. Management styles can be thought of as emanating from particular input variables. For example, tropical agroforestry systems tend to be more common when soil erosion is a recognized factor of production, suggesting a relationship in which tree density on a farm is a function of soil erosion tendency [9]. Such a relationship may be secular and monotonic. However, strong nonlinearities may also be involved, sometimes to the extreme of generating parameter regimes (e.g., a range of soil erosion tendencies) in which alternative "syndromes" (high tree densities versus low tree densities) emerge [10]. This region is referred to as a hysteretic zone, and its edges are normally associated with critical transitions [8,11].

Agriculture is a particularly appropriate study system for this effect since soils are well known for their propensity to undergo hysteresis [1–3]. Here we re-examine a classic model of sediment-nutrient feedbacks known as the Carpenter et al. model (Fig 7.1) [4]. The model was

originally used to describe phosphorous dynamics in lakes but can be generalized for terrestrial systems and other nutrients [4,12,13]. The flux of a nutrient (N) is the difference between source and sink where the source is given as:

$$source = i + \frac{rN^q}{m^q + N^q} \qquad (1)$$

where N is the nutrient of interest, i is the input rate, r is the maximum recycling rate of N in the soil, q describes the shape of the source function following a typical Mechalis-Menton form, where m is the half saturation constant. The sink is taken as a simple proportionality, namely

$$sink = sN \qquad (2)$$

whence the overall flux is

$$\frac{dN}{dt} = source - sink \qquad (3)$$

In agriculture, loss processes include nutrient uptake by plants or consumers and runoff. Sources include microorganisms that decompose soil organic matter and fix atmospheric nitrogen.

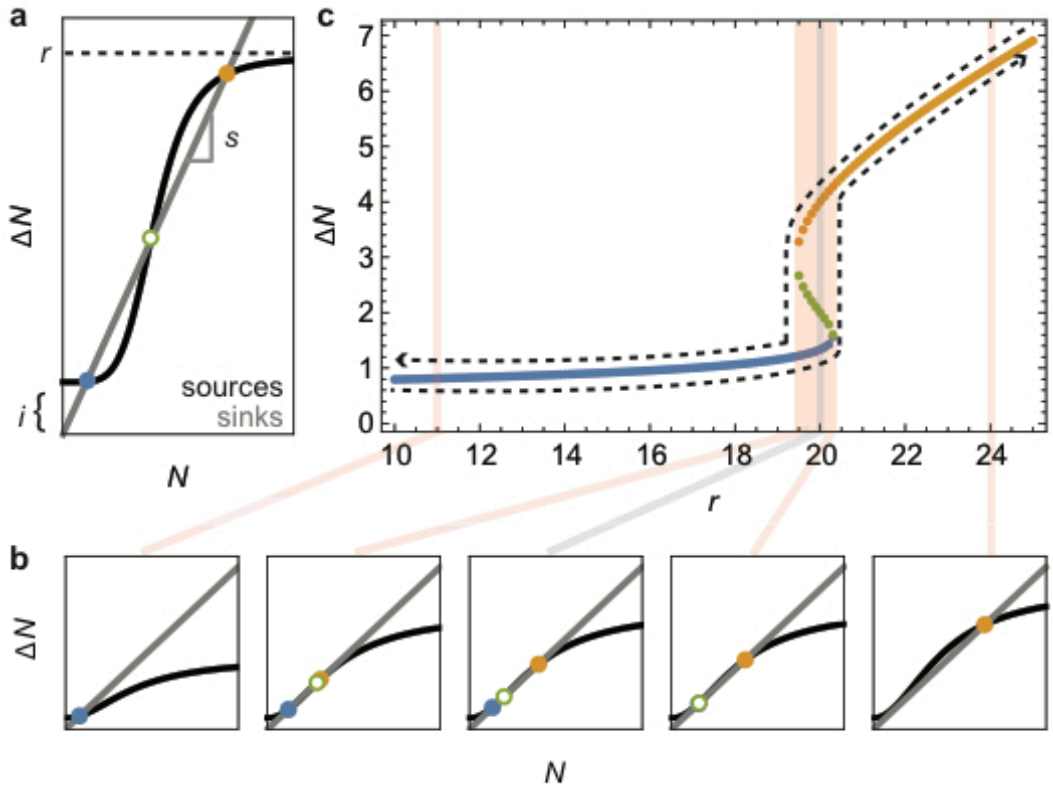

Fig. 7.1 Carpenter et al. model of nutrient-soil hysteresis. (a) Phase diagram of nutrient flux (ΔN) as a function of nutrient density (N). Difference in source (black line) and sink (grey line) functions equal nutrient flux. Rate of nutrient inputs, i and max recycling rate of nutrients within soils r, defines the sigmoid shaped source function. The sink function is a linear term defined by the loss rate of nutrients from the system, s. **(b)** Changes to source and sink functions that occur with increases in r parameter. A single equilibrium point bifurcates into three, and collapses back into one. Stable (blue and orange solid points) and unstable (open green) equilbria are plotted where source and sink functions overlap. Forward and reverse trajectories exhibiting hysteresis displayed as dashed arrows. **(c)** Graph displaying hysteresis resulting from changes in the presence and values of equilibria as r increases. Pink and light grey lines connect source-sink curves in **(b)** to their corresponding positions in the bifurcation graph of **(c)**. Large shaded region marks zone of hysteresis.

We can envision nutrient flux (dN/dt) as a function of nutrient density by plotting source and sink components of (1) as separate functions of nutrient density (Fig. 7.1a). When nutrient sources are larger than sinks, nutrient flux increases. When sinks are larger than sources, nutrient flux decreases. Where sources are equal to sinks, there is no net change in nutrient flux (Fig. 7.1a). Carpenter et al. analyzed the model for $q \geq 2$ (sigmoid source function) since this

formulation has the potential for three equilibrium points, two stable (solid circles) where slight perturbations lead back to the equilibrium points, and one unstable (open circle) where perturbations move the system away from the equilibrium point (Fig 1a) [4]. A sigmoid source function would imply that soils act as a delayed nutrient source, requiring a minimum density of nutrients absorbed before becoming a net source of nutrients with a maximum of *r*. This maximum recycling rate likely depends on the amount of soil organic matter in the system, the main source of nutrients. If soils have a low *r*, the source function crosses the sink function at one stable equilibrium point (blue solid circle) (Fig 7.1b). As *r* increases, the source function crosses the sink function at two additional points—an unstable (green open circle) and a stable equilibrium point (orange solid circle) emerge (Fig 7.1b). If we plot equilibrium values of nutrient flux as a function of *r*, we replicate Carpenter et al.'s original conclusion that hysteresis with alternative stable states can emerge when the maximum rate at which soils recycle nutrients increases (Fig. 7.1c). Varying the rate at which nutrients are lost *s* while keeping *r* constant can also result in hysteresis (Fig S1), as can many other parameters in the model.

Carpenter et al. showed that hysteresis could result from simple nutrient feedbacks in lake sediments, yet their model considered hysteresis from the perspective of each parameter in isolation. We suggest that in agriculture, parameters that drive nutrient flux (ie. nutrient loss and maximum recycling rates) are likely correlated with one another and also with management intensity. For example, transitions between conventional to organic agriculture practices usually involve an increase in soil organic matter. Soils rich in organic matter are expected to recycle nutrients at higher rates. However, nutrient loss rates may also be affected. Loss rates may first decrease as soils improve, but may also increase at some point when soils reach their maximum

capacity for recycling nutrients. Taking into account such correlated effects, we modify the Carpenter et al. model as:

$$\frac{dN}{dt} = i - f(r)N + \frac{rN^q}{m^q + N^q} \qquad (4)$$

It is evident that depending on the nature of the function *f(r)*, a variety of hysteretic patterns are possible. For example, if we arbitrarily allow *f* to be periodic, the sort of complications illustrated in Figure 2 are possible. (Fig. 2).

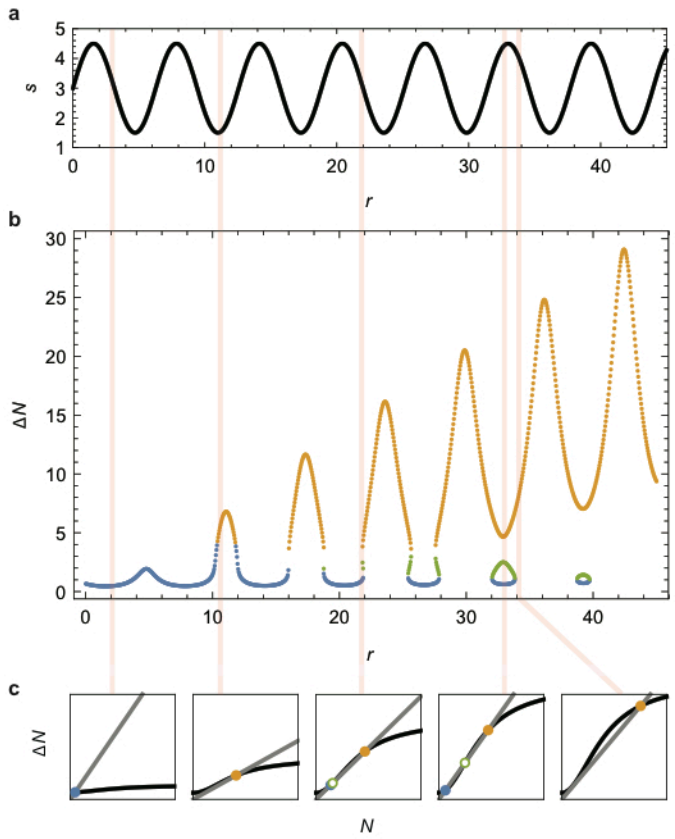

Fig 7.2 Consequences of correlations between max recycling rate *r*, and loss rate, *s*. (a) Sine function relationship between *r* and *s*. **(b)** Resulting hysteretic patterns that occur for stable (blue and orange) and unstable (green) equilibria, shown as a function of *r*. **(c)** Corresponding source-sink functions for nutrient flux. Stable (blue and orange solid points) and unstable (open green)

equilbria are plotted where source and sink functions overlap. Pink lines connect points in **(a)**, **(b)**, and **(c)** with the same *r* values.

Applying a sine function to the relationship between *r* and *s* we can represent a variety of correlation patterns and ranges of each parameter that may be relevant for a given system (Fig. 7.2a). The effects of positive, negative or parabolic relationships between *r* and *s* for nutrient flux can be observed separately by constraining the bifurcation graph to the parameter range of interest (Fig. 7.2b). In contrast to the original Carpenter et al. model, since *r* and *s* are related, source and sink functions change simultaneously (Fig 7.2c). This results in a variety of complex hysteretic patterns including double hysteretic loops and hidden stable states (Fig. 7.2b). Notice that when increasing *r* from 30 to 35, two equilibrium points (green and blue) would never be realized since the system initializes on one stable point and there is no smooth transition to the alternative stable point below (Fig. 7.2b). However, if the system were perturbed at that specific parameter range by artificially decreasing nutrient input rates for instance, the lower equilibrium state could theoretically be achieved. These patterns resemble those described by Ong and Vandermeer in a recent theoretical study where correlating parameters in simple population models revealed a plethora of similarly complex hysteretic patterns (in preparation). Thus, if loss and recycling rates are related, changes to soil management may lead to complicated hysteretic patterns for nutrient flux.

To test for the existence of these patterns we conducted a greenhouse experiment where the same beds of soil were exposed to a weekly fertilizer regimen that was systematically transitioned from 100% organic (earthworm castings) to 100% synthetic sources ($CaNO_3$) and back over the course of several weeks. Forty corn (*Zea mays*) seeds were sown in each bed at the beginning of every week and harvested before the next fertilizer regimen began. Yield in dry

weight, germination rates, NO_2, NO_3, H_20 flux and disease incidence were recorded every week. The same process was conducted for soils beginning initially with 100% synthetic fertilizers (Methods summary). From now on we use the term industrialization to refer to the relative amount of synthetic to organic fertilizer in our experiment. Though total nitrogen input rates were kept constant, transitions from high to low industrialization resulted in different levels of nitrogen flux (NO_3) than when the same beds were transitioned from low to high industrialization. We assumed that non-overlapping forward and reverse trajectories represent alternative stable states in our experiment. According to theory two stable points must be separated by a single unstable point. For each empirical result where hysteresis is apparent we can draw a theoretical unstable state (dashed line) between the stable ones (solid colored arrows). The unstable state is like the top ridge of a mountaintop such that if a ball (current state of the system) were placed on this ridge it would stay balanced until a slight perturbation pushes the ball into one of the valleys below on either side of the mountain (alternative stable states) (Fig 7.3c). We tested for the presence of unstable states by perturbing the system at intermediate industrialization levels to test for sudden jumps between alternative stable states. When we reached intermediate industrialization levels in our experiment, soils from a subset of our forward and reverse replicates were mixed at a 1:1, 1:2, or 2:1 ratio in order to forcefully move the state of the system to lie in between the two alternative states. We then perturb the system with a ±¼ change to industrialization and observe effects on state variables. Changes to the direction and magnitude of state variables allow us to map theoretical unstable state curves that are consistent with empirical results and dynamic rules (Fig 7.3d-f). In some cases hidden stable states best explain empirical results (Fig 7.3d-e).

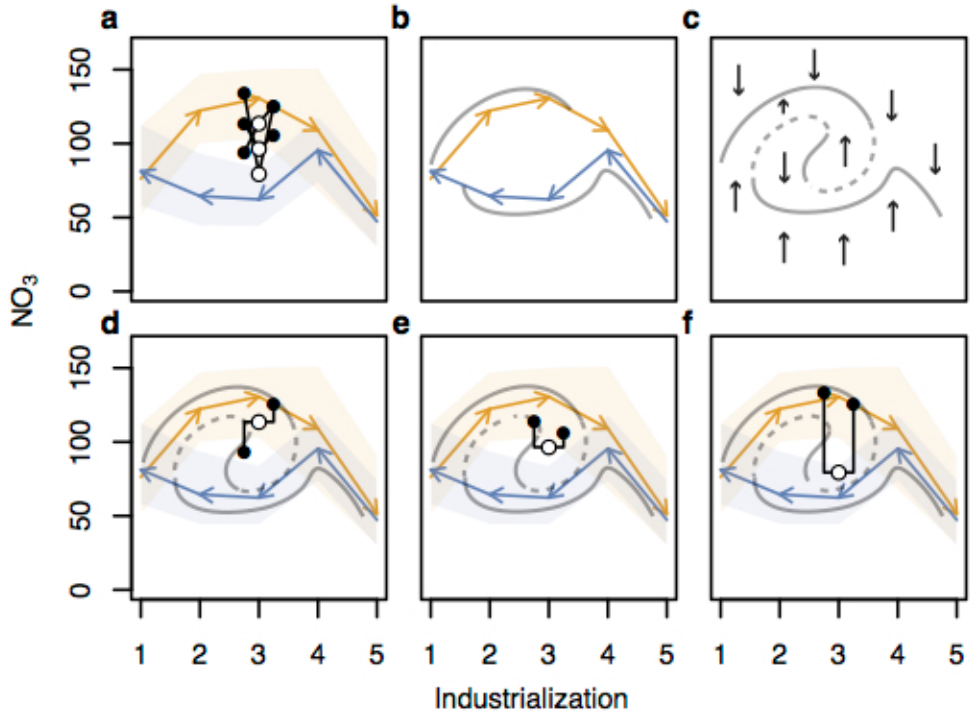

Fig. 7.3. Experimentally derived hysteresis for NO_3 flux. Forward (orange) and reverse (blue) trajectories for NO_3 flux as industrialization is experimentally driven from 100% organic to 100% synthetic nitrogen inputs and back. **(a)** Experimental results plotted as means (arrowheads) and 95% bootstrapped confidence intervals (shaded regions). At mid-industrialization levels, forward and reverse soil beds were mixed at 1:2, 1:1: and 2:1 ratios (open circles) then subjected to a ±¼ perturbation to the normal full change to industrialization, average NO_3 flux across $n = 5$ replicates for each unique perturbation is plotted as solid black points and connected to their initial conditions (open circles) with black lines. **(b)** Deduced alternative stable states (black curves) from overlap in confidence intervals of **(a)** plotted over experimental results (orange and blue arrows) with confidence removed for clarity. **(c)** Alternative and hidden stable states (solid lines), unstable state (dashed line) deduced from vector field (arrows) and dynamic rule that a single unstable point must be surrounded by two stable points. **(d)** Results (solid points) of experimental perturbation at 1:2 ratio of forward and reverse transitions at mid industrialization levels. **(e)** Results of experimental perturbation at 1:1 ratio and **(f)** 2:1 ratio. For panels **(d-f)** black lines connect initial conditions (open circle), ±¼ perturbation in industrialization and their final NO_3 results (solid points) overlaid on top of experimental results for forward and reverse transitions (blue and orange arrows and corresponding confidence intervals) and deduced hysteretic structure (grey curves).

We found that changes to management drove hysteresis in all state variables measured: NO_3, NO_2, H_2O flux, germination, disease incidence and dry weight yields (Fig 7.3-7.4). For

some state variables, hysteretic patterns were very complex (Fig. 7.4). Empirical results indicate the presence of multiple hysteretic loops (Figs. 7.2 and 7.4). In the case of water flux, perturbations to the system when soils from mid-industrialization forward and reverse treatments were mixed resulted in a jump to a high, possibly hidden stable state (Fig 7.4b). These results are consistent with patterns from theoretical work where driver parameters are related (Ong and Vandermeer, in prep).

An old, but reoccurring question is whether the unpredictability of nature sources from stochastic or deterministic effects[14–17]. Is there such a thing as essential stochasticity or is nature simply an accumulation of complicated relationships we have yet to unravel? Both are likely to play some part, but here we show evidence that complex hysteretic loops can arise from simple relationships between drivers of ecosystem state change. We expect this to be relevant for all systems where driver variables are interrelated, which is to say all natural systems. Difficulty in predicting changes in ecosystem states may arise not only from stochasticity[15] or chaos[18] but also the presence of complicated hysteretic patterns. For agriculture specifically, hysteresis implies that transitions from hi to low-industrialization will result in worse or better conditions than transitions from low to high-industrialization depending on the ecosystem state of interest and the transition period (Figs. 7.3 and 7.4).

In some cases, government incentives may be necessary to support transitions to less industrial states if past management physically constrains potential for economic success.

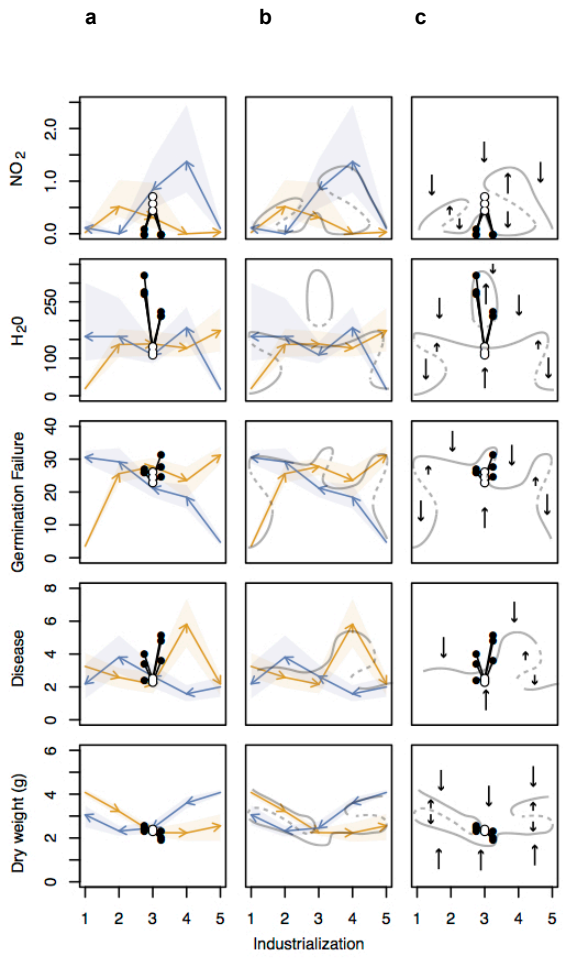

Fig. 7.4. Complicated hysteretic patterns across several experimentally measured state variables. **(a)** Experimental results for state variables NO_2 flux, H_2O flux, number of seeds failing to germinate, disease incidence and dry weight yields (g), as a function of industrialization level when transitioning forwards from low to high industrialization (orange) and backwards from high to low industrialization (blue). 95% bootstrapped confidence intervals (n = 999 replicates) plotted in corresponding colors. Initial conditions for treatments taken at mid-industrialization levels and mixed at 1:2, 1:1, and 2:1 ratios of forward and reverse transitions (open circles) connected via solid black lines to results of ±¼ (from one whole single step) perturbations in industrialization for various state variables (solid black points). **(b)** Deduced hysteretic structures including stable states (solid grey lines) and unstable states (dashed grey lines) overlaid over empirical results (blue and orange arrows and corresponding confidence intervals). We overlay empirical results to show how alternative stable states were deduced from overlap in confidence intervals from empirical results. **(c)** Vector field (black arrows), empirical points perturbed at mid-industrialization levels, initial conditions (open circles) and results of perturbations (solid points) showing how complete hysteretic structures (grey lines) including unstable states (dashed grey lines) were deduced.

7.3 Methods Summary

Model analysis

To graph plots of hysteresis for the original and modified Carpenter et al. models, we calculated equilibria from the intersection of the source (1) and sink (2) curves. These equilibria were plotted as a function of *r,* with *s* held constant or allowed to vary in a correlated fashion with *r* as described in the text.

Experimental set up and measurement of state variables

To test for hysteresis we set up a greenhouse experiment transitioning beds of potting soil from organic to synthetic fertilizer regimes. To remove the confounding effects of initial conditions, we began the experiment with $n = 20$ beds fertilized with 100% organic nitrogen inputs using earthworm castings (1-0-0) supplied at 1488g. Another $n = 20$ beds of soil were fertilized with 100% synthetic nitrogen inputs using $CaNO_3$ (15.5-0-0) supplied at 0.32g. Rates of nitrogen application were calculated so that the total amount of nitrogen supplied would be the same regardless of synthetic or organic nature. Every bed was sown with 40 seeds of *Zea mays*, fertilized, and left to germinate and grow for one week. After one week, the number of seeds that failed to germinate and the incidence of diseased seedlings were tabulated. Each bed of soil was then irrigated with 1L of dH20, and all leached water collected and measured. This water exudate was immediately used to measure NO_3 and NO_2 with simple strip tests. All seedlings and seeds were then extracted from beds of soil, dried and weighed. Soil was then returned to beds and planted with 40 new *Zea mays* seeds.

Transition regimen

Every week, beds of soils were transitioned to a new fertilizer regime, + 25% organic for beds that began 100% synthetic or -25% organic for beds that began 100% organic until 4 weeks

had past and beds reached 100% organic and 100% synthetic. At this point, beds were transitioned back to their original conditions over the course of another 4 weeks to 100% synthetic and 100% organic inputs.

Testing for unstable points

To artificially alter the ecosystem state at intermediate industrialization levels, we waited until soil beds reached 50% organic and 50% synthetic fertilizer inputs during the first round of the experiment, then mixed 9 beds that began with 100% synthetic fertilizer and 9 beds that began with 100% organic fertilizer and reallocated them to beds at ratios of 1:1 (n = 6), 1:2 (n = 6), and 2:1 (n = 6). Beds were immediately sown with 40 new *Zea mays* seeds and then half of the beds subjected to a +¼ of a normal full increase, and the other half a -¼ of a normal full decrease in industrialization, then measured as usual one week following the perturbation. Beds used for testing unstable points were retired after this process. The same process was repeated for 12 additional beds during the second phase of the experiment when beds reached 50% organic and synthetic on their way back towards their initial conditions. Each unique treatment (1:1 ratio and -¼ perturbation, 1:2 ratio and -¼ perturbation, 2:1 ratio and -¼ perturbation, 1:1 ratio and +¼ perturbation, 1:2 ratio and +¼ perturbation, 2:1 ratio and +¼ perturbation) had 5 total replicates.

Data analysis

Averages of state variables were calculated across all beds with the same level of industrialization and moving in the same direction (forward towards more industrialization or backwards towards less industrialization). Data was pooled across beds that began with 100% synthetic and 100% organic inputs to remove the effects of initial conditions. We calculated bootstrap confidence intervals using n = 999 replicates for each industrialization level (1-5) and

transition direction (forwards or backwards). Averages of mid-industrialization level perturbations are plotted over regular forward and reverse trajectories. Hysteresis is significant when forward and reverse confidence intervals do not overlap in their confidence intervals. We compared overlap in confidence intervals and mean point values of beds perturbed at mid-industrialization levels to reconstruct putative unstable curves.

Acknowledgements

Thank you to Azucena Lucatero and Damie Pak for assistance gathering and inputting data. The Department of Ecology and Evolutionary Biology and the Rackham Graduate School of the University of Michigan provided funding.

7.4 Literature Cited

1. Li, J. *et al*. Asymmetric responses of soil heterotrophic respiration to rising and decreasing temperatures. *Soil Biol. Biochem*. **106,** 18–27 (2017).
2. Huang, W., Yu, H. & Weber Jr., W. J. Hysteresis in the sorption and desorption of hydrophobic organic contaminants by soils and sediments: 1. A comparative analysis of experimental protocols. *J. Contam. Hydrol*. **31,** 129–148 (1998).
3. Groffman, P. M. & Tiedje, J. M. Denitrification Hysteresis During Wetting and Drying Cycles in Soil. *Soil Sci. Soc. Am. J*. **52,** 1626–1629 (1988).
4. Carpenter, S. R., Ludwig, D. & Brock, W. A. Management of eutrophication for lakes subject to potentially irreversible change. *Ecol. Appl*. **9,** 751–771 (1999).
5. Staver, A. C., Archibald, S. & Levin, S. A. The global extent and determinants of savanna and forest as alternative biome states. *Science* **334,** 230–232 (2011).
6. Hirota, M., Holmgren, M., Van Nes, E. H. & Scheffer, M. Global resilience of tropical forest and savanna to critical transitions. *Science* **334,** 232–235 (2011).
7. Petrie, B., Frank, K. T., Shackell, N. L. & Legget, W. C. Structure and stability in exploited marine fish communities: quantifying critical transitions. *Fish. Oceanogr*. **18,** 83–101 (2009).

8. Scheffer, M. *Critical transitions in nature and society*. (Princeton University Press, 2009).

9. Sanchez, P. A. in *Agroforestry: Science, policy and practice* 5–55 (Springer, 1995).

10. Vandermeer, J. Syndromes of Production: an Emergent Property of Simple Agroecosystem Dynamics. *J. Environ. Manage.* **51,** 59–72 (1997).

11. Scheffer, M. *et al*. Anticipating Critical Transitions. *Science* **338,** 344–348 (2012).

12. van Nes, E. H. & Scheffer, M. Implications of Spatial Heterogeneity for Catastrophic Regime Shifts in Ecosystems. *Ecology* **86,** 1797–1807 (2005).

13. Scheffer, M., Brock, W. & Westley, F. Socioeconomic Mechanisms Preventing Optimum Use of Ecosystem Services: An Interdisciplinary Theoretical Analysis. *Ecosystems* **3,** 451–471 (2000).

14. Chase, J. M. & Leibold, M. A. *Ecological niches: linking classical and contemporary approaches*. (University of Chicago Press, 2003).

15. Hubbell, S. The unified theory of biogeography and biodiversity. (2001).

16. Chase, J. M. & Myers, J. A. Disentangling the importance of ecological niches from stochastic processes across scales. *Philos. Trans. R. Soc. Lond. B Biol. Sci.* **366,** 2351–2363 (2011).

17. Desharnais, R. A. *et al*. Experimental support of the scaling rule for demographic stochasticity. *Ecol. Lett.* **9,** 537–547 (2006).

18. Hastings, A. & Powell, T. Chaos in a Three-Species Food Chain. *Ecology* **72,** 896–903 (1991).

APPENDIX 5

Supplementary Information

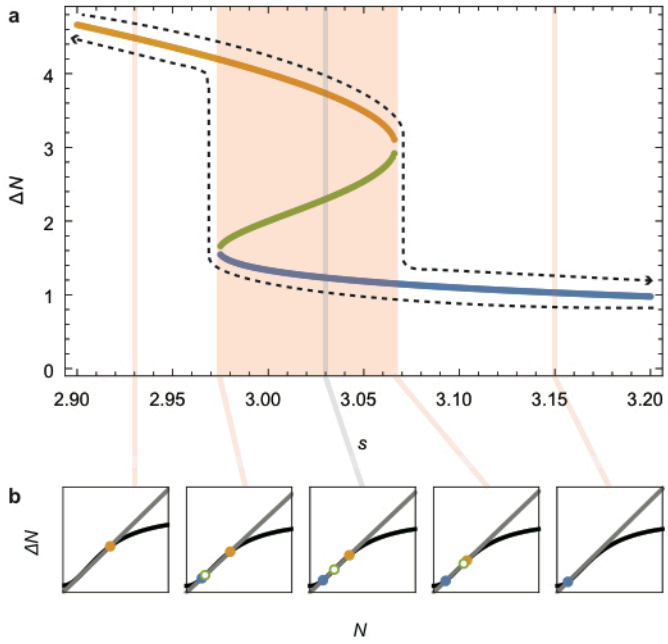

Fig. S7.1. Carpenter et al. model of nutrient-soil hysteresis using *s* as the bifurcating parameter. (a) Hysteresis in nutrient flux (ΔN) resulting from changes in the presence and values of stable (orange and blue) and unstable (green) equilibria as loss rate *s*, increases or decreases (dashed arrows). Large shaded region marks zone of hysteresis.
(b) Stable (blue and orange solid points) and unstable (open green) equilbria are plotted where source (black) and sink (grey) functions overlap in phase diagrams of nutrient flux (ΔN) and nutrient density (N). Pink and light grey lines connect source-sink curves in **(b)** to their corresponding positions in the bifurcation graph of **(a)**.

FINAL CONCLUSIONS

Historically, ecology has focused on conserving natural systems. Yet human impositions in the forms of agriculture and urbanity continue to increase (Pimentel et al. 1992, 2005). In an attempt to create ecologically resilient farms and cities, many argue that we should incorporate the complexities of nature into the systems we manage (Elton 1958, Vandermeer et al. 2010). Though ecological systems are inherently multi-dimensional and context dependent, the consequences of complexity for ecosystem stability are unclear. This dissertation examines the role of biocomplexity in effecting stability in biological control systems and agriculture more generally. Here, I summarize its main conclusions and implications.

Autonomous biological control

Autonomous biological control is the notion that a diversity of natural enemies prevents herbivores from reaching pest densities in natural systems (Lewis et al. 1997, Vandermeer et al. 2010). However, strong negative interspecific interactions between biological control agents are considered detrimental for species coexistence and effective biological control of pests (Denoth et al. 2002, Louda et al. 2003, Straub et al. 2008, Letourneau et al. 2009). The theoretical literature surrounding coexistence of species is extensive and complicated, but one common feature throughout is an underlying presumption that subsystems of large networks are initially stable (May 1972, 2001, Murdoch 1975, McCann et al. 1998, McCann 2000). Here, I re-evaluate

the role of strong negative interactions in effecting stability of complex networks when subsystems are initially unstable. This is the first time that the stability of subcomponents has been considered when assessing the stability of larger, complex networks. By starting with unstable subcomponents we find that strong interspecific competition for pest resources and intraguild predation between control agents can effectively rescue control, stabilizing the system. Specifically, we model a predator control agent that becomes ineffective once it reaches a carrying capacity, external to its pest resource. We also model a pathogen that cannot control outbreaks of pests because of the lag that is required for a critical density of pests to build before a pathogen epidemic can occur. With each epidemic, pest populations decline dramatically, only to build again to critical densities creating cyclical boom-bust dynamics. Strong competition and intraguild predation prevent the predator from reaching carrying capacity and prevent the pathogen from creating epidemics that would otherwise spiral the system out of control. Here, for the first time, we provide a theoretical scenario where diversity is maintained rather than hindered through strong negative interactions. We further confirm this in an experiment. These results may help explain a long-standing paradox in ecology: the coexistence of many, strongly negative interacting organisms in natural systems—a phenomenon that is particularly common for biological control systems in agriculture (Denoth et al. 2002, Straub et al. 2008).

The role of space and perceptions of space

Since Huffaker first assessed the coexistence of predator and prey mite species on spatial arrays of oranges, space has generally been considered a stabilizing force for ecological systems (Huffaker 1958, Hastings 1977, Levin 1992, Durrett and Levin 1994, Hassell et al. 1994). Spatial heterogeneity creates niches across landscapes and allows for a diversity of organisms, including

predators and prey to coexist (Hastings 1977, Liere et al. 2012). Yet, if changing initial conditions such that subcomponents of complex systems are unstable to begin with can reverse the implications of strong negative interactions for species coexistence, the effects of space may also change. In this dissertation, I extend Huffaker's classic experiment to test the effects of space when two competing natural enemies are combined to control a pest resource. The results confirm that spatial heterogeneity is stabilizing, but rather than artificially imposing spatial heterogeneity in the landscape as Huffaker had done, we show that stabilizing spatial heterogeneity can arise spontaneously from interactions between organisms. Thus, endogenous spatial heterogeneities may be an essential component of autonomous biological control in natural systems. Spatial heterogeneity is generally considered a feature of the landscape, even when there are behavioral mechanisms associated with the landscape features. For example, scale insects were found to coexist with ladybird beetle predators by finding spatial refuges at the base of their host trees where the beetles could not reach (Caltagirone and Doutt 1989). Here we show that even in a completely homogenous landscape (where there is no physical refuge), prey can find spatial refuges by dispersing across landscapes at a different rate and direction than their predators and pathogens.

In this dissertation I propose that if interactions between organisms can generate spatial structure where there is none, landscapes should not be organized solely on the size and frequency of habitat features. In the classic metapopulation framework, populations existing in fragmented landscapes with many small patches of habitats are thought to exist as metapopulations, whereas populations in landscapes with one main large patch and smaller peripheral patches of habitats are more likely source-sink populations (MacArthur and Wilson 1967, Levins 1969, Pulliam 1988, Hanski and Gilpin 1991). Yet if the movement and behavior

of organisms is important, a single landscape may be perceived very differently from organism to organism, regardless of the static layout of habitat features in the landscape. This dissertation presents a novel theoretical framework that links the synchrony of populations sampled across a landscape to how fragmented landscapes are perceived by organisms on a scale between metapopulation and source-sink. We apply a power function scaling law between population means and variances known as Taylor's law to assess perceptions of space by different organisms coexisting in the same landscape. Though known to apply almost universally to populations sampled across space or time, the power of Taylor's law varies from 1 to 2, and there is no consensus yet as to what different powers signify (Taylor 1961, Eisler et al. 2008). We suggest that this power should depend on how synchronous sampled populations are from one another, and that synchrony depends on how much dispersal is happening across the entire landscape. Furthermore, since Taylor's law is derived from a fundamental relationship between means and variances, it can help assess population synchrony for datasets that are limited in replications across time but not space. We applied our framework to test perceptions of space across the urban landscape of Ann Arbor for populations of aphids, ladybird beetles and parasitoid wasps. Our results suggest that aphids experience the landscape at much larger spatial scales than their natural enemies. Aphid populations were much more synchronous across the landscape with power functions closer to 2, while their natural enemy populations were asynchronous and had power functions closer to 1. Again spatial heterogeneity arises not from landscape features, but from different perception of the same landscape by different species. We show for the first time that a single landscape can be both metapopulation and source-sink depending on what organism is the focus of study. We expect that endogenous disjunctions in

spatial scales between prey and their predators can promote coexistence just as well as exogenous landscape barriers.

These results were further verified for aphids using genetic markers to measure dispersal across the city of Ann Arbor. As predicted we find evidence of a source-sink structure, since genetic diversity decreases with urbanity, and the most diverse populations came from the most rural sites on the outskirts of the city. Theory, survey data, and population genetics combined all point to the same general conclusion: aphids perceive the urban landscape of Ann Arbor at large scales corresponding to a source-sink structure. Even though this is a single case study, the remarkable concordance across the three distinct methods employed in this dissertation suggest that Taylor's law may indeed be useful for assessing how permeable fragmented landscapes are for different organisms. This is particularly useful considering the widespread applicability of Taylor's law, one of the few general laws recognized in ecology.

Irreversible consequences of human management in agriculture

The goal of this dissertation was to assess how biocomplexity can contribute stability to agricultural systems so that we may effectively transition conventional agriculture systems that rely heavily on inputs of pesticides and fertilizers to agroecological systems that are capable of autonomous biological control and nutrient regulation. Vandermeer and Perfecto have suggested that conventional and agroecological forms of agriculture may represent alternative stable states that are driven by socio-ecological forces (Vandermeer and Perfecto 1997). If this is the case, we should expect changes in management of agriculture to have long-term consequences that are irreversible, or in formal terms, hysteretic. This phenomenon is common for human-managed systems: fisheries, fire-managed forests/savannas, and eutrophic lakes are a few examples

(Carpenter et al. 1999, Scheffer 2009, Petrie et al. 2009, Staver et al. 2011). Examples of alternative stable states (high or low fish populations, forest or savanna, eutrophic or oligotrophic lakes) in the literature are always represented by changes in a single driver variable (harvest rates, fire, nutrient loads). In reality there are many potential driver variables and human management is likely to have effects on more than one driver variable at a time.

For example, correlations in vital rates of biocontrol agents can easily result when agents interact with the environment and pests in a nonlinear fashion. Changes in management to improve the carrying capacity of a control agent (ie. providing nesting sites) can have unintended consequences on growth rates (ie. increases at first followed by declines from disease outbreaks or intraspecific competition at high densities) (Luck 1990, Arditi and Berryman 1991). Thus, to expand the critical transition literature to include more realistic complexities, this dissertation examines the effects of correlated driver variables on patterns of hysteresis. For biological control systems, simple correlations between carrying capacities and growth rates result in very complicated hysteretic patterns that have never before been discussed in the critical transition literature. These hysteretic patterns include hidden stable states. The standard form of hysteresis implies that though transitions to alternative stable states are difficult to reverse, all systems will eventually revert to their original state given a large enough reversion of the driver variable. The presence of hidden stable states completely changes this perspective. Hidden states can only be achieved via an external perturbation of the system that changes the state variable irrespective of the driver variable. If the system is driven out of a hidden stable state, recovery of the state via changes in the driver variables is impossible no matter how far they are reversed.

To examine agroecological transitions more broadly, I also applied this new hysteretic framework to soil-nutrient dynamics (Carpenter et al. 1999). Simple correlations between max

nutrient recycling rates and loss rates produce similar complexities in hysteretic patterns that were confirmed to exist in a carefully designed greenhouse experiment. For the first time, we show that changes in agricultural management from organic to synthetic inputs can result in hysteresis, and that hysteresis is often complicated and includes hidden stable states. We carefully designed the experiment to test for unstable states, and found that we could perturb systems at unstable points and that those perturbations resulted in predictable jumps between alternative stable states. To our knowledge this is the first experiment to assess the instability of points within a hysteretic loop. If hysteresis and correlations between driver variables is as common as the current ecological literature suggests, the presence of the complex hysteretic patterns though currently unacknowledged, is likely ubiquitous.

Implications

Though counterintuitive, we found that complexity is often a stabilizing force in agriculture. Strong negative interactions between control agents can stabilize pest populations. That stability is often complex, and sometimes chaotic. Yet regardless, pests never exceed economic thresholds that would threaten the livelihood of a farmer. A single landscape can actually be perceived very differently depending on what organism is occupying it. This complexity may help maintain coexistence of predator-prey populations, especially in homogenous landscapes like agriculture. Complexity, whether endogenous or exogenous, creates the necessary disjunctions between consumers and their resources that allow them to coexist. Yet complexity also makes approaching Elton's vision of naturally managed systems complicated. Past management regimes are likely to constrain future yields or pest control services for agriculture, and if systems are driven out of ideal states they may never be recovered. In such a

scenario, rescue of ideal states depends entirely on knowledge of the underlying hysteretic pattern for the system. Thus, to effectively stabilize pest and nutrient dynamics in agriculture, we must first evaluate and only later manipulate its complexities. Successful transitions from conventional to agroecological systems may depend entirely on our ability to understand and apply complexity appropriately.

Literature Cited

Arditi, R., and A. A. Berryman. 1991. The biological control paradox. Trends in ecology & evolution 6:32.

Caltagirone, L. E., and R. L. Doutt. 1989. The History of the Vedalia Beetle Importation to California and its Impact on the Development of Biological Control. Annual Review of Entomology 34:1–16.

Carpenter, S. R., D. Ludwig, and W. A. Brock. 1999. Management of eutrophication for lakes subject to potentially irreversible change. Ecological Applications 9:751–771.

Denoth, M., L. Frid, and J. H. Myers. 2002. Multiple agents in biological control: improving the odds? Biological Control 24:20–30.

Durrett, R., and S. Levin. 1994. The importance of being discrete (and spatial). Theoretical population biology 46:363–394.

Eisler, Z., I. Bartos, and J. Kertesz. 2008. Fluctuation scaling in complex systems: Taylor's law and beyond 1. Advances in Physics 57:89–142.

Elton, C. S. 1958. The ecology of invasions by plants and animals. Methuen, London 18.

Hanski, I., and M. Gilpin. 1991. Metapopulation dynamics: brief history and conceptual domain. Biological Journal of the Linnean Society 42:3–16.

Hassell, M. P., H. N. Comins, and R. M. May. 1994. Species coexistence and self-organizing spatial dynamics. Nature 370:290–292.

Hastings, A. 1977. Spatial heterogeneity and the stability of predator-prey systems. Theoretical Population Biology 12:37–48.

Huffaker, C. B. 1958. Experimental studies on predation: Dispersion factors and predator-prey oscillations. Hilgardia 27:343–383.

Letourneau, D. K., J. A. Jedlicka, S. G. Bothwell, and C. R. Moreno. 2009. Effects of Natural Enemy Biodiversity on the Suppression of Arthropod Herbivores in Terrestrial Ecosystems. Annual Review of Ecology, Evolution, and Systematics 40:573–592.

Levin, S. A. 1992. The Problem of Pattern and Scale in Ecology: The Robert H. MacArthur Award Lecture. Ecology 73:1943–1967.

Levins, R. 1969. Some Demographic and Genetic Consequences of Environmental Heterogeneity for Biological Control. Bulletin of the Entomological Society of America 15:237–240.

Lewis, W. J., J. C. van Lenteren, S. C. Phatak, and J. H. Tumlinson. 1997. A total system approach to sustainable pest management. Proceedings of the National Academy of Sciences 94:12243–12248.

Liere, H., D. Jackson, and J. Vandermeer. 2012. Ecological Complexity in a Coffee Agroecosystem: Spatial Heterogeneity, Population Persistence and Biological Control. PLoS ONE 7:e45508.

Louda, S. M., R. W. Pemberton, M. T. Johnson, and P. A. Follett. 2003. Nontarget effects- the Achilles' heel of biological control? Retrospective Analyses to Reduce Risk Associated with Biocontrol Introductions*. Annual Review of Entomology 48:365–396.

Luck, R. F. 1990. Evaluation of natural enemies for biological control: A behavioral approach. Trends in Ecology & Evolution 5:196–199.

MacArthur, R. H., and E. O. Wilson. 1967. The Theory of Island Biogeography. Princeton University Press.

May, R. M. 1972. Will a Large Complex System be Stable? Nature 238:413–414.

May, R. M. 2001. Stability and Complexity in Model Ecosystems. Princeton University Press.

McCann, K., A. Hastings, and G. R. Huxel. 1998. Weak trophic interactions and the balance of. Nature 395:794–798.

McCann, K. S. 2000. The diversity–stability debate. Nature 405:228–233.

Murdoch, W. W. 1975. Diversity, complexity, stability and pest control. J. appl. Ecol 12:795–807.

Petrie, B., K. T. Frank, N. L. Shackell, and W. C. Legget. 2009. Structure and stability in exploited marine fish communities: quantifying critical transitions. Fisheries Oceanography 18:83–101.

Pimentel, D., U. Stachow, D. A. Takacs, H. W. Brubaker, A. R. Dumas, J. J. Meaney, D. E. Onsi, and D. B. Corzilius. 1992. Conserving Biological Diversity in Agricultural/Forestry Systems. BioScience 42:354–362.

Pimentel, D., R. Zuniga, and D. Morrison. 2005. Update on the environmental and economic costs associated with alien-invasive species in the United States. Ecological Economics 52:273–288.

Pulliam, H. R. 1988. Sources, Sinks, and Population Regulation. The American Naturalist 132:652–661.

Scheffer, M. 2009. Critical transitions in nature and society. Princeton University Press.

Staver, A. C., S. Archibald, and S. A. Levin. 2011. The global extent and determinants of savanna and forest as alternative biome states. Science 334:230–232.

Straub, C. S., D. L. Finke, and W. E. Snyder. 2008. Are the conservation of natural enemy biodiversity and biological control compatible goals? Biological Control 45:225–237.

Taylor, L. 1961. Aggregation, variance and the mean.

Vandermeer, J. 1997. Syndromes of Production: an Emergent Property of Simple Agroecosystem Dynamics. Journal of Environmental Management 51:59–72.

Vandermeer, J., I. Perfecto, and S. Philpott. 2010. Ecological Complexity and Pest Control in Organic Coffee Production: Uncovering an Autonomous Ecosystem Service. BioScience 60:527–537.